

AD\_\_\_\_\_

Award Number: DAMD17-99-2-9007

TITLE: Georgetown Institute for Cognitive and Computational  
Sciences

PRINCIPAL INVESTIGATOR: Alan I. Faden, M.D.

CONTRACTING ORGANIZATION: Georgetown University Medical Center  
Washington, DC 20007

REPORT DATE: April 2001

TYPE OF REPORT: Final, Phase II

PREPARED FOR: U.S. Army Medical Research and Materiel Command  
Fort Detrick, Maryland 21702-5012

DISTRIBUTION STATEMENT: Approved for Public Release;  
Distribution Unlimited

The views, opinions and/or findings contained in this report are those of the author(s) and should not be construed as an official Department of the Army position, policy or decision unless so designated by other documentation.

20010925 242

**REPORT DOCUMENTATION PAGE**Form Approved  
OMB No. 074-0188

Public reporting burden for this collection of information is estimated to average 1 hour per response, including the time for reviewing instructions, searching existing data sources, gathering and maintaining the data needed, and completing and reviewing this collection of information. Send comments regarding this burden estimate or any other aspect of this collection of information, including suggestions for reducing this burden to Washington Headquarters Services, Directorate for Information Operations and Reports, 1215 Jefferson Davis Highway, Suite 1204, Arlington, VA 22202-4302, and to the Office of Management and Budget, Paperwork Reduction Project (0704-0188), Washington, DC 20503

<b>1. AGENCY USE ONLY (Leave blank)</b>		<b>2. REPORT DATE</b> April 2001	<b>3. REPORT TYPE AND DATES COVERED</b> Final, Phase II (1 Feb 00 - 31 Mar 01)	
<b>4. TITLE AND SUBTITLE</b> GEORGETOWN INSTITUTE FOR COGNITIVE AND COMPUTATIONAL SCIENCES			<b>5. FUNDING NUMBERS</b> DAMD17-99-2-9007	
<b>6. AUTHOR(S)</b> Alan I. Faden, M.D.				
<b>7. PERFORMING ORGANIZATION NAME(S) AND ADDRESS(ES)</b> Georgetown University Medical Center Washington, DC 20007  fadena@giccs.georgetown.edu			<b>8. PERFORMING ORGANIZATION REPORT NUMBER</b>	
<b>9. SPONSORING / MONITORING AGENCY NAME(S) AND ADDRESS(ES)</b> U.S. Army Medical Research and Materiel Command Fort Detrick, Maryland 21702-5012			<b>10. SPONSORING / MONITORING AGENCY REPORT NUMBER</b>	
<b>11. SUPPLEMENTARY NOTES</b> Report contains color graphics				
<b>12a. DISTRIBUTION / AVAILABILITY STATEMENT</b> Approved for Public Release; Distribution Unlimited				<b>12b. DISTRIBUTION CODE</b>
<b>13. ABSTRACT (Maximum 200 Words)</b>  The Georgetown Institute for Cognitive and Computational Sciences (GICCS) is a neuroscience research institute whose mission is to elucidate mechanisms of neurological function and dysfunction through interactive collaborative efforts among scientists using multidisciplinary investigative strategies. A cooperative agreement with the Department of Defense provided a component of the initial support required to establish GICCS. One goal was to provide seed funding to establish a variety of multidisciplinary laboratory programs, helping investigators to establish research laboratories and develop independently funded research programs in targeted areas. These efforts have been remarkably successful, both in terms of additional external funding and publication track record. As our investigators have become independently supported, we have used the DOD funds to expand some of our more successful programs and to provide support for new junior investigators. Increased emphasis on central nervous system injuries (e.g. brain trauma, Alzheimer's disease, spinal cord injury) has included studies relating to basic mechanisms (molecular/cellular) of cell death, nervous system plasticity, drug discovery (neuroprotection/cognitive enhancement), computational neuroscience/structural biology, and clinical studies related to cognition and Alzheimer's disease.				
<b>14. SUBJECT TERMS</b> brain trauma, Alzheimer's disease, spinal cord injury, mechanisms of cell death, nervous system plasticity, drug discovery, cognition, computational neuroscience/structural biology				<b>15. NUMBER OF PAGES</b> 75
				<b>16. PRICE CODE</b>
<b>17. SECURITY CLASSIFICATION OF REPORT</b> Unclassified	<b>18. SECURITY CLASSIFICATION OF THIS PAGE</b> Unclassified	<b>19. SECURITY CLASSIFICATION OF ABSTRACT</b> Unclassified	<b>20. LIMITATION OF ABSTRACT</b> Unlimited	

**Cooperative Agreement No. DAMD17-99-2-9007**

**TABLE OF CONTENTS**

Cover .....	1
SF 298 .....	2
Table of Contents.....	3
Introduction.....	4
Human Cognitive Neuroscience .....	5
Dr. Michael Ullman .....	5
Dr. Paul S. Aisen .....	17
Computational/Developmental Neuroscience .....	21
Dr. Geoffrey Goodhill .....	21
Dr. Alexander Yakovlev .....	26
Drug Discovery and Design.....	41
Dr. Alan Kozikowski .....	41
Dr. Shaomeng Wang.....	45
CNS Injury: Mechanism and Treatment.....	50
Dr. Alan Faden.....	50
Dr. Robert Vink .....	56
Dr. Susan Knoblach.....	60
CNS Injury: Models, Plasticity and Regeneration.....	66
Dr. Linda MacArthur .....	66
Dr. Lisa Rosenberg .....	70
Faculty publications during the last year .....	72

## INTRODUCTION

The Georgetown Institute for Cognitive and Computational Sciences (GICCS) is a neuroscience research institute whose mission is to elucidate mechanisms of neurological function and dysfunction through interactive collaborative efforts among scientists using multidisciplinary investigative strategies. A cooperative agreement with the Department of Defense provided a component of the initial support required to establish GICCS. One goal was to provide seed funding to establish a variety of multidisciplinary laboratory programs, helping investigators to establish research laboratories and develop independently funded research programs in targeted areas. These efforts have been remarkably successful. Since its initiation, GICCS faculty members have obtained approximately 40 competitive, federal grants totalling more than \$16,000,000. The publication track record has been equally impressive, with a strong history of full-length publications over the initial five-year funding cycle. As our investigators have become independently supported, we have used the DOD funds to expand some of our more successful programs and to provide support for new junior investigators.

In 1999, a new Department of Neuroscience was established at Georgetown University Medical Center, and many of the GICCS faculty moved into this department. Other investigators elected to remain in the Department of Neurology or to move to Departments most reflective of their primary research interests, such as Physiology or Tumor Biology. With these changes and following bill language in Congress, which provided continuation support, the research focus of the past two years has increasingly emphasized central nervous system injuries (e.g. brain trauma, Alzheimer's disease, spinal cord injury). This has included studies relating to basic mechanisms (molecular/cellular) of cell death, nervous system plasticity, drug discovery (neuroprotection/cognitive enhancement), computational neuroscience/structural biology, and clinical studies related to cognition and Alzheimer's disease.

Present faculty include four professors, two associate professors, seven assistant professors, and one instructor. A total of 22 post-doctoral fellows and 5 research technicians/ assistants support this research team. Among this group, there are extensive collaborations, particularly in areas relating to mechanisms of cell death, plasticity, and drug discovery.

**HUMAN COGNITIVE NEUROSCIENCE:** Dr. Ullman investigates neural bases of language and memory. Dr. Aisen studies the mechanisms and treatment of Alzheimer's disease.

**MICHAEL ULLMAN, Ph.D.**

In the study of language, a fundamental distinction is drawn between the memorized "mental lexicon" and the computational "mental grammar." The lexicon contains memorized words — that is, pairings of sound and meaning. The grammar contains rules, which underlie the productive sequential and hierarchical combination of lexical forms and abstract representations into complex structures, including complex abstract representations, words, phrases, and sentences. That is, the grammar subserves the computation of compositional linguistic forms whose meanings are transparently derivable from their structures. For example, a mental rule which specifies that English past tense forms are derived from the concatenation of a verb stem and an *-ed* suffix would allow us to productively compute past tenses from new words (e.g., *fax* + *-ed* → *faxed*) and from novel forms (e.g., *blick* + *-ed* → *blicked*). Rule-derived forms can thus be computed in real-time, and so do not need to be memorized — although even compositional forms (*walked*) could in principle be memorized.

We have proposed a mental model of lexicon and grammar, which addresses representational, computational, and neural aspects of the two language capacities. The *declarative/procedural model* of lexicon and grammar posits that, for native speakers of a language, aspects of the lexicon/grammar distinction are tied to the distinction between two well-studied brain memory systems, each of which has been implicated in a particular set of non-language functions.

One system is often referred to as the "declarative" memory system. It has been implicated in the learning, representation, and use of knowledge about facts ("semantic knowledge") and events ("episodic knowledge"). It may be particularly important for learning arbitrarily related information — that is, for the associative/contextual binding of information. It has been argued that the information learned by this system is not informationally encapsulated, being accessible to multiple response systems. Moreover, this information may be consciously ("explicitly") recollected. The memory system is subserved by medial temporal lobe regions (the hippocampus and related structures), which are connected largely with temporal and parietal neocortical regions. Learning new information involves all parts of the system. However, the medial temporal components appear to be required to consolidate new memories. Memories eventually become independent of the medial temporal lobe structures, and dependent upon neocortical regions, particularly in the temporal lobes, possibly primarily (but not only) in the left hemisphere see.

The other system is usually referred to as the "procedural memory," "skill," or "habit" system. It has been implicated in the learning of new, and the control of long-established, motor and cognitive "skills" or "habits" (e.g., from simple motor acts to riding a bicycle to skilled game playing). Neither the learning nor the remembering of these procedures appear to be accessible to conscious memory — thus the system is often referred to as an "implicit memory" system see. It has been argued that the procedural system is largely "informationally encapsulated" see, having relatively little access to other response systems. The system may be particularly important for learning and performing skills involving sequences. Evidence from animal studies suggests that its circuitry may also be critical in the expression of innate behavioral routines, such as grooming sequences in rodents.

The procedural system is rooted in frontal/basal-ganglia structures, with a possible role for inferior parietal regions. Evidence from impairments in expressing established motor skills (in ideomotor apraxia) suggests that the system may be especially dependent upon left hemisphere structures. Inferior parietal structures may serve as a repository of stored knowledge of skills, including information on stored sequences. The basal ganglia and the Supplementary Motor Area (SMA) may play a particularly important role in the processing of sequences. The basal ganglia also appear to play an important role in the learning of new skills and habits. The basal ganglia circuits are connected largely with frontal cortex. These circuits appear to be parallel and functionally segregated, each receiving projections from a particular set of cortical and subcortical structures, and projecting via the thalamus to a particular cortical region, apparently largely in frontal cortex. Thus a basal ganglia "motor circuit" projects to frontal motor areas, while other circuits project to other frontal areas. The different basal ganglia circuits may have similar synaptic organizations, suggesting that similar neuronal operations might be performed at comparable stages of each circuit. It has been independently hypothesized that the frontal lobes, to which the basal ganglia project, may also be organized in a similar manner, with distinct topographically organized regions playing the same or similar computational roles in different domains.

According to the declarative/procedural model, the declarative memory system subserves an associative memory that underlies stored knowledge about words, including their sounds, their meanings, and other memorized information. The consolidation of new words relies on medial temporal lobe structures. Eventually the knowledge of words becomes independent of these structures, and dependent on neocortex, particularly in temporal and temporo-parietal regions. Temporal-lobe regions may be particularly important in the storage of word meanings, whereas temporo-parietal regions may be more important in the storage of word sounds, including their phonological sequence information. Extrapolating from evidence from the study of declarative memory leads to the suggestion that lexical memory is not informationally encapsulated, being accessible to multiple response systems.

It is posited that the procedural memory system subserves the non-conscious (implicit) learning and use of aspects of a symbol-manipulating grammar, across grammatical sub-domains, including syntax, non-lexical semantics, morphology, and phonology. This system may be particularly important in the learning and computation of sequential and hierarchical structures (i.e., in grammatical structure building). Once learned, knowledge of sequences may depend upon left inferior parietal (that is, temporo-parietal) regions, which thus may serve as a locus of convergence between the declarative and procedural systems. The learning of rules is expected to be at least partially dependent upon basal ganglia structures. One or more particular basal ganglia circuits or sub-circuits, projecting to particular frontal region(s), may subserve grammatical processing, and perhaps even finer-grained distinctions, such as morphological (morpho-phonological) versus syntactic structure-building. On this view, the frontal/basal-ganglia structures are domain-general in that they subserve non-linguistic as well as linguistic processes, but contain parallel domain-specific circuits.

The declarative/procedural model contrasts with two previously proposed theoretical frameworks, both of which have addressed the computational and neural basis of language.

Previously proposed (here termed "traditional") "dual-mechanism" theories posit distinct cognitive and neural components for the two capacities. On this view, the learning, representation, and/or processing of words and associated information in a rote or associative memory is subserved by one or more components, which may be specialized and dedicated ("domain-specific") to these functions. It has been claimed that the use of stored words may be especially dependent upon left

posterior regions, particularly temporal and temporo-parietal structures. In contrast, the learning, knowledge, and/or processing of grammar are posited to be subserved by one or more components that are specialized and dedicated to their linguistic functions, and whose computations depend upon innately-specified constructs. The use of grammar has been claimed to be dependent on left frontal cortex, particularly Broca's area (the inferior left frontal gyrus, which contains the cytoarchitectonic Brodmann's areas 44 and 45 ) and adjacent anterior regions.

"Single-mechanism" theories posit that the learning and use of the words and rules of language depend upon a single computational system with broad anatomic distribution. On this view, there is no categorical distinction between non-compositional and compositional forms. Rather, rules are only descriptive entities, and the language mechanism gradually learns the entire statistical structure of language, from the arbitrary mappings in non-compositional forms to the rule-like mappings of compositional forms. Modern connectionism has offered a computational framework for the single mechanism view. It has been argued that the learning, representation, and processing of grammatical rules as well as lexical items takes place over a large number of inter-connected simple processing units. Learning occurs by adjusting weights on connections on the basis of statistical contingencies in the environment.

Thus the declarative/procedural model of language differs from both traditional dual-mechanism theories and single-mechanism theories. Although the model shares the perspective of traditional dual-mechanism theories in positing that lexicon and grammar are subserved by distinct (separable) computational systems, with posterior and anterior neural correlates, respectively, it diverges from these theories where they assume components dedicated (domain-specific) to each of the two capacities. Conversely, while the model shares with single-mechanism theories the view that the two capacities are subserved by domain-general circuitry, it diverges from them where they link both capacities to a single mechanism with broad anatomic distribution.

The three perspectives make different theoretical claims with respect to four issues: separability, computation, domain-generality, and anatomical localization. The differing theoretical claims in turn lead to distinct predictions, allowing the theories to be distinguished empirically.

Separability. Both traditional dual-mechanism models and the declarative/procedural model posit separability — that lexicon and grammar are subserved by separable cognitive systems, with at least partially distinct neural correlates. Thus these two models predict double dissociations between the two language capacities. In contrast, single mechanism models do not posit separate underpinnings for lexicon and grammar, and therefore do not predict double dissociations between the two capacities.

Computation. The declarative/procedural model's assumption that one component is an associative memory, and that the other underlies symbol-manipulation, is consistent with traditional dual-mechanism models — although these often adopt the distinct perspective that lexical memory is a rote list of words. Thus psychological or neural markers of memory (e.g., frequency effects), and in particular of associative memory (e.g., phonological neighborhood effects) , should be found with memorized lexical items, but not with linguistic forms posited to be computed by grammatical rules. In contrast, single-mechanism models predict associative memory effects for all linguistic forms.

Domain-Generality. According to the declarative/procedural model, but to neither competing theoretical framework, lexicon and grammar are subserved by distinct systems, each of which underlies a specific set of non-language functions. Only the declarative/procedural model predicts associations

— in learning, representation, and processing — among lexicon, facts, and events, and among grammar, skills, and habits.

Localization. The declarative/procedural model makes specific claims about links between lexicon and particular temporal/temporo-parietal structures, and between grammar and left frontal/basal-ganglia structures, as a function of the roles of those neural structures in the two memory systems (see above). Traditional dual-mechanism models expect similar links, although the particular neuroanatomical claims made by the declarative/procedural model are not predicted by traditional dual mechanism models. Single mechanism models do not predict the same function-structure associations.

Thus the declarative/procedural model, but not traditional dual-mechanism or single-mechanism models, predict double dissociations, with (1) associations among associative memory markers, lexical items, facts and events, and temporal/temporo-parietal regions (including medial temporal lobe structures in the learning of new information); and (2) a distinct (dissociated) set of associations among grammar, motor and cognitive skills and habits (especially sequences), and frontal/basal-ganglia structures.

Testing for lexicon/grammar dissociations has been problematic because tasks probing for lexicon and for grammar usually differ in ways other than their use of the two capacities. For example, it is difficult to match measures of grammatical processing in sentence comprehension with measures of lexical memory see. A more productive approach to investigate the brain bases of lexicon and grammar may be to examine simple language phenomena that are well-studied from linguistic, psycholinguistic, developmental, and computational perspectives.

We have therefore focused (though not exclusively) on English past tense inflection. This linguistic phenomenon has been intensively studied, and is therefore relatively well understood. It offers a crucial contrast between two otherwise well-matched types of inflected word: regular past-tenses (*walked*), which can be described as a combination of stem (*walk*) and affix (*-ed*), and which may be composed in real-time; and irregulars (*kept*, *sang*), which do not follow a predictable pattern, and which therefore must depend upon memorized representations. The declarative/procedural model, but not traditional dual system models nor single system models, posits that regulars are real-time rule products whose computation depends upon left frontal/basal-ganglia structures; whereas irregulars are memorized in and retrieved from the temporal lobe declarative/lexical memory system. Although we have focused on regular and irregular English past tense inflection, we have also examined the regular/irregular contrast in English plural inflection, Japanese adjectival past tense inflection, and Italian present tense and past participle inflection. In addition, a number of our studies have examined aspects of syntactic processing at the sentence level.

## PROJECT 1. PSYCHOLINGUISTIC INVESTIGATIONS

We have shown that generation times and acceptability judgments of past tense forms of irregular (*dig-dug*) but not regular (*walk-walked*) verbs correlate with their frequencies, even when holding stem frequencies or stem acceptability ratings constant. We have found a similar result in children. These data suggest that irregular but not regular past tense forms are retrieved from memory. In addition, we have reported that acceptability ratings of real and novel past-tenses correlate with a measure of the number of similar-sounding verbs for irregulars (e.g., *spring-sprang*, *spling-splang*; c.f., *sing-sang*, *ring-rang*) but not for regulars (e.g., *walk-walked*, *nawk-nawked*; c.f. *stalk-stalked*, *lock-locked*). This suggests that the computation of irregulars but not regulars is dependent on an associative



memory in which the phonological patterns of stem-past pairs can be generalized to other verbs, as predicted by the dual-system model. We have shown a similar pattern in Japanese regular and irregular adjectival past tense inflection.

## **PROJECT 2. DEVELOPMENTAL DISORDERS: SPECIFIC LANGUAGE IMPAIRMENT**

Specific Language Impairment (SLI) refers to a developmental disorder of language in the relative absence of other cognitive impairments. We have examined two groups of subjects (including children and adults) with hereditary SLI and with syntactic processing deficits. Subjects in one of the groups had motor sequencing impairments and basal ganglia and frontal abnormalities, suggesting a dysfunctional procedural memory system. We found that both groups failed to produce novel regular forms (*plam-plammed*) and over-regularizations (*dig-digged*), suggesting that they were unable to use the past tense suffix productively, as predicted by a grammatical deficit.

## **PROJECT 3. NEUROLOGICAL STUDIES OF LANGUAGE: APHASIA, AD, PD, AND HD**

We have carried out a number of studies testing for the predicted dissociations of associations in adult-onset brain damaged patients.

### **Project 3A: Aphasia**

In several studies we have reported that non-fluent aphasics with left anterior (frontal/basal-ganglia) damage and agrammatism (grammatical impairments) are worse at producing reading and judging regular than irregular English past tense forms. In contrast, we have found that fluent aphasics with left posterior (temporal/temporo-parietal) damage and anomia (word-finding problems) show the opposite pattern in past tense production, reading, and judgment. These double dissociations suggest that regular and irregular past tense computation depend on distinct neural underpinnings. They also link the computation of regulars to left anterior structures and to grammar, and the computation of irregulars to left posterior regions and to the lexicon.

### **Project 3B: Neurodegenerative Diseases – AD, PD and HD**

Our studies of adults with degenerative brain disease have revealed double dissociations between the production of irregularly and regularly inflected forms, and have linked irregulars to memorized words and facts and to temporal lobe regions, and regulars to syntax and motor skill function and to frontal/basal-ganglia structures.

Alzheimer's disease (AD) is associated with severe degeneration of temporal and temporo-parietal regions, and relative sparing of the basal ganglia and frontal cortical regions, particularly Broca's area. The temporal and temporo-parietal damage may explain AD impairments at retrieving and recognizing words. In contrast, the majority of studies suggest that AD patients are relatively unimpaired at syntactic processing. AD patients are also relatively spared at performing motor and cognitive skills.

In studies of English regular and irregular past tense, we have shown that AD patients with severe deficits at object naming or fact retrieval make more errors producing past tenses of irregulars

than of regulars or *-ed*-suffixed novel verbs. Moreover, across AD patients, error rates at object naming and at fact retrieval correlate with error rates at producing irregular but not regular or *-ed*-suffixed novel past tenses. Similarly, Cappa and Ullman reported that Italian AD patients had more difficulty producing irregular than regular present tense and past participle forms in Italian.

Parkinson's disease (PD) is associated with the degeneration of dopaminergic neurons in the basal ganglia, causing high levels of inhibition in the motor and other frontal cortical areas to which the basal ganglia circuits project. This is thought to explain why PD patients show the suppression of motor activity (hypokinesia) and have difficulty expressing motor sequences. PD patients may also have difficulty with grammar, both in comprehension and production. In contrast, temporal-lobe regions remain relatively undamaged and the recognition of words and facts remains relatively intact in low- or non-demented PD patients.

In our investigations of the PD production of regular and irregular past tense forms, we found that severely hypokinetic PD patients showed a pattern opposite to that found among the AD patients, making more errors producing regular and *-ed*-suffixed novel past-tenses than irregular past-tenses. Moreover, across PD patients, the level of right-side hypokinesia, which reflects left basal ganglia degeneration, correlated with error rates at the production of regular and *-ed*-suffixed novel forms but not irregular forms. Intriguingly, left-side hypokinesia, which reflects right basal ganglia degeneration, did not show the analogous correlations with error rates in the production of any past tense type, underscoring the role of left frontal/basal-ganglia structures in grammatical rule use.

Patients with Huntington's disease (HD) show the opposite pattern to that of PD patients. Although HD is like PD in causing degeneration of the basal ganglia, it strikes different portions of these structures. Unlike in PD, this damage results in the disinhibition of frontal areas receiving basal ganglia projections. This is thought to lead to the unsuppressible movements (chorea, a type of hyperkinesia) found in patients with HD. Patients with HD show the opposite pattern to those with PD not only in the type of movement impairment (the suppressed movements of hypokinesia vs. the unsuppressed movements of hyperkinesia), but also in the type of errors on *-ed*-suffixed forms. HD patients produce forms like *walkeded*, *plaggeded*, and *dugged* — but not analogous errors on irregulars like *keptet*, suggesting that these errors are not attributable to articulatory or motor deficits. Rather the data suggest unsuppressed *-ed*-suffixation. This conclusion is strengthened by the finding that the production rate of these over-suffixed forms correlates with the degree of chorea, across patients. These contrasting findings in PD and HD, linking movement and *-ed*-suffixation in two distinct types of impairments related to two types of basal ganglia damage, strongly implicate frontal/basal-ganglia structures in *-ed*-suffixation. They also support the hypothesis that these structures underlie the expression of grammatical rules as well as movement, and suggest that the structures play a similar role in the two domains.

#### **PROJECT 4. ELECTROPHYSIOLOGICAL INVESTIGATIONS OF LANGUAGE: ERP**

We have been investigating the brain bases of lexicon and grammar using the electrophysiological technique of measuring the Event Related Potentials (ERPs) associated with the presentation of stimuli. Previous evidence had suggested that lexical or semantic violations yield central/posterior negativities ("N400"), whereas grammatical violations can yield left anterior negativities ("LAN"). Unfortunately, the tasks tapping these lexical and grammatical capacities have not been well-matched in factors other than the two capacities. Therefore we have been investigating

the electrophysiological basis of lexicon and grammar by probing the use of irregular and regular forms.

In a recent ERP study of regular and irregular English past tense morphology, we presented regular and irregular verbs in past tense context sentences either as incorrect stem forms (e.g., Yesterday I walk after lunch) or as correct past tense forms (e.g., Yesterday I dug a hole). In comparisons to ERP waves of correctly inflected forms, incorrect regulars (i.e., an illicit absence of past-tense affixation) yielded a LAN, whereas incorrect irregulars (i.e., an illicit absence of a memorized past-tense form) yielded a more central distribution. In a second study designed to directly compare regular/irregular morphology and syntax/lexical-semantics, subjects viewed sentences with and without violations of syntactic phrase structure and lexical-semantics (following ), as well as the violations of regular and irregular past-tense morphology described above. Violations of regular verb inflection and syntactic phrase structure yielded LANs, whereas the waveforms yielded by the incorrect irregulars and the lexical-semantic anomalies were more posterior. We argue that both of these posterior negativities are N400 ERP components. These results tie regular morphology to syntax, link irregular morphology to lexical-conceptual processing, and dissociate regular morphology and syntax from irregular morphology and lexical-conceptual processing.

## **PROJECT 5. HEMODYNAMIC STUDIES OF LANGUAGE: FMRI**

In a recent fMRI study, we examined syntactic and semantic processing directly, rather than focussing on regular and irregular morphology. We used event-related functional magnetic resonance imaging to identify brain regions involved in syntactic and semantic processing. Healthy adult males read well-formed sentences randomly intermixed with sentences which either contained violations of syntactic structure or were semantically implausible. Reading anomalous sentences, as compared to well-formed sentences, yielded distinct patterns of activation for the two violation types. Syntactic violations elicited significantly greater activation than semantic violations primarily in superior frontal cortex. Semantically incongruent sentences elicited greater activation than syntactic violations in the left hippocampal and parahippocampal gyri, the angular gyri bilaterally, the right middle temporal gyrus, and the left inferior frontal sulcus (Fig. 1). These results demonstrate that syntactic and semantic processing result in non-identical patterns of activation, including greater frontal engagement during syntactic processing and larger increases in temporal and temporo-parietal regions during semantic analyses.

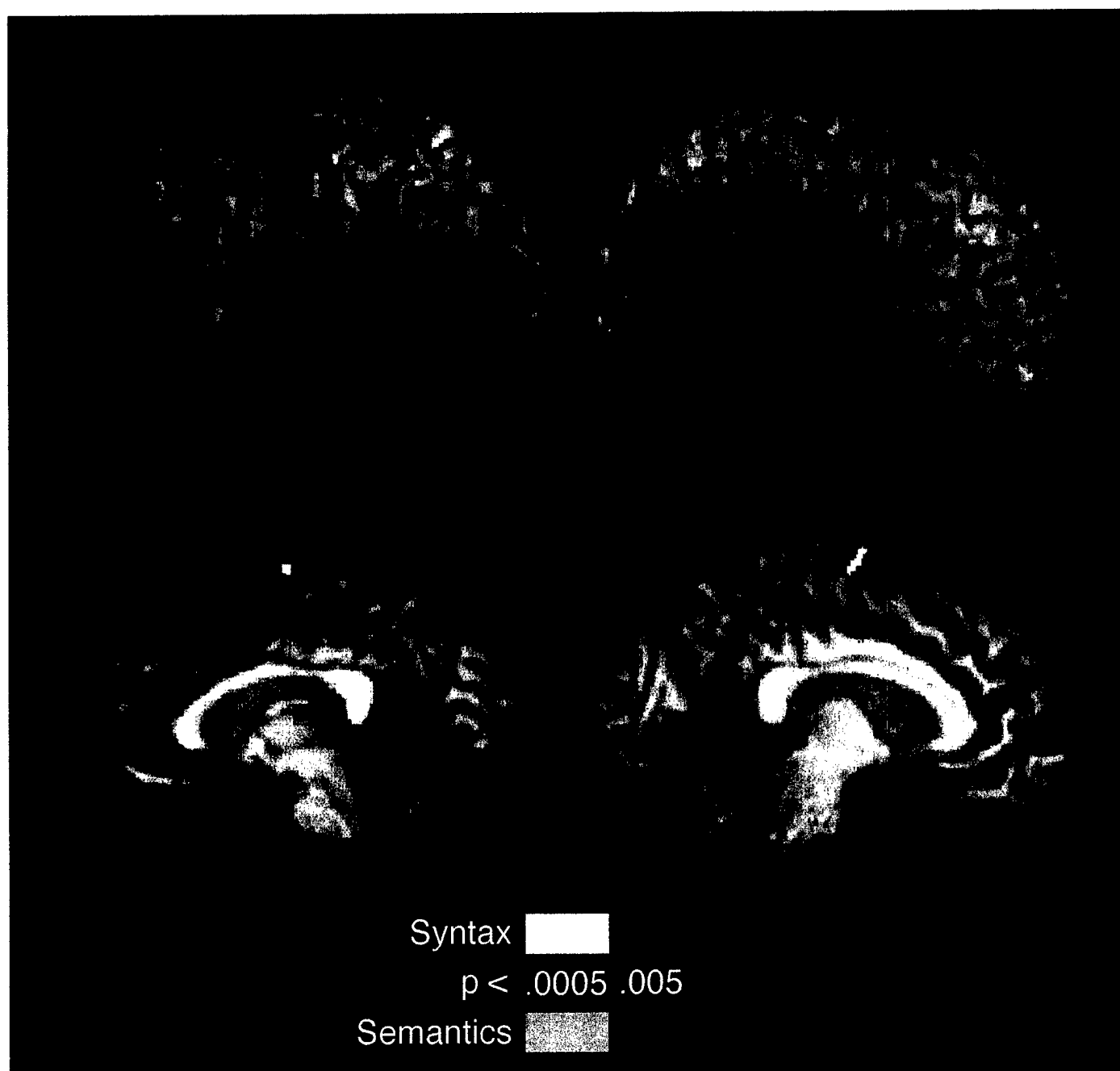


**Figure 1.** Activations (thresholded at  $p \leq 0.005$ ) for syntactic (yellow/red) and semantic (green/blue) anomalies on the lateral (top) and medial (bottom) surfaces of each hemisphere. The data have been averaged over all 14 subjects following stereotaxic normalization, resampled to 1mm voxels using cubic interpolation, and superimposed on a stereotaxically normalized anatomical image (1mm resolution) from one subject.

## **PROJECT 6. MAGNETOENCEPHALOGRAPHY (MEG)**

This technique provides a method for investigating the real-time spatio-temporal dynamics associated with the production of regular and irregular past tense forms. Rhee, Pinker, & Ullman recorded from a whole-head 64-channel magnetometer while subjects produced past tenses of regular and irregular verbs. Satisfactory solutions to the inverse problem of dipole fitting for data averaged over all subjects were found at a number of 10 millisecond time-slices following stimulus presentation. No right-hemisphere dipoles were found. Dipoles in both the regular and irregular verb conditions were localized to a single left temporal/parietal region (250 to 310 milliseconds). Dipoles in left frontal regions were found only for regular verbs, and only for time-slices immediately following the left temporal/parietal dipoles (310-330 milliseconds). The results are consistent with a dual-system model in which temporal/parietal-based memory is searched for an irregular form, whose successful retrieval blocks the application of a frontal-based suffixation rule.

## **PROJECT 7. FUNCTIONAL REORGANIZATION AND RECOVERY OF LANGUAGE**

### **Project 7A: Specific Language Impairment (SLI)**

We have investigated language dysfunction in two groups of subjects with hereditary SLI and syntactic processing deficits (see above). Unlike cognitively unimpaired subjects, patients in both groups were not only unable to use the past tense suffix productively (see above), but also showed frequency effects for *regular* as well as irregular past tense forms. This suggests that their difficulty at learning or using grammatical rules resulted in the memorization of regular as well as irregular forms in a relatively intact lexical/declarative memory system.

### **Project 7B: Anterior (Agrammatic) Aphasia**

We asked 9 agrammatic anterior aphasics and 5 posterior aphasics to read aloud regular and irregular past-tense forms see. The posterior aphasics, like healthy subjects, showed past-tense frequency effects for irregulars, but not for regulars. In contrast, the anterior aphasics showed frequency effects for regulars as well as irregulars, suggesting both were memorized. Moreover, a positive correlation between the number of years since the lesion and frequency correlation *r*-values was obtained only for the anterior aphasics and only with regulars, suggesting that the anterior aphasics memorized regulars following lesion-onset. These results support the hypothesis that anterior aphasics depend upon temporal/temporo-parietal structures to memorize regular past-tense forms following lesion onset, whereas posterior aphasics are like unimpaired subjects in depending upon frontal structures to compute regulars compositionally. Thus the data underscore the relative plasticity of the temporal-lobe system and its role in the recovery of grammatical function.

## **PROJECT 8. SEX DIFFERENCES IN LANGUAGE AND MEMORY**

Males and females clearly differ in various perceptual, motor and cognitive domains. However, the existence of sex differences in the neurocognition of language remains highly controversial. Robust differences might become apparent only when separately probing the distinct domains of language, as

motivated by theories of language. Moreover, whereas most investigations have compared overt behavioral performance between the sexes, the detection of certain cognitive sex differences may require methods which directly probe underlying processing mechanisms or their neural correlates.

The goal of this project is to examine sex differences in the computational and neural bases of language learning and processing in two domains: the mental lexicon containing memorized words, and the mental grammar, whose rules underlie the combination of lexical forms into complex representations: words (morphology), phrases and sentences (syntax). "Dual-system" theories of language hold that distinct neurocognitive systems underlie lexicon and grammar. Grammatical computations are processed automatically in real-time. Evidence suggests that the learning and use of lexical knowledge depends upon a well-studied bilateral temporal-lobe "declarative memory" system implicated in the learning and use of conceptual/semantic knowledge (i.e., knowledge about the world), while aspects of grammatical computations rely on left frontal/basal-ganglia circuits implicated in the acquisition and expression of motor and cognitive skills (e.g., riding a bicycle).

Girls and women are much better than boys and men at memorizing words ("verbal memory"). This suggests the novel hypothesis that whereas males generally compute complex forms compositionally in real-time (e.g., *play* + *-ed*), females may tend to store previously encountered complex forms (*played*) as entries in the mental lexicon.

In a recent series of studies, we have examined this sex difference hypothesis by focusing on regular and irregular English past tense. As discussed above, according to the dual-system declarative/procedural model, the *-ed* morpho-phonological affix is grammatically combined in real-time with regular verb forms (e.g., *play*) by a rule which depends upon frontal/basal-ganglia structures; irregular past-tense representations are memorized in and retrieved from the temporal-lobe based lexical/declarative memory system. Whereas this dichotomy is expected in males, females may tend to memorize regulars along with irregulars. Both sexes should rule-compute novel *-ed*-suffixed past-tenses (*proy* + *-ed*). We tested these predictions with psycholinguistic, neuropsychological, and neuro-electrophysiological experiments.

*Experiment 1.* If past-tense representations are retrieved from memory, more frequent ones should be remembered better and faster than less frequent ones. If they are rule-products, such past-tense frequency effects are not expected. Sixteen men and 17 women were asked to produce past tenses of regular and irregular verbs in sentence contexts. Men showed past-tense frequency effects for irregulars but not regulars. Women showed past-tense frequency effects for both verb types.

*Experiment 2.* Parkinson's disease is associated with frontal/basal-ganglia degeneration. The basal-ganglia lesions lead to suppressed movements (hypokinesia). These brain structures may also underlie grammatical composition: It was previously shown that past-tense production rates of novel (*proyed*) and regular (*played*) verbs correlate with hypokinesia, but not with lexical abilities. Conversely, production rates of irregular past-tenses (*broke*) correlate with lexical abilities, but not hypokinesia. This suggests that the production of *-ed*-suffixed forms involves frontal/basal-ganglia circuits, whereas irregular past-tenses are retrieved from lexical memory.

Fifteen men and 14 women with Parkinson's disease produced past-tenses in sentence contexts. The men showed the correlation pattern reported in the previous study (in which 22 of the 28 patients

were male). The women's production rates of regular as well as irregular past-tenses correlated with lexical abilities but not hypokinesia. Like the males, however, their production rates of novel *-ed*-suffixed past-tenses correlated with hypokinesia; surprisingly, these also correlated with lexical abilities.

*Experiment 3.* Event-Related Potentials (ERPs) reflect the real-time electrophysiological brain activity of cognitive processes that are time-locked to the presentation of target stimuli. Difficulties in lexical/semantic processing elicit centro-parietal negativities ("N400s") that peak about 400 milliseconds post-stimulus, and depend upon bilateral temporal lobe structures. Difficulties in grammatical processing yield early (150-500 ms) left anterior negativities ("LANs") linked to rule-based automatic computations and left frontal structures; and late (600 ms) centro-parietal positivities ("P600s") associated with controlled processing and posterior brain regions.

Twenty-six men and 26 women were visually presented with anomalous and control sentences probing four conditions: regular and irregular past-tense, syntactic word-order, and lexical/semantic processing. Among the men, incorrect (vs. correct) regulars and word-order violations yielded statistically indistinguishable left fronto-central negativities (LANs). Incorrect irregulars patterned with the bilateral N400 elicited by lexical/semantic incongruities. Among the women, the negativities produced by violations of regulars, irregulars, and word-order patterned with the lexical/semantic N400.

The experiments support the language sex difference hypothesis, in expressive and receptive language, in morphology and syntax. Presumably, retrieving a representation blocks the rule system. The memory-dependence of novel past-tense and syntactic word-order processing is consistent with a productive associative memory; and with the memorization of already-computed complex representations containing affixal, word or phrasal categories, and their relations. The three experiments pose a challenge to theories which posit that all complex forms are computed in associative memory. No performance differences were found, suggesting that the computational and neural sex differences do not lead to achievement differences.

Multiple lines of evidence suggest that the female advantage at lexical memorization involves the medial-temporal-lobe structures of declarative memory. The word learning and medial-temporal sex differences are clearly linked to estrogen. As expected if lexical memory depends on declarative memory, the female memorization advantage extends beyond verbal material. Women have shown an advantage at remembering abstract figures, events, and object locations. Such memory abilities involve medial-temporal structures, are tied to estrogen, and may explain computational sex differences in navigation: Women (and female rats) rely on landmarks, and men (and male rats) on geometric cues or "dead-reckoning". Thus in (at least) language and navigation, parallel computational strategies are available, with females relying more than males on declarative memory.

The predicted sex differences have educational, neurocognitive and clinical implications. They may account for girls' superiority in the use of words and complex grammatical structures, and girls' and women's advantage at second language learning. Greater bilateral temporal lobe activation in women than in men while listening to sentences is consistent with a greater female reliance on complex representations stored in the temporal-lobe memory system. The hypothesized sex differences may be relevant to reports of sex differences in aphasia and its recovery. Sex differences in the incidence of various brain disorders could be partly explained by a greater cognitive dependence of females than

males on temporal-lobe structures, and of males on frontal/basal-ganglia structures: This would lead to a higher detection rate in females of diseases largely affecting the temporal lobes (e.g., Alzheimer's disease), and a higher detection rate in males of frontal/basal-ganglia diseases (e.g., Parkinson's disease and a variety of developmental disorders). Finally, the sex differences offer intriguing clues on the evolutionary origins of language and its neural substrates.

## **PROJECT 9. SECOND LANGUAGE ACQUISITION AND PROCESSING**

Critical/sensitive period effects are found in both first and second language (L1 and L2) acquisition. Later language exposure affects the use of grammar much more adversely than the use of lexical items that do not play an important grammatical role. We have shown that, presumably in order to compensate for reduced grammatical abilities, adult late learners of English as a second language tend to memorize morphologically complex linguistic forms that are typically computed compositionally in real-time by adult native English speakers.

We have posited that the greater sensitivity to age-of-exposure for grammar than for lexicon leads to a compensatory shift of reliance from the grammatical computational system in L1 to lexical memory in L2: Complex linguistic representations that are compositionally computed by the grammatical system in L1 may simply be memorized in the lexicon in L2. As described above, we have observed this effect in Specific Language Impairment, which, like L2, is associated with difficulties in acquiring grammar. Moreover (also see above), we have found that agrammatic aphasics memorize complex forms during recovery. Finally, Ullman has carried out an exhaustive retrospective examination of the neurolinguistic literature, which supports the predicted increase in dependence upon lexical memory in second language learners.

To directly test the hypothesis, we asked three groups of adults to produce English regular and irregular past tenses and plurals (item-matched on past-tense/plural frequency, stem frequency, and phonological structure) in sentence contexts: 33 native speakers of English (L1), 32 native speakers of Chinese (L2), and 33 native speakers of Spanish (L2). All L2 subjects had their first substantial exposure to English after age 17, and had at least three years of exposure. Reaction time to past tense or plural production constituted the dependent variable.

In the L1 group, both past tense and plural production times correlated significantly with past-tense frequency for irregulars ( $p's < .001$ ) but not regulars ( $p's > .15$ ). In both the Chinese and Spanish L2 groups, all the correlations were significant (regulars:  $p's \leq .001$ ; irregulars:  $p's \leq .01$ ).

The results indicate a sharp contrast between native speakers and late-learning non-native speakers. These and other data indicate that in L1, regular past-tenses and plurals are generally compositionally computed in real-time, whereas irregular past-tenses and irregular plurals have memorized representations. In contrast, in L2 both regular and irregular forms depend on memorized representations. The findings support the novel hypothesis that there is a shift between L1 and L2, such that linguistic forms computed compositionally in L1 tend to be memorized in L2. The contrast between the L1 and L2 patterns also further strengthens the existence of distinct grammatical and lexical systems in L1.



**PAUL S. AISEN, M.D.**

**TRANSLATIONAL RESEARCH PROGRAM IN ALZHEIMER'S DISEASE**

We proposed to use Department of Defense funding to support, in part, the establishment of a Memory Disorders Program, along with clinical and basic projects aimed at development of better therapies for Alzheimer's disease.

The Memory Disorders Program, in the Department of Neurology, has grown steadily since its inception in 1999. At present, the staff includes two physicians (one with a Ph.D. in Neuropsychology), a linguist, a study coordinator, a research assistant and a research nurse. Over one hundred patients with memory disorders, primarily Alzheimer's disease, are followed in the program.

The Memory Disorders Program has been the central site for multiple therapeutic trials:

**PROJECT 1. MULTICENTER TRIAL OF NAPROXEN AND ROFECOXIB IN AD**

Evidence that inflammatory mechanisms contribute to neuronal injury in Alzheimer's disease along with a number of epidemiological studies suggest that non-steroidal anti-inflammatory drugs (NSAIDs) may slow the rate of cognitive deterioration. We have selected two such drugs for a therapeutic trial: rofecoxib, a new selective cyclooxygenase (COX)-2 inhibitor, and naproxen, a non-selective NSAID. The trial employs a double-blind parallel design with three primary treatment groups: rofecoxib (25mg daily), naproxen (200mg twice daily) and placebo. A total of three hundred patients will be enrolled in the trial and randomized to the three groups. Stable use of cholinesterase inhibitors, estrogen, low dose aspirin and vitamin E will be allowed. Patients with inflammatory diseases that might respond to the study medications will be excluded. The primary outcome measures will be the one year change in the cognitive subscale of the Alzheimer's Disease Assessment Scale (ADAScog) and the Clinical Dementia Rating Scale sum of boxes (CDR-SOB). The attainment of significant endpoints (4 point and 7 point declines from baseline ADAScog score, death, institutionalization, 1 point worsening on the global CDR, 15 point decline on the ADCS activities of daily living (ADL) inventory) will be examined as a secondary outcome measure. Other secondary measures include the Neuropsychiatric Inventory, the Quality of Life-AD and the ADCS pharmacoeconomic scale.

This nationwide trial is directed and coordinated by the Memory Disorders Program staff. Enrollment for the trial closed in November, 2000, with a total of 349 subjects at 40 sites (including 10 subjects at Georgetown). The study will be completed early next year.

## **PROJECT 2. PILOT STUDY OF NIMESULIDE IN AD**

Clinical and laboratory experience with nimesulide, an NSAID with preferential cyclooxygenase-2 inhibition, suggests that it may be a good candidate for AD therapy. This pilot study (conducted at Mount Sinai under the direction of the Georgetown Memory Disorders Program staff) investigated the clinical feasibility of nimesulide treatment in AD. Forty subjects with probable AD were enrolled in a randomized, controlled parallel group trial designed to assess the tolerability and short-term cognitive/behavioral effects of nimesulide. In the initial 12 week double-blind phase, subjects were treated with nimesulide 100mg po bid or matching placebo; during the second 12 week phase all subjects received active drug. Subjects who tolerated the drug well and perceived benefit were invited to continue open-label nimesulide treatment.

This trial has now been completed, and data analysis and manuscript preparation are under way. Short-term therapy with nimesulide, compared to placebo, had no significant effect on total assessment scores of measures of cognition, clinical status, activities of daily living, affect or behavior. Post-hoc analysis of individual items suggested possible benefit on clinical assessment of orientation and judgment, and possible mood elevation. Long-term therapy was well tolerated for periods exceeding 2 years. These findings support the feasibility of nimesulide therapy in AD; assessment of efficacy will require a larger, long-term treatment study.

## **PROJECT 3. PILOT STUDY OF HIGH-DOSE VITAMINS TO REDUCE HOMOCYSTEINE IN AD**

In recent years, homocysteine, a sulfur amino acid, has been recognized as an important risk factor for vascular disease. Individuals with relatively high blood levels of homocysteine are at markedly increased risk for heart attack, stroke and peripheral vascular disease. The mechanism by which homocysteine promotes vascular disease may involve direct toxicity on endothelial cells (the lining cells of blood vessels), and increased blood clotting. Homocysteine elevations can be related to several factors, including aging, certain genetic factors, inadequate nutrition, and kidney disease. Regardless of the factors leading to homocysteine elevations, levels can be reduced by treatment with high doses of three vitamins: folate, vitamin B<sub>12</sub> and vitamin B<sub>6</sub>. Large scale trials have now been initiated to determine whether supplementation with these vitamins can reduce the risk of vascular disease.

There is now evidence that homocysteine is also a risk factor for dementia, including Alzheimer's disease (AD). Five separate studies have shown that homocysteine levels are higher in individuals with AD compared to non-demented individuals of similar age. Further, one careful study has demonstrated that AD patients with relatively high levels of homocysteine show more rapid disease progression (as measured by brain atrophy) than AD patient with lower levels. Possible explanations for this association between homocysteine and AD include a link between cerebrovascular disease and AD, and a direct toxic effect of homocysteine on brain cells.

The link between high homocysteine levels and AD suggests that reducing homocysteine levels with nutritional supplements may be beneficial in slowing disease progression. Since such supplementation is expected to be safe and inexpensive, any significant beneficial effect on the disease would justify widespread use of such supplements. A prospective therapeutic trial is necessary to

determine whether supplementation is indeed beneficial. However, little is known regarding the extent to which such supplements can actually lower homocysteine in patients with AD, so rational design of such a trial is not yet possible.

In preparation for a large scale therapeutic trial of high dose nutritional supplements to treat AD, we are conducting a pilot study to determine the effect of supplementation on homocysteine metabolism in this population. A group of 80 patients with AD, half of whom will be taking standard multivitamin supplements, will be enrolled in this study (at Georgetown and three other sites). After collection of clinical data and assessment of genetic factors that may influence homocysteine metabolism, levels of homocysteine will be measured before and after an oral methionine load (intake of the amino acid methionine raises homocysteine levels). All subjects will be treated with daily supplements consisting of folate 5mg, vitamin B<sub>12</sub> 1mg and vitamin B<sub>6</sub> 50mg for eight weeks. Fasting and post-methionine homocysteine levels will then be repeated.

This pilot study will provide data on the effect of high dose supplements on homocysteine metabolism in a heterogeneous population of AD patients. This information is essential to the design of a definitive multicenter therapeutic trial of folate and B vitamin supplementation for the treatment of AD. That large-scale study (Multicenter Trial of Homocysteine Reduction in Alzheimer's Disease, Aisen, P.I.) has just been awarded funding from NIA, and will begin late in 2002.

#### **PROJECT 4. MULTICENTER VITAMIN E TRIAL IN AGING PERSONS WITH DOWN SYNDROME**

The goal of this project is to determine whether the administration of vitamin E, which has been shown to delay the progression of Alzheimer disease, will slow the rate of cognitive/functional decline in older individuals with Down syndrome. Individuals with Down syndrome 50 years of age or older, with or without a diagnosis of Alzheimer disease, will be eligible for enrollment. A total of 400 persons functioning at all levels of mental retardation will be enrolled at approximately 20 sites. A vitamin E regimen (1,000 international units twice daily, plus a multivitamin) will be compared to a multivitamin alone in a two-arm parallel group design. The treatment period is three years, with study visits at six-month intervals. The primary outcome measure is a brief test of praxis, measuring cognitive functions expressed as performance of simple, short sequences of voluntary movements. This will be the first large-scale treatment study of Alzheimer disease complicating Down syndrome. It will serve as a model for future efforts at applying treatments developed for sporadic Alzheimer disease to the population of at-risk individuals with Down syndrome. Enrollment at Georgetown and about 20 other sites world-wide will begin in June, 2001.

## **LABORATORY STUDIES:**

While our focus has been therapeutic drug trials, we have also continued our efforts on the development of peripheral biomarkers that may prove useful in conducting these studies.

### **PROJECT 1. PLASMA NEOPTERIN IN ALZHEIMER'S DISEASE**

We chose to test plasma neopterin as a marker of microglial inflammation in AD, because it is a useful marker of inflammation in other conditions, both central and peripheral, and can be easily measured in the blood. Neopterin is formed as a byproduct of tetrahydrobiopterin (THB) synthesis via the guanosine triphosphate-biopterin pathway; THB is a co-factor required for the biosynthesis of catecholamines, serotonin, and nitric oxide. Increased levels of neopterin are released by gamma interferon stimulated monocytes, tissue specific macrophages, and T lymphocytes. Many inflammatory central nervous system disorders are associated with increased neopterin levels. In light of the recent appreciation of the role of inflammatory mechanisms in AD, and the strong correlation between inflammation and elevated neopterin levels in other disorders, we examined plasma neopterin levels in AD.

Our initial effort to characterize the utility of plasma neopterin as an inflammatory biomarker has been completed and published (manuscript attached). Plasma neopterin levels were higher in 51 AD ( $9.3 \pm 5.9$  ng/ml) than in 38 age-matched control subjects ( $6.3 \pm 2.6$  ng/ml,  $p=0.002$ ). There was no correlation between neopterin levels and mini-mental state examination score or duration of disease; there was a weak association between neopterin level and age ( $r=0.26$ ,  $p=0.02$ ). While measurement of plasma neopterin levels is not useful for diagnosis, this assay may provide guidance for the development of anti-inflammatory treatment strategies for AD.

### **PROJECT 2. IMMUNOGENETICS AND ALZHEIMER'S DISEASE**

Several studies from other groups, as well as our own preliminary findings, suggest that immunogenetics may influence inflammatory mechanisms that contribute to AD. In brief, we believe that HLA-DR genotype influences the risk of AD and the rate of disease progression by modulating brain inflammatory activity. This idea departs from established theory, because HLA-DR expression is considered to be important in antigen presentation to lymphocytes, yet there is not much evidence of lymphocytic activity in the AD brain. Nonetheless, we have reported evidence that HLA-DR genotype influences AD glial activity, and hypothesize that this is mediated by an effect on microglial responsiveness.

The goal of this project is to elucidate the relationship between immunogenetics, specifically HLA-DR genotype, and AD progression and on the response of AD patients to anti-inflammatory drug interventions. This effort is linked to the multicenter NSAID trial described above. Genotyping is being performed on each of the 349 study participants, which will allow correlational analyses when the blind is broken next year.

**COMPUTATIONAL/DEVELOPMENTAL NEUROSCIENCE:** Dr. Goodhill has two main research goals, both broadly relating to neural development: understanding the theoretical principles governing the development and structure of cortical mappings; and elucidating quantitatively how gradients of chemotropic factors guide axons to appropriate targets in the developing brain. Dr. Yakovlev studies apoptosis and apoptotic mechanisms in development and after injury.

## **GEOFFREY GOODHILL, Ph.D.**

### **INTRODUCTION**

It has been hypothesized for many decades that growth cones could guide axons to their targets in the developing and regenerating nervous system by sensing concentration gradients of molecules in their environment. In the past few years much progress has been made in identifying the gradient molecules involved (Tessier-Lavigne & Goodman, 1996). However, the understanding of *how* growth cones sense gradients at a mechanistic level has not kept pace. The goal of this project was to develop a new technology to allow the response of axons in precisely controlled gradients to be analyzed and quantified. Particular objectives were:

1. To establish concentration gradients of chemotropic molecules of precisely known steepness in a collagen gel.
2. To grow axons in these gradients and measure how their response depends on the parameters of the gradient.

We have made significant progress on both of these objectives. In particular we have:

- Developed a new technology for establishing precisely controlled molecular gradients in collagen gels.
- Determined how to grow both explants and single cells of dorsal root ganglia (DRGs) and cortex in "dry" collagen without any fluid medium, as required by our technology.
- Purified netrin-1 from a netrin-1-expressing cell line and shown that it is effective at promoting outgrowth (both in terms of extension and direction) from cortex.
- Determined the dose-response curve for extent of neurite outgrowth from DRGs in response to nerve growth factor (NGF), and cortex in response to netrin-1.
- By mathematical simulation determined the range of parameters for which our new technology produces gradients of sufficient stability.
- Quantitatively imaged gradients of fluorescent molecules to both validate the simulations and estimate diffusion constants.
- Quantified the tropic response of neurites from DRG explants to precisely controlled gradients of NGF of exponential shape.

### **RESULTS**

#### **A novel gradient technology**

We have developed a novel *in vitro* assay which allows axonal response to gradients to be measured with unprecedented accuracy. We establish gradients by "printing" chemotropic molecules onto the surface of a long, thin block of collagen gel and allowing the molecules to diffuse into the collagen. Because molecular movement by diffusion is fast over short distances but slow over long distances, initial local unevenness in the concentration smooths out in a few hours, leaving behind a gradient that remains smooth and stable for several weeks. We have complete

control over the shape of this gradient via the pattern of molecules deposited on the surface (Fig. 1A). We can deposit precisely controlled volumes of chemotropic factors onto precisely controlled locations using a method similar to that employed in inkjet printers. A commercially available micropump (Gesim, Germany) consists of a small reservoir between a glass plate and a membrane in contact with a piezo-electric actuator. When a short (100  $\mu$ s) voltage pulse is applied to the pump, the membrane rapidly contracts the reservoir, forcing a small spherical droplet out of the micro-machined nozzle of the micropump (Fig. 1B). The droplet volume depends in a controllable way on the parameters of the voltage pulse, ranging from 0.5 to 1 nl. The amount of factor delivered can be precisely controlled by varying the pulse rate, up to a maximum of 1000 drops per second. The micropump sits above the dish to be printed, which is mounted on a commercial high precision x-y translation stage. By varying the rate of factor delivery from the pump, the length of time the factor is delivered to a particular spot, and the pattern of spots chosen, we have virtually unlimited control over the spatial and temporal characteristics of the factor concentration profile. Although the explant will initially experience a time-dependent concentration of factor, the concentration in between the top and the bottom of the gel (where the explant is located) reaches a nearly stable level (Fig. 1C) within a few hours. By contrast, a smoothly varying difference in concentration between the two ends of the block is maintained for several days or even weeks (Fig. 1D,E,F). The precision of the technique allows for accurate control of the concentration over several orders of magnitude. The technique can also be used to provide a source of factor while axons are growing, since no direct contact is made with the gel.

We have measured a diffusion constant for fluorescein labeled casein (molecular weight 26kD) as follows. A drop of casein was pipetted onto the surface of a 2 mm thick layer of collagen occupying a 35 mm petri dish, and allowed to diffuse over a period of 53 hours. Images of the fluorescence were collected by a CCD camera over this period, smoothed, and fitted to a concentration profile  $C(r, t)$  for a point source on an infinite two dimensional surface (Crank, 1975). A diffusion constant of  $D = 3.5 \times 10^{-7} \text{ cm}^2/\text{sec}$  was obtained, consistent with our previous estimates based on extrapolation from data for other molecules (Goodhill, 1997).

### Growth of DRGs and cortex in “dry” collagen gels

- We have developed a modified form of the collagen gel culture system. Instead of growing in small ( $\approx 0.1$ ml) volumes of collagen submerged in fluid culture medium, explants are now grown in large ( $\approx 1$ ml) volumes of collagen with no serum and no fluid culture medium (see Methods). We refer to these as “dry” collagen gels. This modification is essential for our method for establishing controlled gradients. We have determined conditions for which this arrangement produces good neurite growth, both from explants and from dissociated cells of both cortex and DRGs (Fig. 2).
- We have successfully purified netrin-1 from 293-EBNA cells transfected with the pCEP4 expression vector containing full length netrin-1 (a kind gift of Marc Tessier-Lavigne).
- We have characterized the purely growth-promoting effect of netrin-1 on cortical axons and NGF on DRG axons by adding uniform levels of netrin-1/NGF to the dry gels at a range of concentrations. The results are qualitatively similar to the dose-response curves given in Serafini et al (1994) and Conti et al (1997): growth rises to a peak and then drops off again as the concentration of netrin-1/NGF increases (Fig. 2).

### Tropism of cortex/DRG towards netrin-1/NGF

We have used small pieces of filter paper soaked in our purified netrin-1 solution to demonstrate the efficacy of our purification methods. A tropic response towards the filter paper is observed (Fig. 3). It can be seen that the strength of the tropic response rises to a peak and then drops off again as the concentration of netrin increases.

We have also started to use our new gradient assay to set up controlled gradients of NGF. Fig. 3 shows the response of DRG explants to an exponential gradient of steepness 0.37% over 10  $\mu$ m of NGF set up using the pump technology. A statistically significant bias in growth up the gradient was observed.

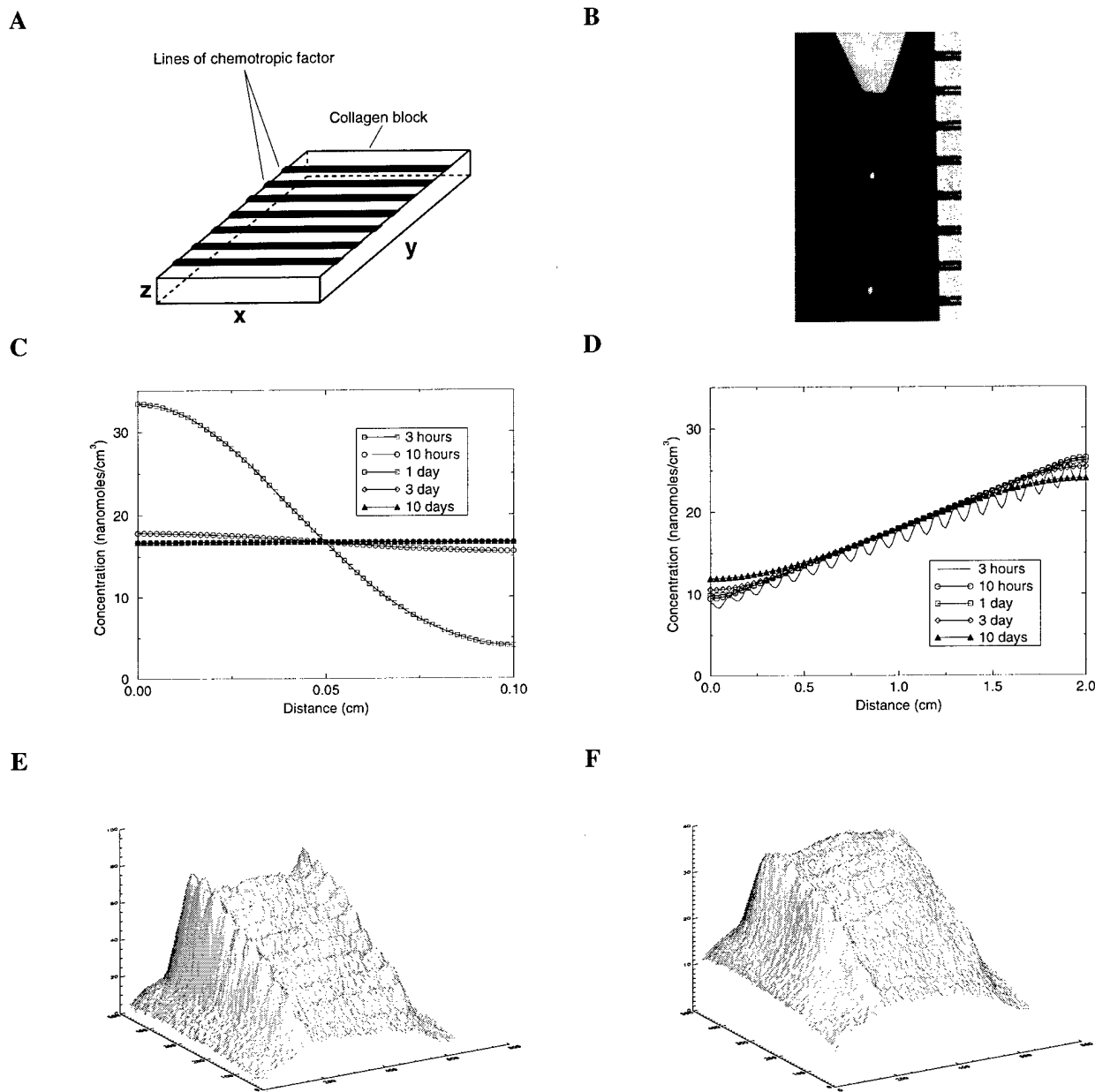


Figure 1: A novel gradient assay. **A**. Basic method for establishing the gradient. **B**. Instantaneous image of a stream of droplets ejected from the pump, captured with strobe illumination: the drops are of volume 1 nl, and the ruler spacing is 1 mm. **C**. Simulation result showing that the gradient (ordinate) rapidly becomes uniform through the vertical thickness of the collagen block (abscissa; z axis in **A**). **D**. Simulation result showing that, after the initial transients have died away, the gradient (ordinate) along the length of the block (abscissa; y axis in **A**) remains highly stable (linear gradient initially consisting of 21 lines 1 mm apart; other gradient shapes have similar stability properties). **E**. Measured gradient of fluorescent dye (casein) in a section of a collagen block 30 minutes after generation of the initial pattern. **F**. Same gradient after 4 days. Note that gradient shape remains highly stable. Total extent of gradient along x, y axes is 1 cm (axis units are pixels), z axis units are arbitrary units of fluorescence intensity (separately normalized for **E**, **F**).

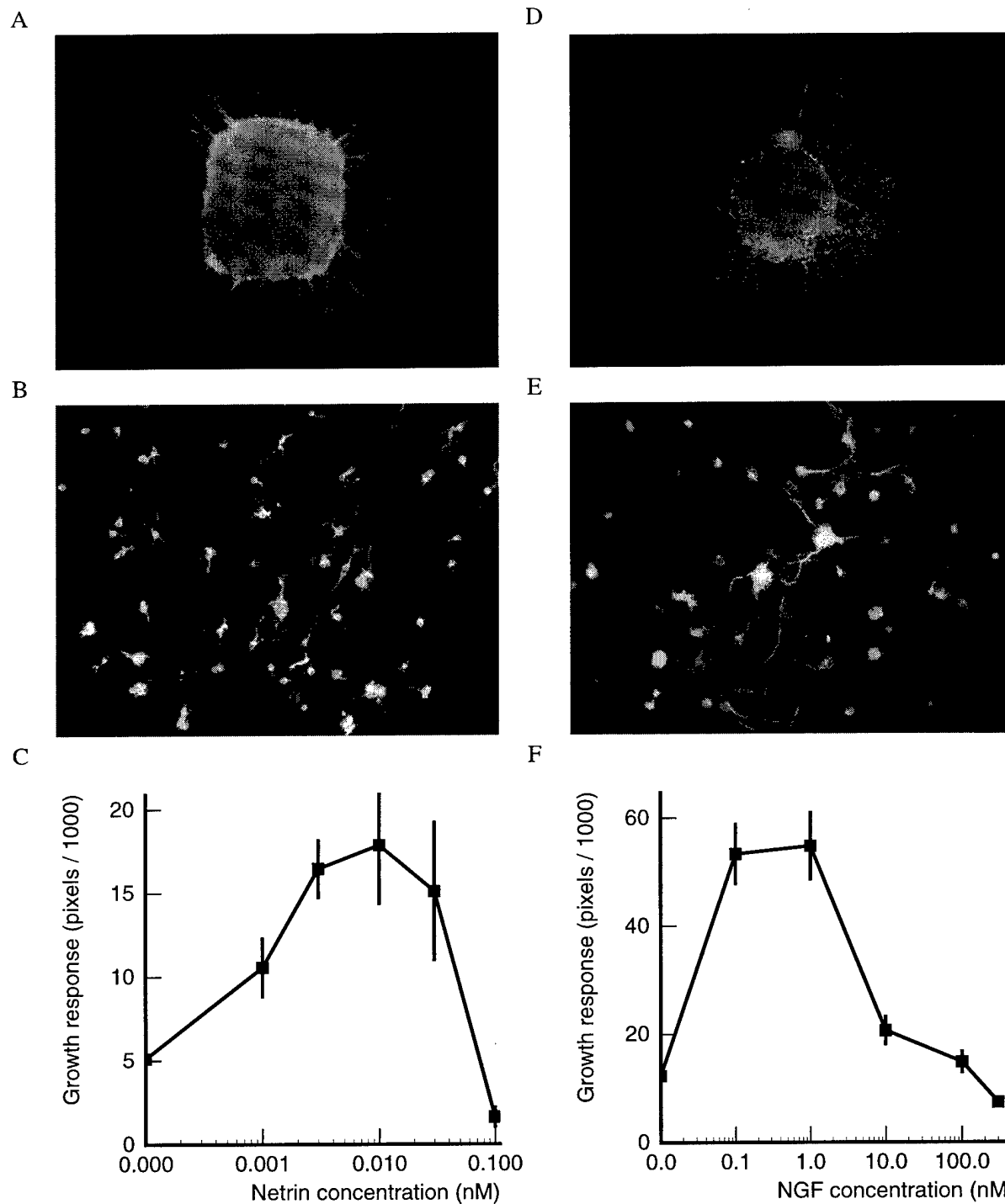


Figure 2: Growth of cortical (left) and DRG (right) neurites in dry collagen gels after 36-40 hours. Both explants and dissociated cell cultures are shown. In each case the degree of growth shows a bell-shaped dependence on ligand concentration.



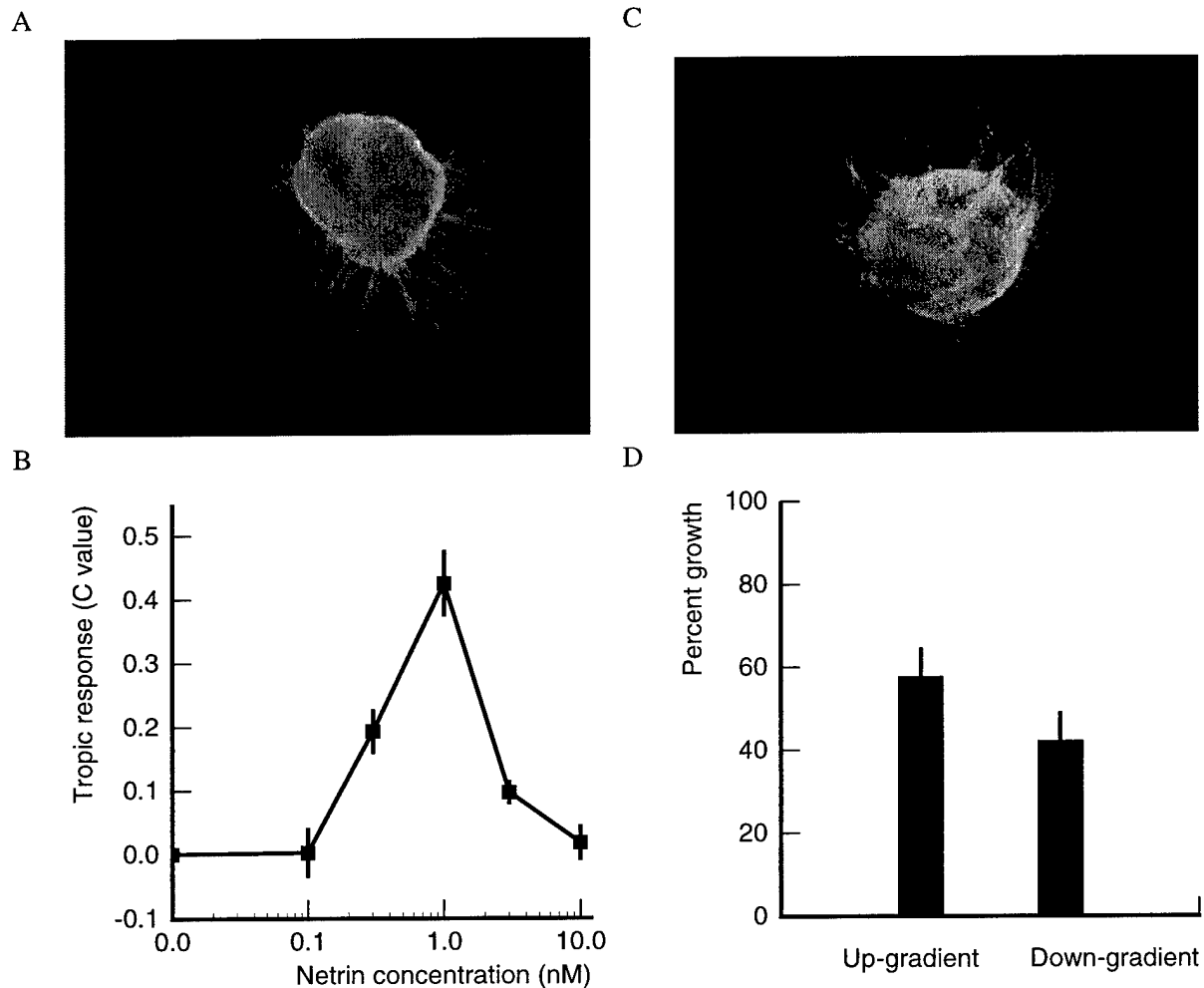


Figure 3: Tropism of cortical (left) and DRG (right) neurites in dry collagen gels after 36-40 hours. In A cortical neurites are growing towards a piece of filter paper soaked in netrin-1 solution. The dose-response curve for tropism in this case is shown in B (the vertical axis gives a statistical measure of the degree to which growth is biased towards the explant, where 1 represents maximum bias and 0 represents no bias). In C, DRG neurites are growing towards a gradient of NGF created by the pump (gradient is up - there is no source of NGF such as filter paper within the gel). D shows the percentage growth (number of neurite pixels) up versus down the gradient averaged over 36 DRG explants. The gradient was exponential in shape with a 0.37% change across each growth-cone diameter.

## ALEXANDER G. YAKOVLEV, Ph.D.

### PROJECT 1. ROLE OF DNA FRAGMENTATION FACTORS IN NEURONAL APOPTOSIS INDUCED BY TRAUMATIC BRAIN INJURY

#### Introduction

Apoptosis plays an important role in delayed neuronal loss following traumatic brain injury (TBI) or cerebral ischemia. Such cell death is characterized by specific morphological and biochemical features; the latter include the activation of caspases and a subsequent cleavage of a variety of substrates including structural proteins, DNA repair enzymes and endonuclease inhibitors. Internucleosomal DNA fragmentation, resulting from activation of endonucleases, represents one of the characteristic biochemical features of apoptosis in a variety of experimental models, including TBI. Potential endonucleases that participate in apoptosis include the caspase-activated enzymes (CAD) and NUC70, divalent cation-dependent neutral or acidic endonucleases, leukemia-associated endonucleases, and  $\text{Ca}^{2+}$ - and  $\text{Mg}^{2+}$ -dependent endonucleases (CMEs).

CAD, also known as DNA fragmentation factor (DFF40), is a 40 kDa protein that is translated in the presence of its inhibitor (ICAD, or DFF45), which functions as a specific chaperone and forms heterodimer with DFF40 in proliferating cells. *In vitro* studies have shown that DFF45 is cleaved by caspase-3, releasing the nuclease activity of DFF40 from inhibitory control and triggering DNA fragmentation. Other recent studies indicate that DFF45 may be essential in various models of apoptosis. Thus, primary thymocytes from DFF45-deficient mice are resistant to apoptosis following exposure to several apoptotic stimuli. After TBI, caspase-3 is activated and DFF45 is cleaved. Consequently, DFF proteins may undergo translocation to cell nucleus and initiate apoptotic DNA degradation postinjury.

Using a combination of *in vivo* and *in vitro* techniques, we have previously investigated neuronal apoptosis caused by fluid percussion-induced TBI in rats. We demonstrated caspase-3-dependent internucleosomal cleavage of genomic DNA in neurons from injured cortex and hippocampus after injury. In the present study we examined a potential role for DFF40 and DFF45 in TBI-induced DNA fragmentation and associated neuronal apoptosis in mice, by comparing effects in DFF45 knockout mice and wild type controls. Neuronal cell culture models and reconstitution of apoptosis *in vitro* were also used to address this issue.

## RESULTS

### DFF45 is essential for expression of DFF40 in mouse brain

To investigate whether DFF45 is essential for expression of DFF40 protein *in vivo*, we estimated levels of expression for the latter in brain cortex from wild type and DFF45 knockout mice using Western blot analysis. Staining of protein samples from mouse brain cortex with DFF45-specific antibodies confirmed expression of DFF45 in wild type animals, whereas it was not detected in samples from DFF45 knockout mice (Fig.1). Staining of the samples with DFF40-specific antibodies demonstrated that DFF40 protein expression was barely detected in DFF45 knockout mice brain, in contrast to its abundant expression in wild type mouse brain samples (Fig. 1).

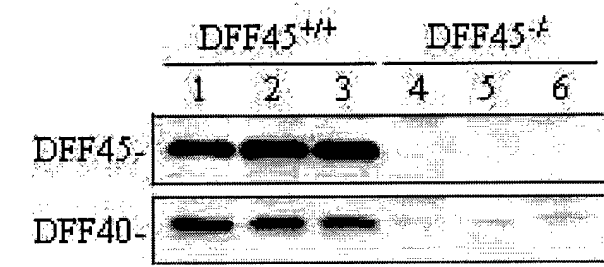


**Fig. 1** Expression of DFF45 and DFF40 proteins in brain cortex tissue from three wild type (lanes 1-3) and three DFF45 knockout mice (lanes 4-6) was monitored by immunoblot analysis. DFF45 is absent and DFF40 protein is markedly reduced in brain cortex from the knockout mice.

### Internucleosomal DNA fragmentation in brain cortex of DFF45 knockout mice

Oligonucleosomal DNA fragmentation in cortex of mouse brain subjected to experimental TBI was examined by gel electrophoresis. Analysis of labeled DNA isolated from cortex of wild type and DFF45 knockout mice demonstrated its fragmentation in affected areas (Fig. 2). DNA fragmentation from samples of injured but not from sham operated cortex was detected at 24h and 72h after trauma. The extent of DNA degradation in wild type mouse cortex appeared higher at 24h rather than 72h after TBI, whereas, in DFF45 knockouts, this process was somewhat delayed, although it should be noted that this method of DNA fragmentation detection is not quantitative.

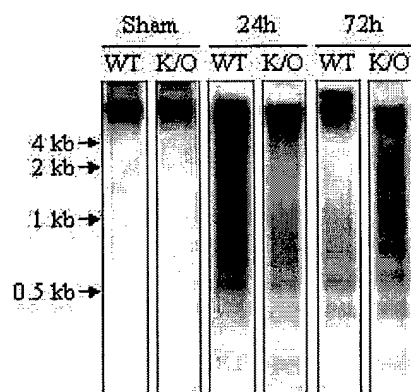


**Fig. 2** TBI induces DNA fragmentation in brain cortex of DFF45 knockout mice. Total DNA was isolated from brain cortex of wild type (WT) or DFF45 knockout mice (K/O) at indicated times after TBI. One microgram of DNA from each sample was labeled with [ $\alpha$ -<sup>32</sup>P] dATP, using *Taq* DNA polymerase, and analyzed in 1.2% agarose gel. Dried gel was exposed with X-ray film and photographed. Data are representative of four separate experiments with similar results.

### Deletion of DFF45 gene does not alter neurological recovery or injury volume after TBI

The number of footfaults was markedly increased in both wild type and DFF45<sup>-/-</sup> animals, with no significant differences observed between the groups at any time point (Fig. 3A). The effect of CCI on place learning in the Morris Water Maze task was analyzed by comparing the daily mean latency ( $\pm$ SEM) to goal location over the four trials for each group. No significant differences were found between the groups from days 14 to day 17 (Fig. 3B). Examination of working memory, performed on days 21-23 showed no significant differences between the groups for any day, although the latencies were consistently longer in the knockout animals (Fig. 3C). Lesion volume measurements, using high field MRI, also showed no significant differences between groups, although there were trends toward larger lesion volumes in DFF45 knockout animals as compared to wild type controls (Fig. 4).

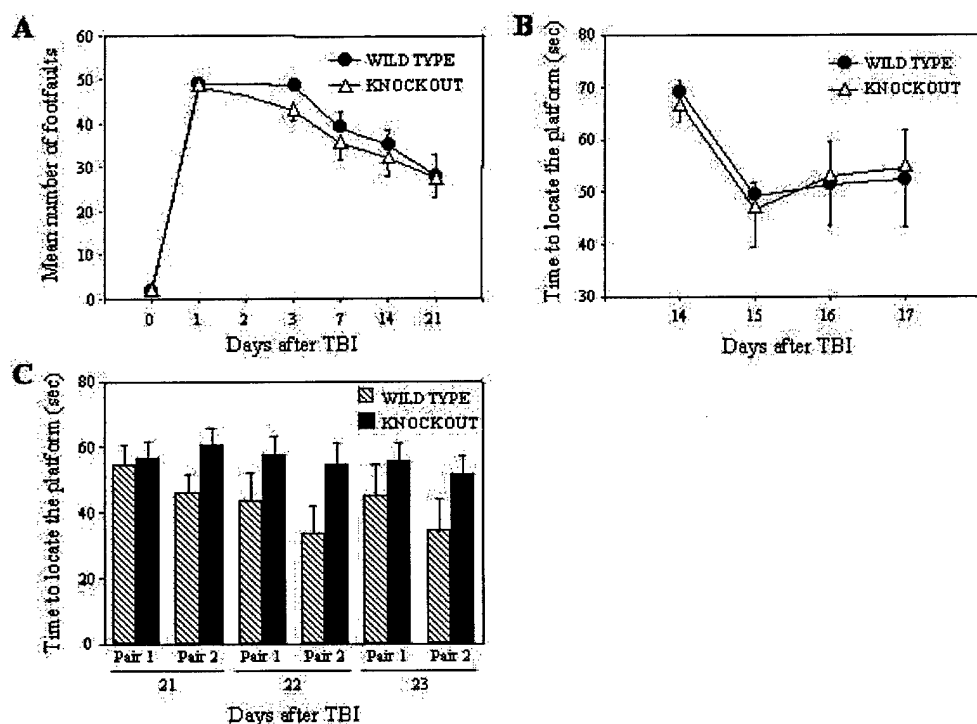


**Fig. 3** Deletion of DFF45 gene does not alter neurological recovery after TBI. (A) Performance of wild type and DFF45 knockout mice in a beam-walking task measuring fine motor coordination. Results are expressed as mean  $\pm$  SEM number of contralateral hindlimb footfaults (maximum 50) per group. (B) Latency to find the hidden platform in a version of the Morris water maze. Results are expressed as daily means  $\pm$  SEM for each group over 4 trials. (C) Mean difference in latency ( $\pm$ SEM) to locate the hidden platform between the first and second of the trial pairs in a working memory version of the Morris water maze, conducted at days 21, 22, and 23.  $n=10$  for the wild type group;  $n=20$  for the knockout group.

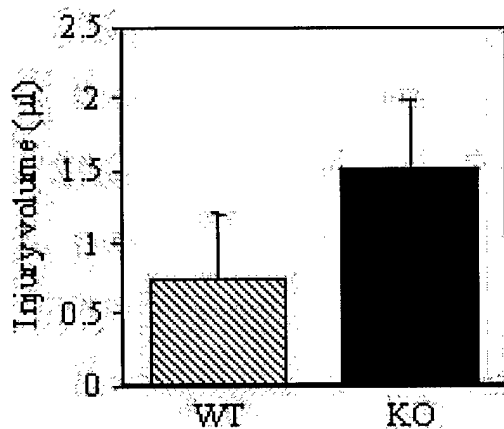


**Fig. 4** Deletion of DFF45 gene does not alter lesion volume after TBI. The graph of lesion volume versus genotype shows that while the DFF45 knockout animals had a slightly larger lesion on average than the wild type strain, this was not a statistically significant difference. Average injury volume for each group ( $\pm$  SEM in  $\mu$ l) was calculated and a one tailed T-test performed to determine significance of reduction in injured tissue in DFF45 knockout mice versus wild type.  $n=11$  for the wild type group;  $n=17$  for the knockout group.

# DNA fragmentation during apoptosis and cell death induced in cultured primary cortical neurons from wild type and DFF45 knockout mice

To verify further a role of DFF40 in DNA fragmentation during neuronal apoptosis, we used primary cultures of cortical neurons from wild type and knockout mice. Neurons in culture were treated with etoposide or staurosporine, established inducers of neuronal apoptosis. Agarose gel electrophoretic analysis of DNA integrity, performed after 24h of treatment, demonstrated that both drugs caused DNA laddering in wild type cells (Fig. 5A). In neurons from DFF45 knockout mice, staurosporine failed to induce DNA fragmentation after 24h incubation, whereas treatment with etoposide resulted in low levels of DNA laddering. When the incubation time with etoposide was increased for 48h, DNA fragmentation in DFF45 knockout neurons became prominent, while it was still not detected in knockout cultures treated with staurosporine. In contrast to neurons, spleen and thymus cells isolated from the knockout mice and exposed to etoposide or staurosporine did not develop DNA laddering even after 48h of treatment, whereas wild type splenocytes and thymocytes underwent extensive DNA fragmentation (Fig. 5B).

Viability of primary neurons was assayed by measuring calcein AM fluorescence. In accord with the difference in the extent of DNA fragmentation, a significant difference in cell viability was observed between wild type and DFF45 knockout neurons after 24 h treatment with etoposide or staurosporine (Fig. 5C). When the treatment time was increased for 48 h, cell viability in both knockout and wild type cultures decreased to a similar level following etoposide treatment, whereas viability of the knockout neurons treated with staurosporine remained significantly higher than that of wild type neurons under the same culture conditions (Fig. 5C).

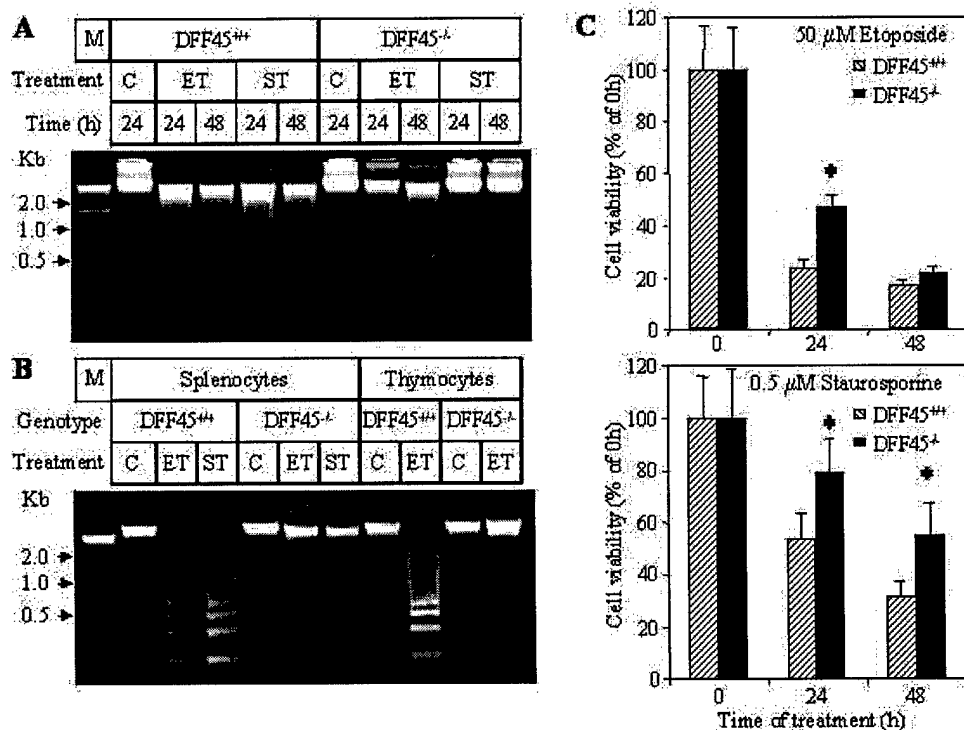


**Fig. 5** Effects of DFF45 expression on DNA fragmentation in (A and B) and viability (C) of primary mouse cortical neurons (A and C), splenocytes, and thymocytes (B) exposed to etoposide (ET) or staurosporine (ST). Primary cells were incubated for 24 or 48 h in the absence or presence of 0.5  $\mu$ M staurosporine or of 50  $\mu$ M etoposide. The integrity of genomic DNA was then examined by electrophoresis through a 2% agarose gel, and cell viability was analyzed by measurement of calcein fluorescence. Data in (C) are expressed as a percentage of the value for control cells (C) not exposed to inducers of apoptosis, and are means  $\pm$  SEM of six samples from an experiment that was repeated 2 times with similar results. \* $p$ <0.05, compared with control, by ANOVA and Dunnett's test.

## Reconstitution of apoptosis *in vitro*

We have previously demonstrated that protein extracts isolated from traumatic rat cortex were able to induce the oligonucleosomal fragmentation of DNA in isolated nuclei. To further examine a role of DFF45 and DFF40 in apoptotic DNA laddering in rat brain we employed such an *in vitro* apoptosis reconstitution system, using rat cerebellar nuclei or pCR2.1 plasmid DNA.

Agarose gel electrophoretic analysis indicated that the degree of DNA fragmentation induced in cerebellar nuclei (Fig. 6A) or plasmid DNA degradation (Fig. 6B) by extracts from injured cortex was consistent with the previously reported results: incubation of nuclei or pCR2.1 DNA with extracts from sham controls did not result in detectable degradation of DNA, whereas extracts from injured tissue isolated 24 hr post-injury produced DNA cleavage. A greater degree of DNA degradation was observed with cortical extracts isolated 3 d after trauma.

To investigate a role of caspase-3-mediated DFF45 cleavage in DNA degradation during apoptosis in brain tissue, we examined the effect of active recombinant caspase-3 on endonuclease activity in cytosolic extracts from sham control rat cortex. Increasing amounts of caspase-3 were incubated with cortical protein extracts. Integrity of DFF45 was monitored using specific anti-DFF45 antibodies. Western blot analysis demonstrated that the recombinant caspase-3 cleaved DFF45 in the incubated extracts in a dose dependent manner (Fig. 7A). However, DFF45 cleavage was not obvious in protein extracts from traumatic rat cortex isolated 3d after TBI (Fig. 7A).

Sham operated extracts incubated with or without caspase-3 and extracts from traumatized rat cortex isolated 3d after trauma were incubated with rat cerebellar nuclei and DNA fragmentation was analyzed by agarose gel electrophoresis. Addition of caspase-3 to control cortical extracts, leading to complete DFF45 cleavage, was not sufficient for induction of DNA laddering, whereas extracts from traumatized rat cortex produced DNA fragmentation without addition of the recombinant caspase (Fig. 7B).

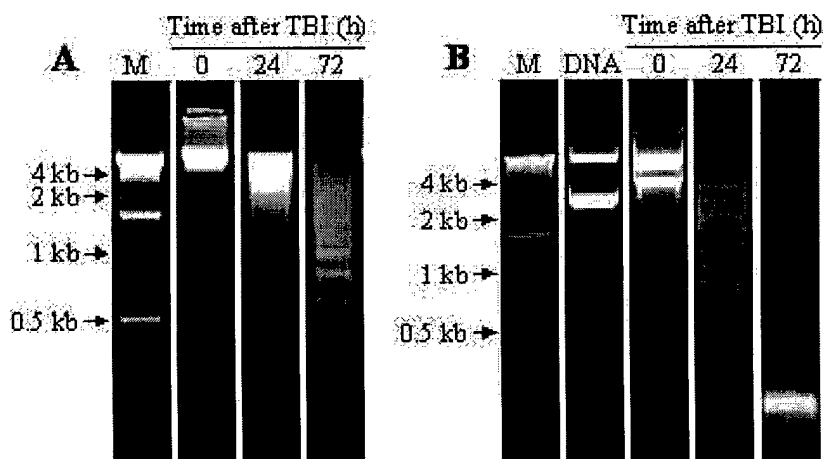


**Fig. 6** DNA cleavage in isolated nuclei (A) and plasmid DNA (B) induced by cytosolic extracts from sham control (0 h) and injured rat cortex (24 and 72 h). Cytosolic extracts from injured brain tissues were isolated at indicated times after TBI. Nuclei from rat normal cerebellum or pCR2.1 plasmid DNA were incubated with extracts, and DNA was analyzed by agarose gel electrophoresis. Data are representative of tens of experiments with similar results. The standard DNA fragments (M) represent a 1 kb DNA ladder

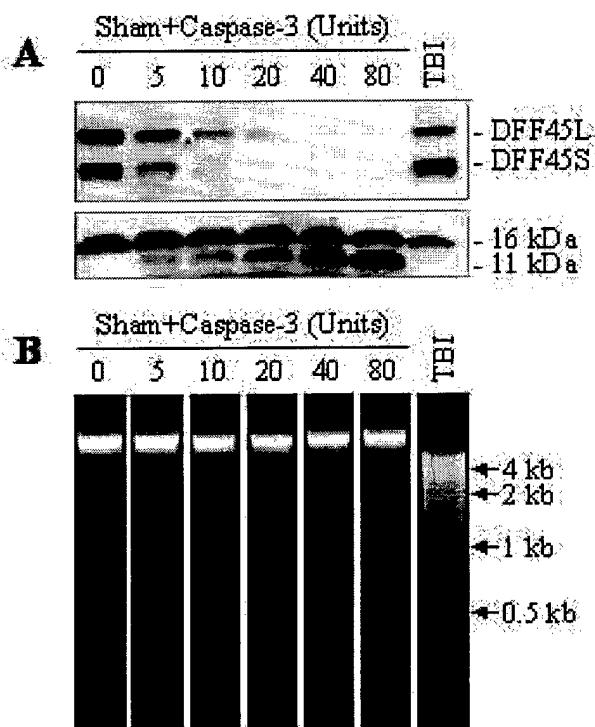


**Fig. 7** A role for caspase-3-mediated DFF45 cleavage in DNA degradation *in vitro*. Protein extracts were isolated from sham operated or injured rat cortex isolated 72 h after TBI. Sham samples were treated with indicated amounts of the recombinant rat caspase-3 for 1 h at 37°C in the extraction buffer (20 mM Hepes, pH7.4, 2 mM EDTA, 1.5 mM MgCl<sub>2</sub>, 5 mM DTT, and 0.1% CHAPS). (A) Half of each extract was then analyzed by western blotting using anti-DFF45 antibodies that recognize two alternatively spliced forms of DFF45 (DFF45L and DFF45S), their cleavage products (11 kDa), and a non-specific band (16 kDa). (B) The other half of the extracts were incubated with rat cerebellar nuclei as described in Materials and Methods. The DNA was then analyzed by electrophoresis through a 1.5% agarose gel and ethidium bromide staining. The result demonstrates that cleavage of DFF45 by caspase-3 is not sufficient for DNA fragmentation induced by protein extracts from control rat brain cortex.

### *Cation dependence of DNA cleavage by endonuclease activity induced by TBI*

To characterize ion dependence of TBI-induced endonuclease activity crude cytosolic extracts were isolated from injured rat cortex 3 d after trauma and tested for nuclease activity in a plasmid DNA cleavage assay. Cleavage of DNA by the extracts, readily observed in the reactions, was inhibited in the presence of 10mM EDTA (Fig. 8A) suggesting that endonuclease activity depended on Ca<sup>2+</sup> and/or Mg<sup>2+</sup> ions. DNA degradation was also inhibited by 20μM aurintricarboxylic acid, which inhibits the formation of protein-nucleic acid complexes and which has been shown to inhibit apoptosis in a variety of experimental models. In contrast, an inhibitor of Ca<sup>2+</sup> and Mg<sup>2+</sup>-dependent endonucleases, 2mM ZnSO<sub>4</sub>, did not inhibit nuclease activity from injured brain.

In addition, the cation dependence of endonuclease activity induced by TBI was examined by adding Ca<sup>2+</sup>, Mg<sup>2+</sup> or Zn<sup>2+</sup> to the reaction mixtures with plasmid DNA. Both 5mM Mg<sup>2+</sup> and 2.5mM Ca<sup>2+</sup> supported the endonuclease activity to similar extent (Fig. 8B). However, the combination of these two cations did not produce a notable additive effect. Addition of 2mM Zn<sup>2+</sup> did not inhibit DNA degradation, as estimated in the presence of both Ca<sup>2+</sup> and Mg<sup>2+</sup>.

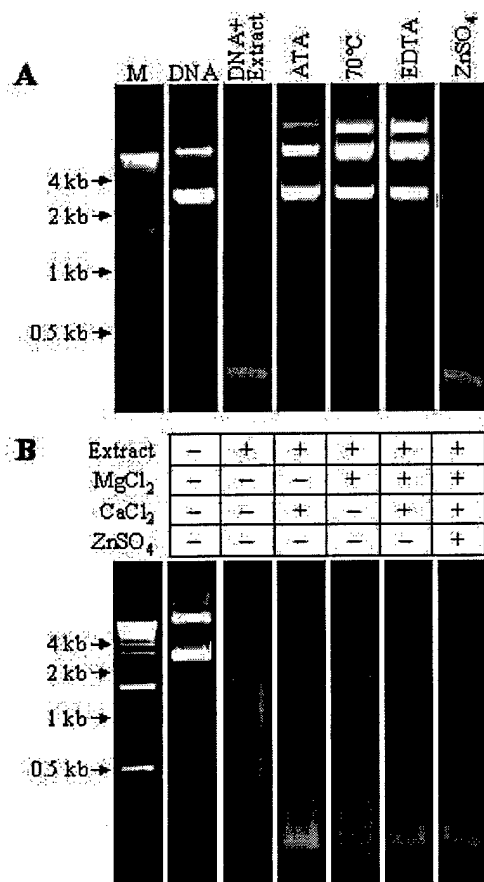


**Fig. 8** Inhibition and cation dependence of TBI induced endonuclease activity. (A) The nuclease activity in cytosolic extracts (0.5 mg/ml final concentration) from injured rat cortex isolated 72 h after TBI was assayed in the presence or in the absence of 20  $\mu$ M aurintricarboxylic acid (ATA), 10 mM EDTA, 2 mM ZnSO<sub>4</sub>, or the protein extracts were preheated at 70°C for 15 min before the reaction. The reactions were carried for 1 h at 37°C with 2  $\mu$ g of pCR2.1 plasmid DNA in the buffer consisting of 10 mM Hepes (pH7.4), 50 mM KCl, 3 mM MgCl<sub>2</sub>, 1 mM EDTA, 1 mM EGTA, 1 mM DTT, 3 mM ATP, 10 mM phosphocreatine, 50  $\mu$ g/ml creatine kinase, and 20% glycerol. The DNA was then analyzed by electrophoresis through a 1.5% agarose gel and ethidium bromide staining. (B) Cation dependence of TBI induced endonuclease activity was assayed in the presence or either 5 mM MgCl<sub>2</sub>, 5 mM CaCl<sub>2</sub>, and 2 mM ZnSO<sub>4</sub>. The reactions were carried and DNA was analyzed as described in the legend (A) for this figure. This results show that the endonuclease activity induced in rat brain cortex following TBI depends on the presence of Mg<sup>2+</sup> and Ca<sup>2+</sup>, but is not inhibited by Zn<sup>2+</sup>.

## CONCLUSION

To address the potential role of DFF40 and DFF45 in TBI-induced apoptotic DNA degradation, we utilized DFF45 knockout mice, which lack DFF40 nuclease activity. Western blot analysis demonstrated that expression of DFF40 is greatly reduced in DFF45 knockout animals. This observation strongly supports a role of DFF45 as a molecular chaperone for DFF40 protein expression *in vivo*. To investigate a role for DFF40 in TBI-induced DNA fragmentation in brain cortex, we examined the extent of DNA degradation in samples from wild type and DFF45 knockout mice. Qualitative analysis of DNA fragmentation suggested that this process was delayed in knockouts. Experiments with primary cortical neuronal cultures also showed delayed DNA degradation in neurons from DFF45 knockouts after treatment with etoposide, as compared to wild type controls. However, treatment of cultured DFF45 knockout neurons with staurosporine failed to induce DNA laddering even after prolonged incubation time. These results indicate that although DFF40 may participate in apoptotic DNA degradation in neurons, other nucleases also are involved and may play a more predominant role in certain models of neuronal apoptosis.

We examined TBI-induced deficits in learning and working memory in the DFF45 knockout and wild type groups of mice. No significant differences between the groups were found with regard to



latency to find the submerged platform, although latencies for the working memory task performed on days 21-23 were consistently longer in the knockout mice. We also applied the MRI technique for measuring of the injured brain tissue volumes following traumatic brain injury in DFF45 knockout and wild type mice. No significant difference in lesion volumes was found between the groups, although there was a trend towards larger lesions in the DFF45 knockouts.

We have previously reported that activation of caspase-3 is necessary for TBI-induced DNA fragmentation in rat brain cortex. Using an *in vitro* reconstitution system, we demonstrated that cleavage of DFF45 by caspase-3 is not sufficient for DNA fragmentation induced by protein extracts from rat brain cortex. The results indicate that activation of enzymes other than caspase-3 and DFF40 may be essential for chromatin degradation during apoptosis in adult brain after TBI.

Finally, we characterized the ion dependence of endonuclease activity induced in rat brain cortex following TBI. This activity depends on the presence of divalent cations such as  $Mg^{2+}$  and  $Ca^{2+}$ , but is not inhibited by  $Zn^{2+}$ . This ion dependence of our "cortical" endonucleases differs from that of both DFF40 and characterized CMEs. Taken together, our results suggest that distinct endonucleases may contribute to genome degradation caused by brain trauma.

## **PROJECT 2. DIFFERENTIAL EXPRESSION OF APAF-1 AND CASPASE-3 GENES AND SUSCEPTIBILITY TO APOPTOSIS DURING BRAIN DEVELOPMENT AND AFTER TRAUMATIC BRAIN INJURY.**

### **Introduction**

Recent studies have established a role for apoptosis in neuronal loss following stroke, spinal cord or traumatic brain injury (TBI). Furthermore, clinical data suggest that outcomes and mortality after acute brain injury are age-dependent, with more severe responses in infants than in adults. Such differences in response to injury may be explained, in part, by differential susceptibility to apoptosis and associated caspase-3 activity in brain as a function of developmental age. However, the molecular mechanisms underlying such age-dependent differences in apoptotic response to neuronal injury have not been identified. Because caspase-3 appears to be the major executioner caspase involved in neuronal apoptosis, we hypothesized that suppression of apoptotic capability during maturation of mammalian brain results from repression of genes involved in the caspase-3 activation pathway, and that injury-induced neuronal apoptosis in the mature brain results from reactivation of these genes.

Two major caspase-3 activating pathways have been identified — an extrinsic pathway involving cell-surface receptors and an intrinsic pathway resulting from alterations at the level of the mitochondrion and activation of the apoptosome. The intrinsic pathway can be triggered by a variety of proapoptotic stimuli and is initiated by release of cytochrome c from mitochondria to the cytosol. In the presence of ATP (or dATP), cytochrome c binds to the cytosolic adaptor protein, apoptotic protease-activating factor-1 (Apaf-1). Binding of cytochrome c to Apaf-1 allows the recruitment and activation of caspase-9 within the apoptosome. Caspase-9 and Apaf-1 bind to each other via their respective N-terminal Ced-3 homologous domains. This event leads to caspase-9 activation. Active caspase-9, in turn, activates executioner caspases-3 and -7. Activated caspase-3 is required for the activation of four other caspases (-2, -6, -8, and -10) in this pathway and also participates in a feedback amplification loop involving caspase-9. Here, we evaluated the role of the intrinsic pathway in neuronal apoptosis at

different stages of rat brain development and during maturation of primary cortical neurons *in vivo*, as well as in response to brain injury.

## RESULTS

To assess effectiveness of the cytochrome c-dependent caspase-3 activation pathway in rat brain at different stages of development, we used a well-established assay of reconstitution of cytochrome c-dependent caspase-3 activation *in vitro*. Cytochrome c and dATP are necessary for the oligomerization and binding of Apaf-1 to procaspase-9 followed by autoactivation of this caspase. Active caspase-9, in turn, cleaves and activates downstream caspases including caspase-3. Therefore, we incubated cell-free cytosolic extracts isolated from rat brain cortex on embryonic day 17 (E17) or postnatal days 2, 7, 14, and 60 (P2-60) in the absence or presence of cytochrome c, and dATP. As an outcome, we used a fluorogenic substrate assay to measure caspase-3-like (DEVDase) enzyme activity levels in the cortical extracts (Fig. 9A). High levels of cytochrome c-induced DEVDase activity were found in extracts from E17 and P2 rat cortex with no considerable difference between these two age groups. In contrast, activity of DEVDase in P7 protein extracts decreased to approximately 65% of embryonic and neonatal level. DEVDase activity in P14 extracts decreased further reaching nearly 10% of E17 and was not detected in extracts from mature (P60) brain. No DEVDase activity was detected also in extracts preincubated in the absence of cytochrome c (Fig. 9A).

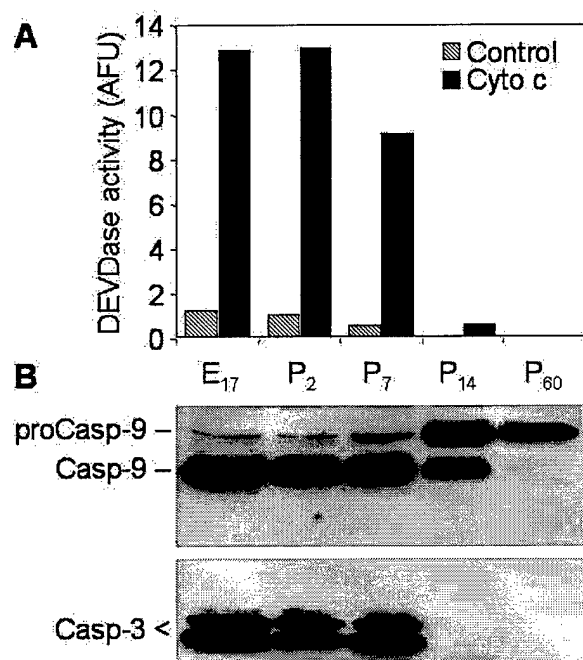


**Fig. 9** Age-dependent susceptibility of cytosolic protein extracts from rat cortex to cytochrome c/dATP-dependent activation of caspase-3. (A) Fifty  $\mu$ g aliquots of cytosolic protein extracts isolated from cortex of embryonic (E, day 17) or postnatal (P, days 2, 7, 14, and 60 after birth) rat brains were incubated in the presence or absence of cytochrome c and dATP in caspase activation buffer as described in "Materials and Methods". Caspase-3-like activity in treated and control extracts was assayed fluorometrically by measuring the accumulation of free AMC resulted after cleavage of Ac-DEVD-AMC. Protease activity is expressed in arbitrary fluorescence units (increase of fluorescence per minute). (B) Fifty  $\mu$ g aliquots of cytosolic extracts were treated as described in Figure 1A, subjected to 12% SDS-PAGE and transferred to a nitrocellulose filters. The filters were probed with a monoclonal anti-caspase-9 antibody (clone 5B4, MBL, Japan) or with a rabbit polyclonal antibody against p17 cleaved form of caspase-3.

Because cytochrome c-dependent activation of caspase-3 requires activation of caspase-9, we next examined cleavage of these two caspases by Western blot analysis. Using a monoclonal 5B4 anti-caspase-9 antibody (MBL, Japan) that recognizes both rat procaspase-9 and its large subunit we observed nearly complete cleavage of procaspase-9 in E17, P2, and P7 extracts (Fig.9B). The degree of caspase-9 cleavage was markedly decreased in P14 extracts and was not detected in P60 extracts. Using a polyclonal anti-caspase-3 antibody from Cell Signaling Technology that recognize only the p20 and p17 cleaved fragments we found that, consistent with results of DEVDase activity assay, caspase-3 was

cleaved to its active form in E17, P2, and P7 but not in P14 or P60 extracts (Fig. 9B). Similar age-dependent changes in cytochrome c-dependent apoptotic susceptibility were found in developing mouse brain (data not shown).

In order to identify a potential molecular basis for observed age-dependent change in cytochrome c-dependent apoptotic potential, we examined expression of each component of the apoptosome during rat brain development at mRNA and protein levels. mRNA levels were estimated by RT-PCR analysis. These experiments were based on the available rat Apaf-1, caspase-3, and caspase-9 mRNA sequences (GenBank accession numbers NM023979, U58656, and AF262319, correspondingly). RT-PCR experiments revealed that Apaf-1 and caspase-3 mRNA levels decreased markedly in the rat cortex between 1 week and 2 weeks after birth, and were sustained at these levels in the mature brain (Fig. 10A). In contrast, caspase-9 mRNA expression was not significantly changed during development.

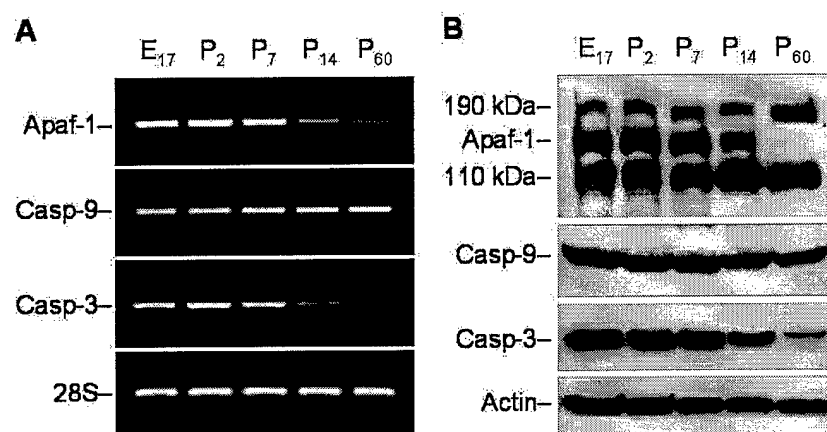


**Fig. 10** Analysis of age-dependent expression of Apaf-1, caspase-9, and caspase-3 mRNA and proteins in rat cortex. (A) RT-PCR analysis of the abundance of transcripts encoding rat Apaf-1, caspase-9, and caspase-3 in cortex of embryonic (E 17) or postnatal (P2-60) rat brains. Total RNA from rat cortex on the indicated days of development was subjected to RT-PCR with primers specific for Apaf-1, caspase-9, or for caspase-3. Amplification of 28S rRNA was used as an internal control. The PCR products were analyzed by electrophoresis through an agarose gel and visualized after staining with ethidium bromide. (B) Western blot analysis of the abundance of Apaf-1, procaspases-9 and -3 in the protein extracts isolated from rat cortex on the indicated days of rat development. Eighty  $\mu$ g aliquots of cytosolic protein extracts isolated from rat brain cortex at indicated developmental stages were subjected to 5% (Apaf-1) or 12% SDS-PAGE and transferred to a nitrocellulose filter. The filters were probed with a polyclonal anti-Apaf-1 antibody (#AB16941, Chemicon International), a monoclonal anti-caspase-9 antibody (clone 5B4, MBL, Japan), or with a rabbit polyclonal antibody against caspase-3 (H-277, Santa Cruz Biotechnology).  $\beta$ -Actin protein abundance was used as an additional control for gel loading and transfer. These experiments were repeated four times with similar results.

To examine if the observed decrease of caspase-3 and Apaf-1 mRNA correlated with decreased expression of the corresponding proteins, we estimated Apaf-1, procaspase-3, and procaspase-9 protein expression in rat cortex at the same times in rat brain development. Protein expression was assayed by Western blot analysis. Identification of procaspase-3 and procaspase-9 was performed by staining with H-277 and 5B4 antibodies (Santa Cruz Biotechnology and MBL, correspondingly) that, in each case, recognized a major protein band of a predicted molecular weight. Among a number of anti-Apaf-1 antibodies tested in this study, only a polyclonal rabbit antibody (#AB16941, Chemicon International) recognized a band of ~140 kDa corresponding to predicted molecular weight of rat Apaf-1 (140 kDa), while the rest of tested antibodies stained a ~110 kDa-protein of unknown origin. Specificity of this antibody was confirmed in preliminary experiments where immunostaining of Apaf-1 in rat brain samples was compared with staining of Apaf-1 preparations purified from bovine thymus (Fig. 11).

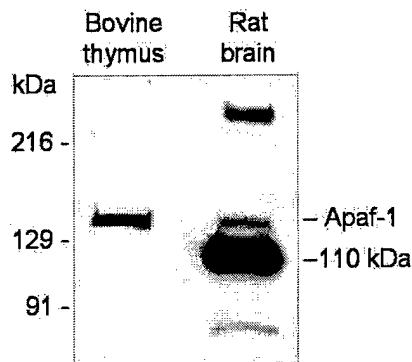


**Fig. 11** Analysis of the anti-Apaf-1 antibody specificity. Fifty  $\mu$ g of cytosolic proteins from 7 days old rat cortex and 10 ng of Apaf-1 purified from bovine thymus were separated in 5% SDS-PAGE followed by staining with a polyclonal antibody (#AB16941, Chemicon International). The preparation of purified bovine Apaf-1 was also tested in the *in vitro* reconstitution system with cytochrome c and demonstrated high Apaf-1 specific activity (data not shown). Results show location of the Apaf-1 protein band above the extensively stained 110 kDa protein of unknown origin.

As shown in Figure 10B, levels of both Apaf-1 and caspase-3 proteins in cortical extracts were markedly decreased after 1 week of age, and were minimal in the mature tissue. In contrast, no significant changes in caspase-9 protein expression were detected in this experiment.

To investigate further age-dependent changes in neuronal susceptibility to apoptosis, we analyzed level of Apaf-1 protein expression, cytochrome c-mediated caspase-3 activation, and etoposide-induced cell death in primary rat cortical neurons cultured for 1 or 14 days *in vitro* (DIV). Western analysis showed that Apaf-1 expression was clearly decreased in 14 DIV primary neurons compared to 1 DIV cells, a result consistent with Apaf-1 protein expression in developing rat cortex (Fig. 12A). Incubation of cytosolic extracts from 1 DIV primary neurons in the presence of cytochrome c and dATP led to marked activation of caspase-3; in contrast, activation of caspase-3 in extracts from 14 DIV neurons was approximately 5 fold lower than in 1 DIV extracts (Fig. 12B). Similar differences in levels of caspase-3 activity were observed in the cytosol from primary neurons treated with etoposide: 5h treatment of 1 DIV cells resulted in activity of caspase-3 corresponding to  $18.7 \pm 0.4$  AUF; in contrast activity in 14 DIV extracts was only  $4.7 \pm 0.1$  AUF (Fig. 12C). Changes in caspase-3 activity in the etoposide-treated neurons correlated inversely with the degree of cell survival. After 24 h incubation of 1 DIV neurons with etoposide,  $45 \pm 6\%$  of cells survived, whereas in 14 DIV cultures  $79 \pm 5\%$  cells were viable (Fig. 12D).

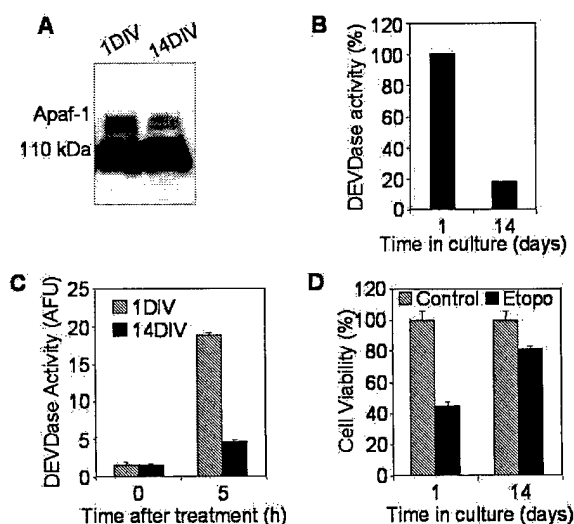


**Fig. 12** Analyses of Apaf-1 expression, cytochrome c-inducible apoptotic potential, and cell viability in 1 DIV and 14 DIV primary cultures of rat cortical neurons. (A) One hundred  $\mu$ g of cytosolic proteins from 1DIV or 14 DIV primary rat cortical neurons were separated in 5% SDS-PAGE followed by staining with an Apaf-1 antibody (Chemicon International). (B) Protein extracts from 1 DIV or 14 DIV primary rat cortical neurons were incubated in the presence of cytochrome c and dATP as described in "Materials and Methods". Caspase-3-like activity was assayed fluorometrically by measuring the accumulation of free AMC resulted after cleavage of Ac-DEVD-AMC. Data are expressed as percent of 1 DIV induced caspase activity. (C) 1 DIV or 14 DIV primary rat cortical neurons were treated with 50  $\mu$ M etoposide for 5 h. Control cultures (0 h) served as negative controls. Caspase-3-like activity in cytosolic extracts from treated or control cells was assayed fluorometrically. Protease activity is expressed in arbitrary fluorescence units  $\pm$  SD (n=6). \* $p < 0.0001$ , compared with caspase-3 activity in etoposide-treated 1DIV cells, by ANOVA, followed by Dunnett's test. (D) 1 DIV or 14 DIV primary neurons were treated with 50  $\mu$ M etoposide for 24 h, and cell viability was analyzed by measurement of calcein AM fluorescence. Data are expressed as a percentage of the value for control cells not exposed to etoposide  $\pm$  SD (n=6)\* $p < 0.0001$ , compared with viability of 1DIV cells after 24h etoposide treatment, by ANOVA, followed by Dunnett's test.

Our previous report suggested that brain trauma in rats results in activation of caspase-3 (Yakovlev et al., 1997). Because activation of caspase-3 results from specific cleavage of the precursor protein, we examined such cleavage of caspase-3 using Western analysis as a function of time after TBI. Consistent with previous findings, low levels of the cleaved forms of caspase-3 were detected beginning 4h after trauma, but increased markedly at 48h after injury (Fig. 13).

Because apoptotic potential in mature brain tissue is repressed and such repression may be predetermined by downregulation of both Apaf-1 and caspase-3 gene expression, we hypothesized that elevation of caspase-3 activity after TBI may require reactivation of these genes in the mature brain. In part, this hypothesis is supported by results of our previous studies where we found that TBI results in early increase in caspase-3 mRNA content in the injured brain regions. In this study, we examined protein expression of procaspase-3 in injured cortex as a function of time after brain trauma. Using Western blot analysis we found that procaspase-3 protein levels were elevated in injured cortex by 4-to-72 hr after TBI (Fig. 14A).

Because of the limitations of Western blot for quantitative analysis of protein expression, we examined if the apparent increase in procaspase-3 after TBI leads to an increase in corresponding caspase activity after experimental cleavage by active recombinant caspase-9. As shown in Figure 14B, TBI induced a significant elevation of caspase-9-mediated caspase-3 activity in extracts from injured cortex. A 1.5 fold increase in caspase-9-dependent caspase-3 activation was observed in extracts isolated from injured cortex 4 h after TBI. This induced activity was further increased at later time points after TBI, exceeding twice control levels by 2 days after injury. No such changes in caspase-3 activity were detected in contralateral brain regions (data not shown).

**Fig. 13** TBI-induced specific cleavage of procaspase-3 in rat brain cortex. Eighty  $\mu$ g aliquots of cytosolic protein extracts isolated from sham-control or traumatized rat cortex at indicated times after TBI were subjected to 12% SDS-PAGE and transferred to a nitrocellulose filter. The filter was probed with a rabbit polyclonal antibody against p17 cleaved form of procaspase-3 (Cell Signaling Technology). Significant increase in caspase-3 cleavage is observed at 48 h after injury.

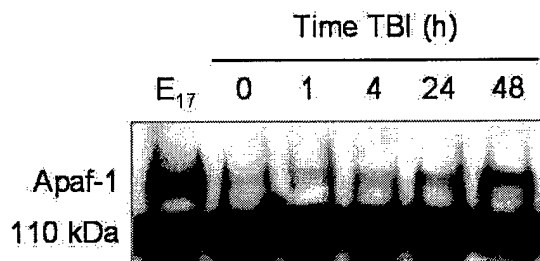
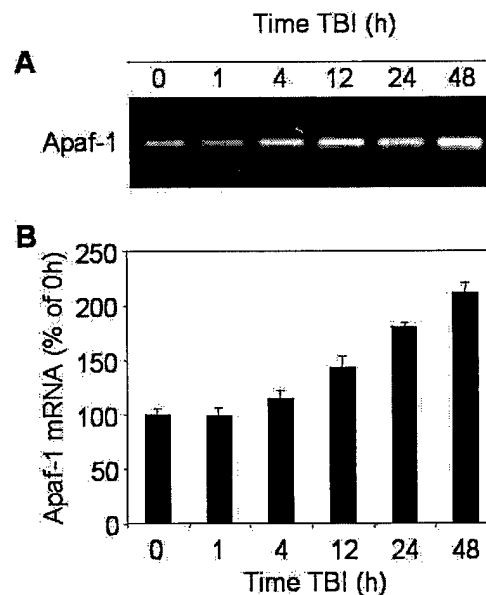


**Fig. 14** A time-course of procaspase-3 protein expression in rat brain cortex after TBI. (A) Fifty  $\mu$ g aliquots of cytosolic protein extracts isolated from sham-control or traumatized rat cortex at indicated times after TBI were subjected to 12% SDS-PAGE and transferred to a nitrocellulose filter. The filter was probed with a rabbit polyclonal antibody against caspase-3 (H-277, Santa Cruz Biotechnology). The antigen-antibody complexes were visualized by an ECL method as described under "Material and Methods." (B) Fifty  $\mu$ g aliquots of cytosolic protein extracts isolated from sham-control or traumatized rat cortex at indicated times after TBI were incubated with or without active recombinant human caspase-9 (20 U, Biomol) in 50  $\mu$ l of caspase activation buffer at 37°C for 1 h. Caspase-3-like activity was assayed fluorometrically by measuring the accumulation of free AMC. Protease activity is expressed as a percent of the activity in sham-operated control extracts.



Injury-induced increases in caspase-3 protein expression observed in this study are consistent with increases in activity of this caspase after TBI. On the other hand, activation of caspase-3 requires prior activation of caspase-9 within the apoptosome. We found that in the mature brain this pathway is repressed, in part, due to downregulation of Apaf-1 expression. Therefore, we hypothesized that neuronal injury may lead to reactivation of intrinsic pathway of apoptosis via reactivation of Apaf-1 gene expression. To test this hypothesis at functional level, we first examined whether specific cleavage caspase-9 could be detected after TBI. This was assessed by Western analysis of cortical protein extracts in time course after trauma.

Amino acid sequence analysis of the rat procaspase-9 revealed that, like human procaspase-9, it contains a SEPD potential autoactivation cleavage site and a DQLD caspase-3 recognition site. Correspondingly, cytochrome c-mediated autoactivation is expected to produce 39 kDa large subunit recognizable by the antibodies, whereas, a 41 kDa large fragment is expected after cleavage with caspase-3 (Fig. 15). Indeed, treatment of P17 cortical extracts with cytochrome c and dATP resulted in cleavage of caspase-9 corresponding to the 39 kDa subunit, whereas treatment of the extracts with recombinant active rat caspase-3 (Alexis) primarily resulted in appearance of 41 kDa fragment. Notably, processing of procaspase-9 by caspase-3 was less efficient compared to that by cytochrome c treatment (Fig. 15).

Western blot analysis of protein samples of injured cortex showed accumulation of the 39 kDa caspase-9 subunit after TBI. At 48h after injury, the 41 kDa caspase-9 fragment also became apparent, reflecting increased caspase-3 activity in the samples at this time point (Fig. 15). Injury-induced cleavage of procaspase-9 at autoactivation specific site presumes that injury reactivates the apoptosome complex, which, as we show here, is normally repressed in the mature brain. Therefore, we next examined whether expression of Apaf-1 mRNA and protein are affected by TBI.

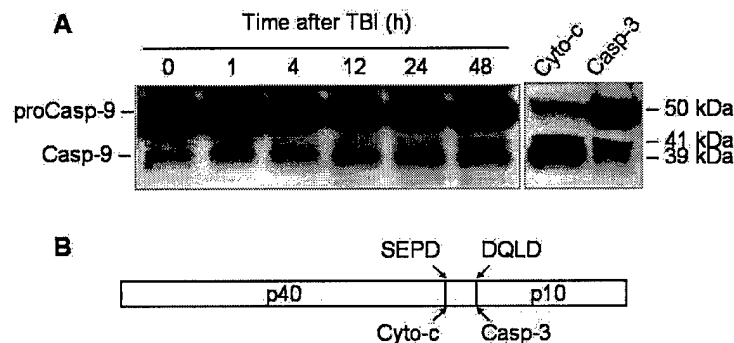


**Fig. 15** TBI induces time-dependent cleavage of procaspase-9 in rat brain cortex. (A) Eighty  $\mu$ g aliquots of cytosolic protein extracts isolated from sham-control or traumatized rat cortex at indicated times after TBI were subjected to 10% SDS-PAGE and transferred to a nitrocellulose filter. As a positive control for cleavage specificity, 80  $\mu$ g aliquots of protein extracts from 2 days-old rat cortex were preincubated in presence of either recombinant active rat caspase-3 (20 U, Alexis) or cytochrome c and dATP for 1 h at 37°C. The filter was probed with a monoclonal antibody against caspase-9 (clone 5B4, MBL, Japan). The antigen-antibody complexes were visualized by an ECL method as described under "Material and Methods." (B) A schematic diagram illustrating processing of procaspase-9. Procaspase-9 is processed preferentially at SEPD site within the apoptosome and at DQLD site by caspase-3 to generate the large subunit (p40) and small subunit (p10) of mature caspase-9.

Results of semi-quantitative RT-PCR showed that Apaf-1 mRNA content increased in the injured cortex reaching  $143\% \pm 10\%$  of control (sham) levels by 12h,  $180\% \pm 5\%$  by 24h, and  $211\% \pm 9\%$  by 48h after TBI (Fig. 16A and 16B). Furthermore, Western blot revealed increased intensity of Apaf-1 protein band in cortical extracts isolated 24h after injury, with a peak expression at 48h (Fig. 17).

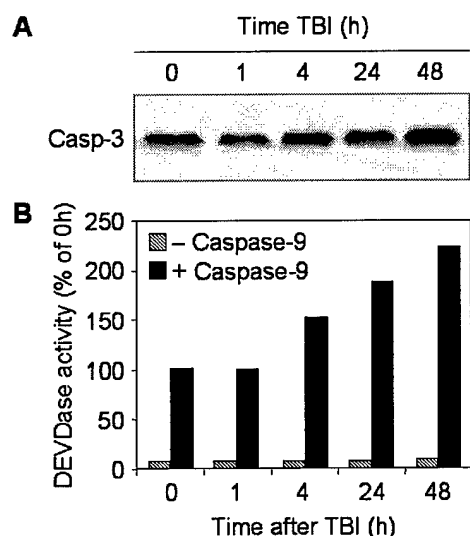


**Fig. 16** The time course of Apaf-1 mRNA expression in rat cortex at indicated times after TBI or in sham-operated controls (0 h). (A) Levels of mRNA were measured by using semiquantitative RT-PCR as indicated under "Material and Methods". (B) Levels of Apaf-1 mRNA are expressed as the proportion of individual RT-PCR product mean optical density to GAPDH RT-PCR product optical density of the same RNA sample. mRNA content is expressed as a percentage of sham controls  $\pm$  SEM (n=5). \*p < 0.05; \*\*p < 0.005, compared with control, by ANOVA, followed by Dunnett's test.

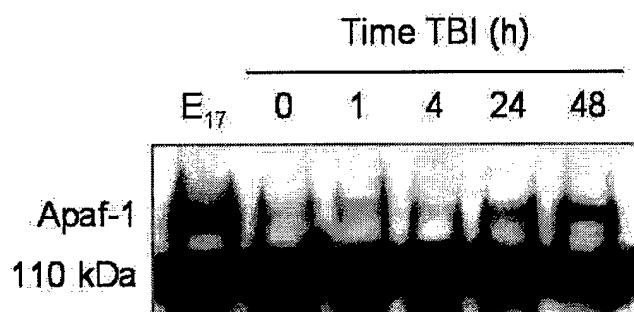


**Fig. 17** TBI induces time-dependent increase in Apaf-1 protein content in rat brain cortex. Eighty  $\mu$ g aliquots of cytosolic protein extracts isolated from rat brain cortex at the embryonic day 17 (E17) or from sham-control (0 h) or traumatized rat cortex at indicated times after TBI were subjected to 5% SDS-PAGE and transferred to a nitrocellulose filter. The filter was probed with a rabbit polyclonal antibody against human Apaf-1 (Chemicon, #AB16941).

## CONCLUSION

Using an *in vitro* system, we demonstrated that the ability of cytochrome c to induce activation of caspase-3 was decreased during maturation of rat brain and was undetectable by the caspase activity assay and by Western blot in rat (and mouse, data not shown) brain samples after 2 weeks of age. This observation is consistent with recent reports on age-dependent differences in injury-induced caspase-3 activation and susceptibility to apoptosis in mammalian brain.

Results of Western blot experiments showed that age-dependent declines in cytochrome c-dependent activation of caspase-3 in rat brain cortex paralleled the extent of procaspase-9 processing in the *in vitro* assay. This suggests that repression of cytochrome c-dependent apoptotic potential might be regulated at the level of the apoptosome. To address this issue, we analyzed Apaf-1, caspase-9, and caspase-3 gene expression as a function of developmental age. We found that mRNA and protein

expression for both Apaf-1 and caspase-3 were markedly decreased in rat cortex during brain development. The age-dependent decrease in caspase-3 mRNA content in rat brain tissue is consistent with previously published data. Profiles of both Apaf-1 and caspase-3 gene expression were comparable to the developmental profile of cytochrome c-mediated caspase-3 activation in rat brain. Interestingly, caspase-9 gene activity, at both mRNA and protein levels, did not change notably during brain development, suggesting that activation of this caspase in the brain may depend on the Apaf-1-mediated pathway. Developmental downregulation of caspase-3 gene activity may serve as a supplementary mechanism that protects the mature brain from apoptosis initiated by other caspases, such as caspase-8, -11, or -12.

Because of poor specificity of available anti-Apaf-1 antibodies, we were not able to examine directly whether downregulation of Apaf-1 during brain maturation occurs in neurons. Therefore, we examined Apaf-1 protein expression, cytochrome c-dependent activation of caspase-3, and etoposide-induced apoptosis in primary rat cortical neurons cultured for 1 day or 14 days *in vitro*. Both Apaf-1 expression and apoptosome-mediated activation of caspase-3 were markedly decreased in 14 DIV neurons. Decreased levels of caspase-3 activity and highly significant reduction of associated apoptosis were also found in neurons at 14 DIV (vs. 1 DIV) treated with etoposide. In transfection studies using dominant negative mutant constructs of caspase-8 and caspase-9, we have demonstrated that etoposide-induced apoptosis in rat primary cortical neurons, as well as in the SH-SY5Y neuroblastoma cell line, proceeds through a caspase-9-dependent pathway (data not shown). Collectively these data support the hypothesis that neuronal maturation *in vitro* leads to repression of cytochrome c-dependent apoptotic susceptibility and that this process parallels to decrease in Apaf-1 protein expression in rat cortical neurons.

Given the present findings and previous observations that brain injury causes activation of caspase-3 and related neuronal apoptosis, we examined whether TBI recapitulates apoptotic potential via coordinated reactivation of caspase-3 and Apaf-1 genes. Increased caspase-3 mRNA levels following neuronal injury have been demonstrated previously in various models of apoptosis, including TBI; however, changes in procaspase-3 protein levels have not been reported. Therefore, we examined expression of procaspase-3 protein as a function of time after brain trauma, using Western analysis and by measuring caspase-9-induced caspase-3 activity in extracts from injured cortex. Both techniques showed a marked increase of procaspase-3 after TBI. Preliminary analysis of caspase-8 cleavage and activation in cortical protein extracts after brain injury did not suggest a role for caspase-8 in TBI-induced cell death (data not shown). In contrast, brain trauma resulted in accumulation of cleavage fragments of caspase-9 in rat cortex after injury that paralleled activation-specific cleavage of caspase-3.

Given the repression of Apaf-1 in normal mature brain cortex, we examined whether its levels were increased after brain injury. RT-PCR and Western blot showed that Apaf-1 mRNA and protein content were substantially increased after fluid percussion-induced TBI, as compared to sham-injured controls.



**DRUG DISCOVERY AND DESIGN:** Dr. Kozikowski's work relates to the design and synthesis of new pharmacological research tools for understanding brain mechanisms, including cognitive drug development. Dr. Wang utilizes molecular modeling techniques as part of drug development, as well as studies relating to structural biology.

**ALAN P. KOZIKOWSKI, Ph.D.**

**Rational Design and Synthesis of a Novel Selective CPP 32 Inhibitor**

Apoptosis is highly conserved mechanism by which eukaryotic cells commit suicide. Excessive or failed apoptosis is a prominent morphological feature of several human diseases. Its prevalence makes it both a tempting and a troublesome target for therapeutic treatments.<sup>1</sup> The caspases (Cysteiny ASPartic proteASES) appear to be the key mediators in programmed cell death.<sup>2</sup> Thus, inhibitors of casepases may be of therapeutic value in the treatment of inflammatory and neurodegenerative diseases.<sup>3</sup>

The tetrapeptide aldehyde AcDEVD-CHO (**1**) (designed to mimic the CPP32/apopain recognition site within poly(ADP-ribose)polymerase(PARP) is a very potent inhibitor of CPP32/apopain.<sup>4</sup> Both crystal structure<sup>5</sup> and structure-activity studies<sup>6</sup> indicate that the P2 amide nitrogen is not utilized in a hydrogen bonding interaction with the enzyme, and that the backbone conformation of the bound inhibitor may allow for the introduction of conformational constraints from this amide nitrogen to either the P2 or P3 side chains. Recently, we prepared compound **2** and in collaboration with the Merck group found this compound to possess excellent inhibitory potency and selectivity for CPP32. Although these peptide inhibitors have served as important pharmacological tools, they are of limited utility for advanced drug development due to their metabolic instability and membrane impermeability.

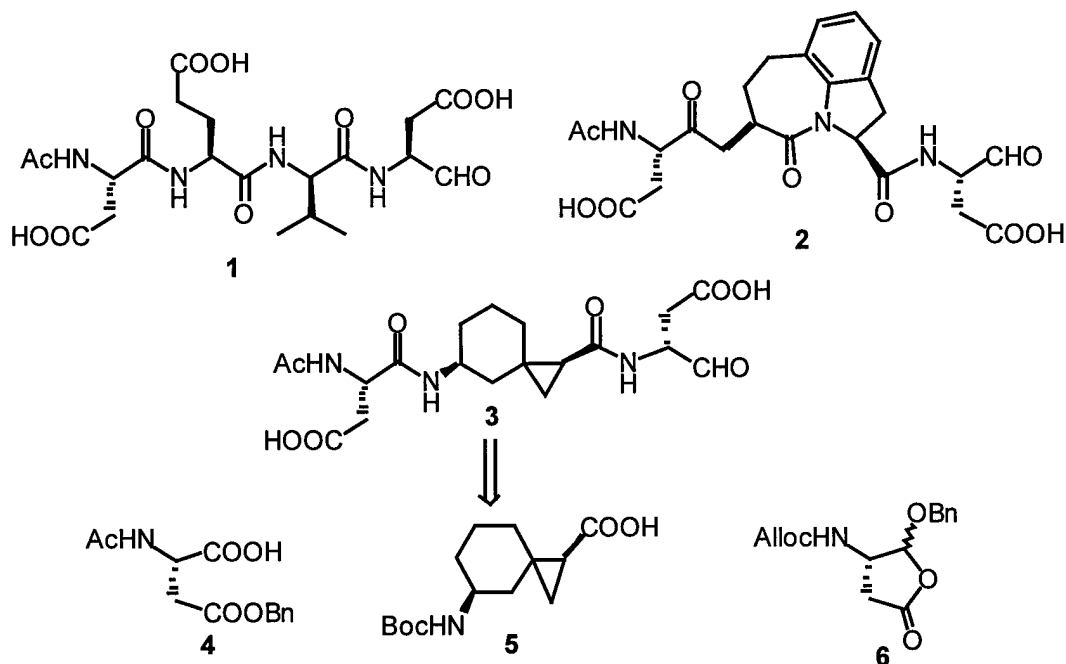
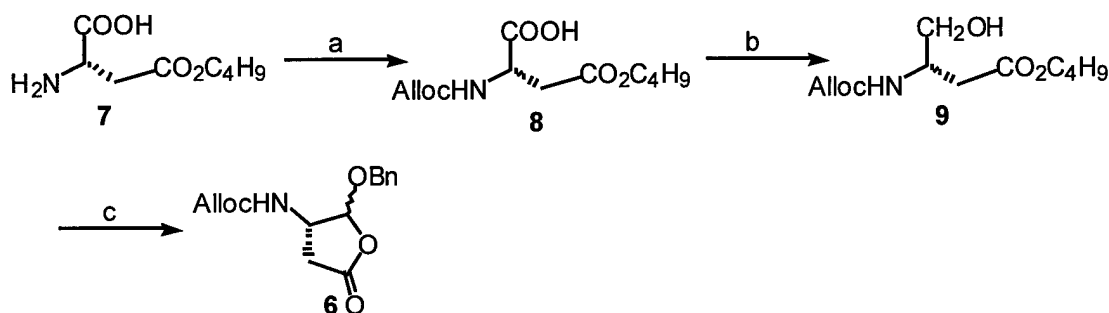


**Figure 1.** Structures of caspase inhibitors and retrosynthetic analysis of our designed inhibitor **3**.

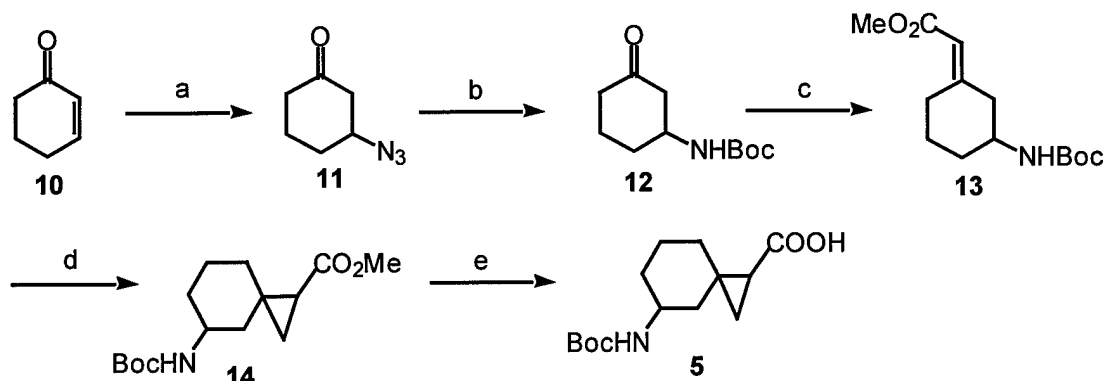
In order to make further advances in this field of caspase inhibitors, it has been our intention to identify other turn mimics that may replace the tricyclic portion of **2** (thus allowing for altered caspase selectivity), with the eventual goal of deleting all amide bonds from the final inhibitor structure. Our initial strategy for the design of such a caspase inhibitor was therefore to keep the P1 and P4 Asp residues and to first find a non-peptidic replacement for inner tricyclic segment of **2** that has approximately the same shape when bound to the enzyme. Based on our modeling studies compound **3** was identified as a possible mimic of compound **2**. Initially, we planed to synthesize the racemic **3** for its biological assay. According to our retrosynthetic plan, compound **3** gave rise to the three building blocks **4**, **5** and **6** (Fig.1).

The protected aspartic acid aldehyde **6** was synthesized as delineated in Scheme 1. Commercially available aspartic acid- $\beta$ -*tert*-butyl ester **7** was N-protected with allylchloroformate in the presence of  $\text{NaHCO}_3$ . The carboxylic acid **8** was then converted to an anhydride and reduced to the corresponding alcohol **9** with sodium borohydride. The alcohol **9** was oxidized to the aldehyde under Swern conditions and immediately treated with benzyl alcohol and PTSA in the presence of 3A° molecular sieves. After 16h, addition of TFA to this solution effected cyclization to the desired O-benzylacetal **6**, which was isolated as 1:1 mixture of diastereomers.<sup>7</sup>



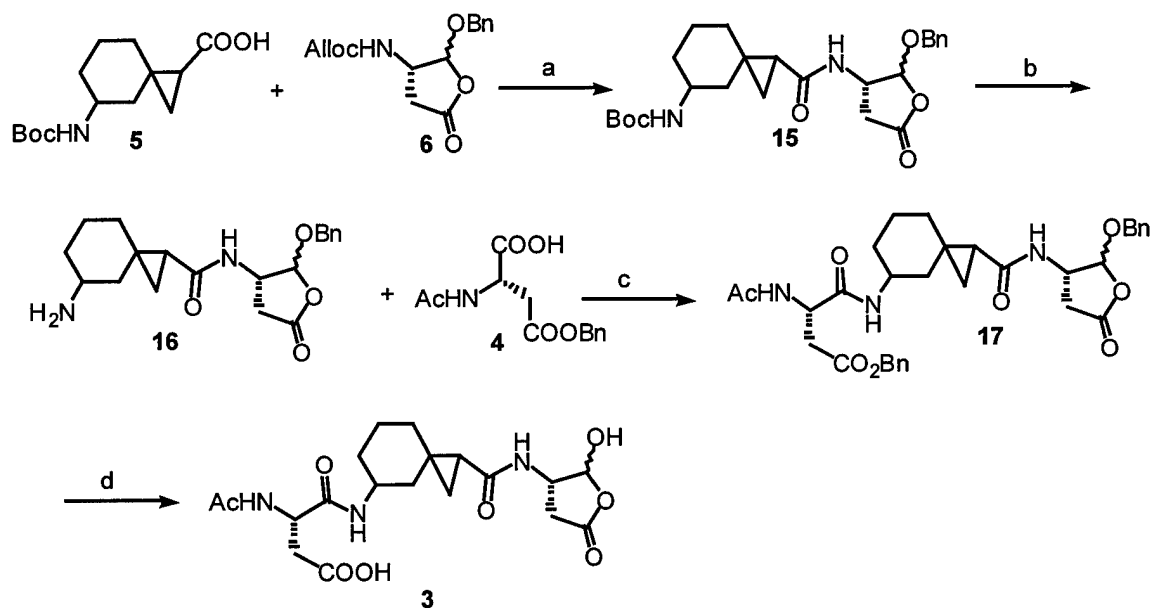
**Scheme 1.** Reagents and conditions: (a) allylchloroformate,  $\text{NaHCO}_3$ , THF,  $\text{H}_2\text{O}$ , 12h, rt, 68%, (b) (i) Isobutyl chloroformate, NMM, THF, 0 °C, 0.5h, (ii)  $\text{NaBH}_4$ , MeOH, -78 °C, 2h, 70%, (C) (i)  $(\text{COCl})_2$ , DMSO, DIEA, -78 °C, 0.5h, (ii) BnOH, PTSA,  $\text{CH}_2\text{Cl}_2$ , 15h, then TFA 0.5h, 74%.

The synthesis of spiro-amino acid **5** is presented in Scheme 2. Cyclohexenone **10** underwent 1,4 conjugate addition with  $\text{TMS-N}_3$  in the presence of AcOH to afford the azido-ketone **11**. Compound **11** was converted to the protected amino-ketone **12** by catalytic hydrogenation and in situ protection using  $(\text{Boc})_2\text{O}$ . The ketone **12** was then subjected to olefination under Wittig-Horner reaction conditions in the presence of NaH and  $(\text{MeO})_2\text{P}(\text{O})\text{CH}_2\text{CO}_2\text{Me}$  to yield the  $\alpha,\beta$ -unsaturated ester **13**. Cyclopropanation of **13** with  $(\text{CH}_3)_3\text{SOI}$  in the presence of NaH afforded compound **14** which was hydrolyzed to acid **5**.



**Scheme 2.** Reagents and conditions: (a) TMS-N<sub>3</sub>, AcOH, DBU, CH<sub>2</sub>Cl<sub>2</sub> 7h, rt., 92%, (b) Pd/C, (Boc)<sub>2</sub>O, EtOH, rt., 5h, 82%, (c) (MeO)<sub>2</sub>P(O)CH<sub>2</sub>CO<sub>2</sub>Me, NaH, THF, 6h, -78 °C to rt., 82%, (d) (CH<sub>3</sub>)<sub>3</sub>SOI, NaH, DMF, 50 °C, 3h, 73%, (e) LiOH, THF: MeOH: H<sub>2</sub>O (3:1:1), rt., 15h, 79%.

The synthesis of inhibitor 3 was completed as shown Scheme 3. Removal of the Alloc protecting group in 6 using Bu<sub>3</sub>SnH and a catalytic amount of (PPh<sub>3</sub>)<sub>2</sub>PdCl<sub>2</sub> in the presence of compound 5 followed by the addition of the coupling reagents HOBt and EDCI afforded the desired intermediate 15. The Boc group was then cleaved with TFA, and the resulting amine 16 was coupled with the protected aspartic acid 4 using the indicated coupling reagents to give 17.



**Scheme 3.** Reagents and conditions: (a) (i) Bu<sub>3</sub>SnH, (PPh<sub>3</sub>)<sub>2</sub>PdCl<sub>2</sub>, DMF, 0.5h (ii) HOBt, EDCI, 15h, 75% (b) TFA, CH<sub>2</sub>Cl<sub>2</sub>, 4h, (c) HOBt, EDCI, DMF, rt, 74% (2 steps), (d) Pd(OH)<sub>2</sub>, H<sub>2</sub>, EtOH, rt, 24h, 90%.

Hydrogenolysis of 17 using Pd(OH)<sub>2</sub> in ethanol gave peptide 3 in good yield. Preliminary biological assays reveal that the stereoisomeric mixture of 3 does indeed possess caspase inhibitory activity. Consequently, efforts are now being made to prepare this inhibitor in a stereodefined manner to allow

testing of a single isomer. The absolute stereochemistry that is required has been predicted with the aid of computer modeling (Fig. 2).

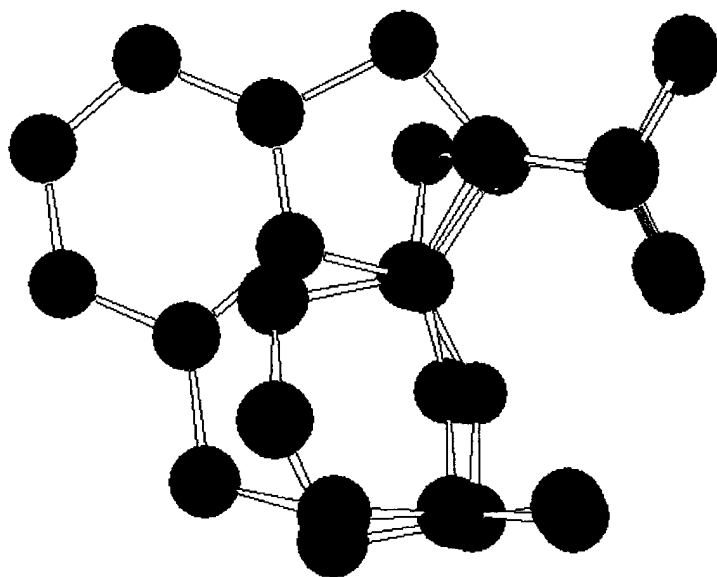


**Fig. 2** Overlay of the central portion of the newly designed caspase inhibitor **3**(red) with the tricyclic portion of **2** (blue).

## References:

1. Kerr, J.F.; Wyllie, A. H.; Currie, A. R. *Br. J. Cancer* **1972**, *26*, 239. (b) Martin, S. J., Green, D. R.; Cotter, T. G. *Trends biochem. Sci.* **1994**, *19*, 26. (c) Barr, P. J.; Tomei, L. D. *Biotechnology* **1994**, *12*, 487.
2. Schwartz, L. M.; Milligan, C. E. *Trends Neurosci.* **1996**, *19*, 388. (b) Steller, H. *Science* **1995**, *267*, 1445.
3. Talanian, R. V.; Brady, K. D.; Cryns, V. L. *J. Med. Chem.* **2000**, *43*, 3351.
4. Nicholson, D. W.; Ali, A.; Thronberry, N. A.; Vaillancourt, J. P.; Ding G, C. K.; Gallent, M.; Gareau, Y.; Griffin, P. R.; Labelle, L. Y. a.; Munday, N.A.; Raju, S. M.; Smulson, M. E.; Yamin, T. T.; Yu, V. L.; Miller, D. K. *Nature* **1995**, *376*, 37.
5. Rotona, J.; Nicholson, D. W.; Fazil, K. M.; Gallent, M.; Gareau, Y.; Labelle, M.; Peterson, E. P.; Rasper, D. M.; Ruel, R.; Vaillancourt, J. P.; Thronberry, N. A.; Backer, J.W. *Nat. Struc. Biol.* **1996**, *3*, 619.
6. Karernewsky, D. S.; Bai, X.; Linton, S. D.; Kerbs, J. F. Wu, J.; Pham, B.; Tomselli, K. J. *Bioorg. Med. Chem. Lett.* **1998**, *8*, 2757.
7. Chapman, K. T. *Bioorg. Med. Chem. Lett.* **1992**, *2*, 613.

## SHAOMENG WANG, Ph.D.

Dr. Wang is interested in computational structural biology (protein folding, drug and receptor interactions), design and discovery of novel therapeutic agents for neuroprotection.

**PROJECT 1.** Molecular modeling can be utilized to elucidate ligand/receptor interactions, with particular reference to caspases and phosphatases, and pharmacophore modeling may help to identify novel neuro-protective small molecule drugs.

### Methods/Approach:

In recent years, molecular modeling has been used to elucidate ligand/receptor interactions in atomic details. Molecular modeling can be used to characterize the active site of a receptor, to quantitatively analyze the crucial hydrophobic and hydrogen bonding interactions between a ligand and its receptor. With such atomic-detailed understanding on the molecular interactions, it is then possible to rationally design novel neuro-protective small molecule drugs for a particular molecular target such as caspases and phosphatases that play a role in programmed cell death (apoptosis).

Dr. Wang's lab has been in the forefront in molecular modeling-assisted, rational drug design research. The two key methods Dr. Wang developed and used are pharmacophore-based and structure-based approaches, as detailed below.

The first step in the pharmacophore-based drug design is the development of a pharmacophore model, which would include the crucial binding elements in a ligand and their three-dimensional geometrical relationship. Using a 3D-pharmacophore model, one can search for large 3D-chemical libraries to identify potential small molecule drugs that meet the requirements specified in the pharmacophore model. One can also use the pharmacophore model to design *de novo* small molecule drugs. Dr. Wang has been a pioneer in this field. Over the years, Dr. Wang has built several large 3D chemical databases (libraries) of more than 700,000 drug-like small molecules [1]. Using the 3D-database pharmacophore searching technique, he has discovered and designed novel ligands for protein kinase C [2], HIV-1 protease[3], HIV-1 integrase[4] and dopamine transporter [5].

Dr. Wang proposes to employ this powerful technique for the discovery of novel neuro-protective agents. In collaboration with Dr. Faden's lab, Dr. Wang is going to focus on one highly promising target PTEN for designing novel neuro-protective agents.

Another powerful and effective approach is then so-called structure-based drug design. The central idea of this approach is that using the 3D structure of the receptor, we can identify and design small molecule drugs that can fit into the active site the receptor, just like "hand-and-glove". Over the last few years, Dr. Wang has developed a number of molecular docking methods for structure-based drug design, including MCDOCK method [6]and the q-jumping method [7]. Dr. Wang proposes to use this approach for the discovery of small molecule inhibitors for PTEN as novel neuro-protective agents.

PTEN phosphatase is a tumor suppressor gene that dephosphorylates phosphatidylinositol phosphates. PTEN restrains the function of a major antiapoptotic and survival pathway involving

phosphoinositol 3-kinase (PI-3 kinase) and Akt kinase. Our major hypothesis is that small molecule inhibitors of PTEN will activate a number of kinases, including Akt and PI-3 kinases and may have neuro-protective effects. The X-ray structure of the PTEN phosphatase domain has been solved. This X-ray structure provides us the essential structural information for designing small molecule inhibitors of PTEN.

Based upon the X-ray structure, a number of pharmacophore models have been proposed. Using the pharmacophore models, Dr. Wang proposes to search through a number of large 3D-databases of over 700,000 small molecules. Furthermore, Dr. Wang proposes to use the X-ray structure to perform structure-based database searching to identify potential small molecule inhibitors for PTEN.

### **Results:**

To date, we have completed the search of the NCI-3D database of 200,000 compounds. Nearly two hundred small molecule candidates have been selected for biological testing. We have discovered 15 compounds which potently inhibit the activity of PTEN with a  $K_i$  value better than 10  $\mu$ M. In collaboration with Dr. Faden, we have selected several compounds that potent activity and good selectivity for PTEN to test their neuro-protective effects in a number of models Dr. Faden developed in his lab.

### **Future Studies:**

The discovery of novel, potent small molecule antagonists of PTEN represents a first but very exciting step toward the development of highly potent and selective PTEN antagonist as potential neuro-protective therapy. Toward this goal, we will perform structure-based design of new analogues of the lead compounds, following by chemical synthesis in our lab. Several new analogues have been designed based upon the most potent and selective lead compound. It is expected that a highly selective and potent small molecule antagonist of PTEN will be created. A potent small molecule antagonist of PTEN will not only serve as a powerful pharmacological tool to test the roles of PTEN and AKT in neuro-injury but also may have a great therapeutic potential as novel therapy for neuro-protection.

### **References:**

1. G.W.A. Milne, Marc C. Nicklaus, Wang, S., John Driscoll and Dan Zaharevitz. The NCI drug information system 3D database, *J. Chem Inf. Comput. Sci.*, **1994**, 34, 1219-1224.
2. Wang, S., Milne, G.W.A., Dan Zaharevitz, Rajiv Sharma, Victor E. Marquez, Nancy Lewin, and Peter Blumberg. The discovery of novel, structurally diverse PK-C agonists through computer 3D-database pharmacophore search. Molecular modeling studies, *J. Med. Chem.*, **1994**, 37, 4479-4489.
3. Wang, S., G.W.A. Milne, Xinjian Yan, Isadora Posey, Marc Nicklaus, and William G. Rice, Discovery of Potent, Non-peptide HIV Protease Inhibitors Through 3D-database Pharmacophore Search and Molecular Modeling Studies, *J. Med. Chem.*, **1996**, 39, 2047-2054.
4. Abhijit Mazumder, Wang, S., Nouri Neamati, Marc Nicklaus, Sanjay Sunder, Julie Chen, G.W.A. Milne, William G. Rice, and Yves Pommier, Antiretroviral Agents as Inhibitors of Both Human Immunodeficiency Virus Type 1 Integrase and Protease, *J. Med. Chem.*, **1996**, 2472-2481.

5. Wang S., Sukumar Sakamuri, S. Istvan J. Enyedy, I. J., Kozikowski, A. P., Deschaux, O., Bidhan C. Bandyopadhyay, B. C., Tella, S. R., Zaman, W. A., Kenneth M. Johnson K. M. Discovery of a novel dopamine transporter inhibitor as a potential cocaine antagonist through 3D-database pharmacophore searching. Molecular modeling, structure-activity relationships, and behavioral pharmacological studies, *J. Med. Chem.*, **2000**, 43, 351-360.
6. Liu, M. and Wang, S. MCDOCK: A New Monte Carlo Docking Method for Molecular Docking Problem, *J. Computer-Aided Molecular Design*, **1999**, 13, 435-451.
7. Pak, Y. and Wang, S. Application of a new molecular dynamics simulation method with a generalized effective potential to the flexible docking problems. *J. Physical Chemistry (B)*, **2000**, 104, 354-359.
8. Rotonda, J., Nicholson, D. W., et al. The three-dimensional structure of apopain/CPP32, a key mediator apoptosis. *Nat. Struct. Biol.* **1996**, 3, 619.
9. Lee, et al. Crystal structure of the PTEN tumor suppressor: Implication for its phosphoinositide phosphatase activity and membrane association. *Cell*, **1999**, 99, 323-334.

**PROJECT 2.** Molecular dynamics simulation can be used to elucidate the folding and mis-folding mechanism of amyloid (1-42) in Alzheimer's Disease (AD), and such information can be used to identify potential small molecule drugs that can prevent conversion of the amyloid from the  $\alpha$  to the  $\beta$  form.

#### **Methods/Approach:**

Amyloid peptide (1-42) has been proposed to play a crucial role to the pathology of AD development. A major hypothesis is that amyloid peptide (1-42) can undergo a conformational change from a soluble  $\alpha$ -form to an insoluble  $\beta$ -form, which deposits and becomes neuro-toxic. Understanding the folding and mis-folding mechanism of amyloid (1-42) in Alzheimer's Disease is of a major importance for the discovery and development of potential small molecule drugs that can prevent conversion of the amyloid from the  $\alpha$  to the  $\beta$  form. Such small molecules have the therapeutic potential for the treatment and prevention of AD. Dr. Wang proposes to continue his study to employ a newly developed molecular dynamics simulation technique to study the folding and mis-folding mechanism of several amyloid peptides, including 1-28, 1-40 and 1-42 in atomic details.

Although many people have been interested for carrying out such studies, a major problem encountered is the conventional MD simulation requires computer power that easily exceeds current available computer power. To overcome this problem, Dr. Wang developed a new molecular dynamics simulation method, termed the self-guided molecular dynamics (SGMD method) simulation method [1, 2, 3, 4, 5]. As compared to the conventional MD method, the SGMD method enhances the conformational searching capability by a factor of 1000-times, as having been demonstrated by a number of studies. The SGMD method is now considered as a major breakthrough in molecular dynamics simulation field and has greatly enhanced our capability to study protein folding and mis-folding that are important for a number of neurological diseases, including AD.

Using the SGMD method, Dr. Wang showed that he can easily study the folding of peptides and small proteins. For example, within 10 ns SGMD simulations, the amyloid 1-28 peptide forms a

predominantly helical conformation, consistent with NMR experimental results. The 10 ns or longer SGMD simulations can be easily carried out using a workstation or computer clusters.

### **Preliminary Results:**

To date, we have tested our powerful SGMD method for folding of peptides and small proteins in explicit water molecules. We have demonstrated that SGMD is 100-1000 times more efficient in its conformational searching efficiency than conventional MD method [1, 2]. Using this method, we have investigated the folding mechanism of elemental protein secondary structures such as turns and helices [3, 4]. More recently, we have shown that SGMD affords efficient folding of small proteins in water [5]. These studies pave the way for our ultimate goal of investigating the folding and mis-folding of amyloid peptides and their implication to the development of a therapy for the treatment of Alzheimer's Disease.

### **Future Studies:**

Through extensive SGMD simulations, it is expected that we will be able to gain fundamental insights into the folding and mis-folding mechanism of amyloid peptides. For example, the influence of temperature, solvent and pH on the folding and mis-folding of amyloid peptides will be elucidated. The structural information obtained from this study will be used for the design and discovery of small molecule drugs that can prevent the conversion of the amyloid from the  $\alpha$  to the  $\beta$  form.

### **References:**

1. Wu, X.-W. and Wang, S., Self-guided molecular dynamics simulation for efficient conformational search, J. Physical Chemistry, **1998**, 102, 7238-7250.
2. Wu, X.-W. and Wang, S., Enhancing Systematic motion in molecular dynamics simulation. J. Chemical Physics, **1999**, 110, 9401-9410.
3. Wu, X. and Wang, S. Folding Studies of a Linear Pentamer Peptide Adopting a Reverse Turn Conformation in Aqueous Solution through Molecular Dynamics Simulation, Journal of Physical Chemistry B, **2000**, 104(33), 8023-8034.
4. Wu, X.-W. and Wang, S. Helix folding of an alanine-based peptide in explicit water, Journal of Physical Chemistry (B), **2001**, 105, 2227-2235.
5. Wu, X.-W. and Wang, S. Simulation study of protein A: Identification of the protein folding topology through computational simulation. Journal of Molecular Biology, 2001, (in review).



**PROJECT 3.** More powerful computational methods can be developed for the study of protein/drug docking and protein/protein interactions.

#### **Methods/Approach:**

The structure-based drug design of novel neuro-protective agents requires powerful computational docking methods to study the precise manner with which a drug interacts with its receptor. Current molecular docking methods suffer a number of deficiencies. For example, the conformational flexibility of a protein molecule is often important for its biological functions. None of the current existing docking method adequately addresses this issue. Solvent effect plays extremely important role for the biological functions of a protein and for its interaction with other proteins and drug molecules. Unfortunately, this solvent effect has not been properly included in computational docking studies. In this project, we propose to develop more accurate, more powerful computational tools to address these fundamental problems.

Over the last two years, Dr. Wang has developed a new docking method, called q-jumping molecular dynamics simulation method [1,2, 3]. This new method is based upon the generalized statistical mechanics and has been found to be able effectively included the flexibility of both the ligand and the receptor into the molecular docking simulation [2, 3]. Dr. Wang plans to further include the solvent effect into the molecular docking simulation. Dr. Wang proposes to use a Generalized Born model to represent the solvent effect into the docking simulations.

#### **Results:**

Dr. Wang expects that the development of a new method by including the conformational flexibility of the ligand and the receptor and the solvent effect can be successfully developed and implemented [1, 2, 3]. This project will be able to allow us more effectively to develop novel neuro-protective agents. The new method will also allow us to study the protein-protein interactions in atomic details. Furthermore, the development of the proposed new docking method will benefit many scientists who are interested to develop novel neuro-protective agents for other molecular targets.

#### **Future Studies:**

It is expected that the q-jumping method will become a powerful method for the study of protein-protein interactions and for structure-based design of novel neuro-protective agents. For example, we are currently using this method to study the interactions between the small molecule PTEN antagonists and PTEN and for the design of more potent PTEN antagonists.

#### **References:**

1. Pak, Y. and Wang, S. Folding of a 16-residue helical peptide using molecular dynamics simulation with Tsallis effective potential, *J. Chemical Physics*, **1999**, 111, 4359-4361.
2. Pak, Y. and Wang, S. Application of a new molecular dynamics simulation method with a generalized effective potential to the flexible docking problems. *J. Physical Chemistry (B)*, **2000**, 104, 354-359.
3. Pak, Y.; Enyedy, I. J.; Varady, J.; Kung, J. W.; Lorenzo, P. S.; Blumberg, P. M. and Wang, S. Structural Basis of Binding of High-Affinity Ligands to Protein Kinase C: Prediction of the Binding Modes through a New Molecular Dynamics Method and Evaluation by Site-Directed Mutagenesis, *J. Medicinal Chem.* **2001**, 44(11), 1690-1701.

**CNS INJURY: MECHANISM AND TREATMENT:** Dr. Faden's group evaluates the molecular and cellular correlates of secondary neuronal injury, including apoptosis, and actively participating in the drug discovery effort (*vide infra*). Dr. Knoblach studies mechanisms and treatment of CNS trauma. Dr. Vink utilizes magnetic resonance imaging and spectroscopy to study both injury and recovery, as well as the effects of treatment.

#### **ALAN I. FADEN, M.D.**

Our laboratory studies the pathobiology of neuronal cell death associated with central nervous system injuries and examines both mechanisms of neuronal cell death, as well as development of novel pharmacological treatment strategies. The central underlying hypothesis being evaluated is that the initial insult (trauma or ischemia) initiates an endogenous autodestructive response, leading to delayed cell death through both necrosis and apoptosis. Elucidating the specific factors involved and their temporal profile can permit the development of drug approaches that serve to limit secondary injury, thereby improving outcome. Complementary *in vivo* and *in vitro* model systems are used to study the molecular and cellular biology of secondary cell death, as well as to examine novel pharmacological strategies.

There are six major lines of investigation in the laboratory: 1) elucidating the role of caspases, and their regulatory pathways, in neuronal apoptosis and traumatic neuronal injury; 2) examining the role of ceramide in neuronal cell death; 3) defining the role of protein kinase B (Akt) in neuronal apoptosis; 4) evaluating the role of metabotropic glutamate receptors (mGluR) in secondary injury; 5) gene profiling changes after brain or spinal cord injury; and 6) drug discovery related to neuroprotection and cognitive enhancement.

#### **PROJECT 1. ROLE OF CASPASES IN NEURONAL APOPTOSIS AND TRAUMATIC NEURONAL INJURY**

Our group was the first to establish an important role for the cysteine protease caspase-3 in posttraumatic cell death and neurological dysfunction, and amongst the first to demonstrate a role for this caspase in neuronal apoptosis. During the past year, we have examined the relative roles of specific caspases in the injury response, including initiator caspases (e.g. caspase-8, -9), effector caspases (caspase-2, -3, -6), and inflammatory caspases (caspase-1). Double and triple labelling immunocytochemistry studies were used to define the temporal profile of specific caspases in specific cell types (neurons, glia, microglia) after traumatic brain injury in rats. These studies underscored the importance of the caspase-9/caspase-3 pathway (intrinsic apoptotic pathways), as compared to the intrinsic pathway or inflammatory related pathways. These studies were extended to a mouse head injury model, demonstrating the strong neuroprotective effects of treatment with the purported selective caspase-3 inhibitor z-DEVD (See Dr. Knoblach's section).

Beta-amyloid (A $\beta$ ) has been implicated as a major factor in Alzheimer's disease. In neuronal cell cultures, A $\beta$  induces dose-dependent apoptosis using both activity assays and selective peptide inhibitors; we showed that multiple caspases were involved in this process (Fig. 1).

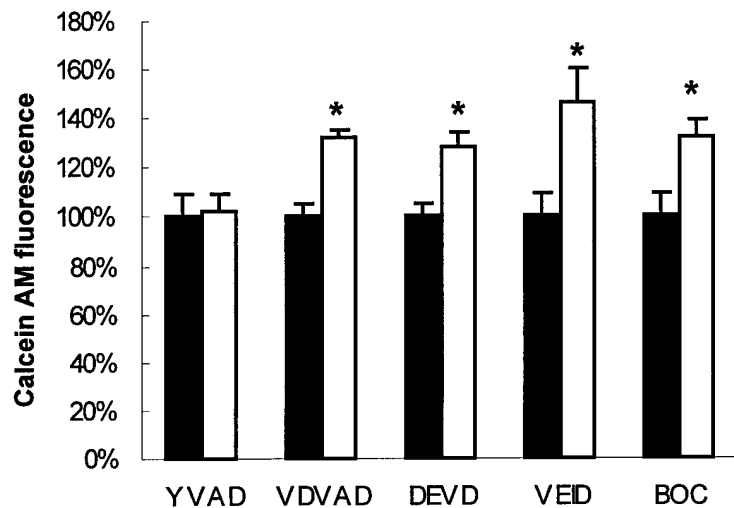


**Fig 1.** Selective inhibition of executioner caspases rescues CGC from  $A\beta_{25-35}$  toxicity with serum withdrawal.  $A\beta_{25-35}$  (25  $\mu$ M) was applied to CGC in the absence of serum for 48 h (filled bars) and the level of cell death was compared to 48 h of treatment with various caspase inhibitors (open bars) as detailed in Materials and Methods. Non-selective inhibition of caspases by Z-Boc-D-FMK (150  $\mu$ M; BOC) significantly reduces  $A\beta_{25-35}$  toxicity in the absence of serum. No significant difference in cell viability occurs after inhibition of caspase-1 by Z-YVAD-FMK (150  $\mu$ M; YVAD). In contrast, selective inhibition of the executioner caspases – caspase-2 by Z-VDVAD-FMK (30  $\mu$ M; VDVAD), caspase-3 by Z-DEVD-FMK (160  $\mu$ M; DEVD) and caspase-6 by Z-VEID-FMK (150  $\mu$ M; VEID) – significantly rescues CGC from  $A\beta_{25-35}$  with concurrent serum deprivation toxicity. Data are expressed as a percentage of calcein AM levels of CGC incubated with  $A\beta_{25-35}$  and simultaneous serum withdrawal in the absence of treatment (control). Bars represent mean  $\pm$  SEM,  $n = 10-15$ . \* $p < 0.05$  versus control. ANOVA followed by Student-Newman-Keuls test.

## PROJECT 2. ROLE OF CERAMIDE IN NEURONAL APOPTOSIS

Ceramide is a lipid produced through the actions of the enzyme sphingomyelinase, which has been implicated in both non-neuronal and more recently neuronal apoptosis. Our studies sought to confirm earlier results relating to the ability of a synthetic ceramide analog to produce neuronal apoptosis *in vitro*, as well as to examine whether endogenous ceramide produced such damage and was upregulated by apoptotic stimuli. Using both CGCs and cortical neurons grown in culture, we showed that the  $C_2$  ceramide analog induced neuronal apoptosis in a dose dependent manner (Fig. 2). Parallel studies showed that administration of sphingomyelinase itself produced similar effects (Fig. 2). In addition, we produced apoptosis in CGCs by removal of serum and potassium; this caused apoptotic cell death associated with increased levels of ceramide. Together, these findings indicate a potentially important role for ceramide in neuronal apoptosis. Follow-up studies using dominant-negative mutants and fluorometric assays indicated that the caspase-9/caspase-8 pathway are involved in this process (Fig. 3).

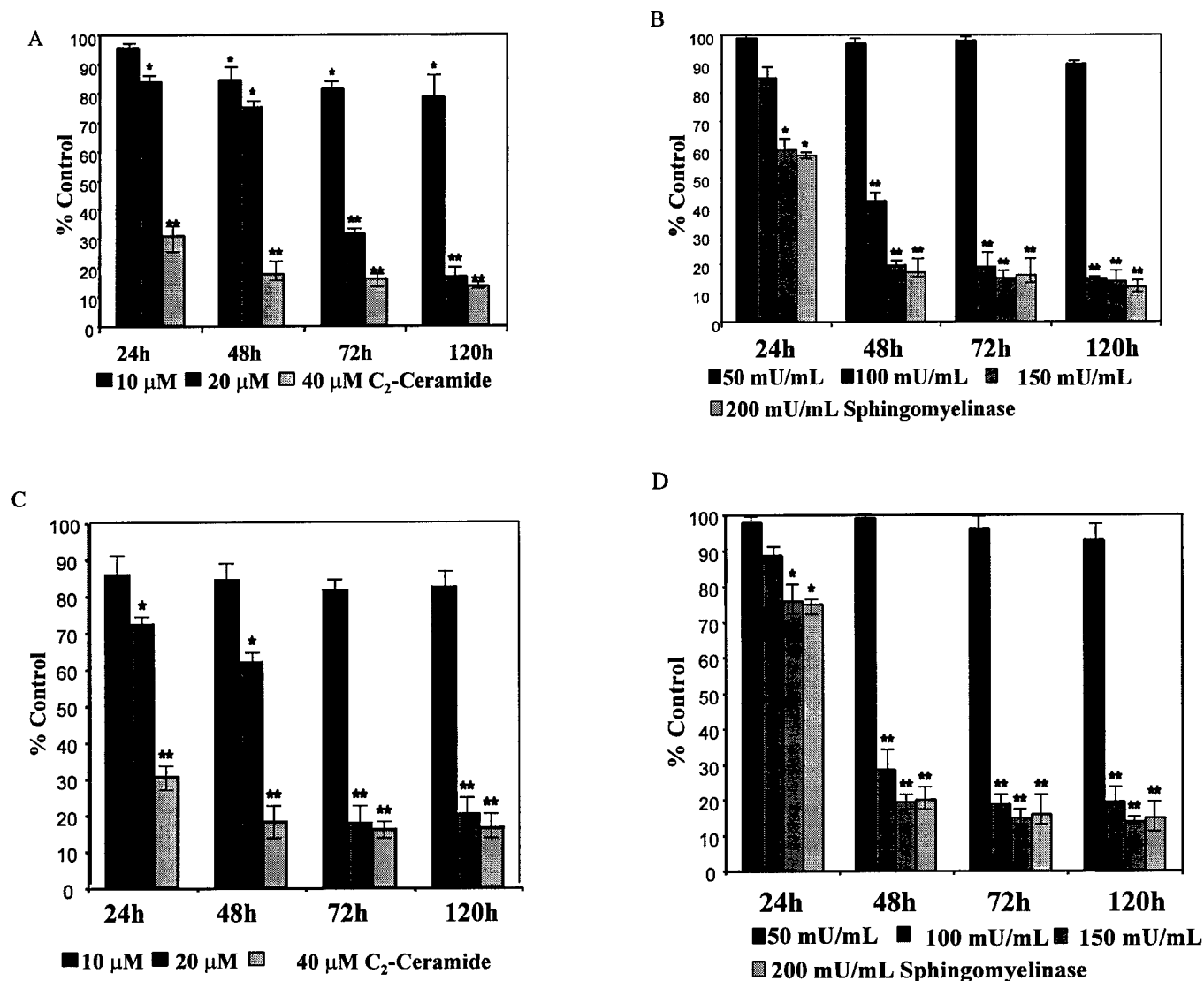


**Fig. 2** Cell viability assays of rat primary cortical neurons treated with C<sub>2</sub>-ceramide (A) and sphingomyelinase (B) and of CGC's treated with C<sub>2</sub>-ceramide (C) and sphingomyelinase (D). The cells were exposed to various doses of ceramide and sphingomyelinase for different time intervals, as indicated, and cell viability was evaluated using Calcein-AM staining method. \*  $p < 0.05$ , Kruskal-Wallis, \*\*  $p < 0.01$ , Kruskal-Wallis.

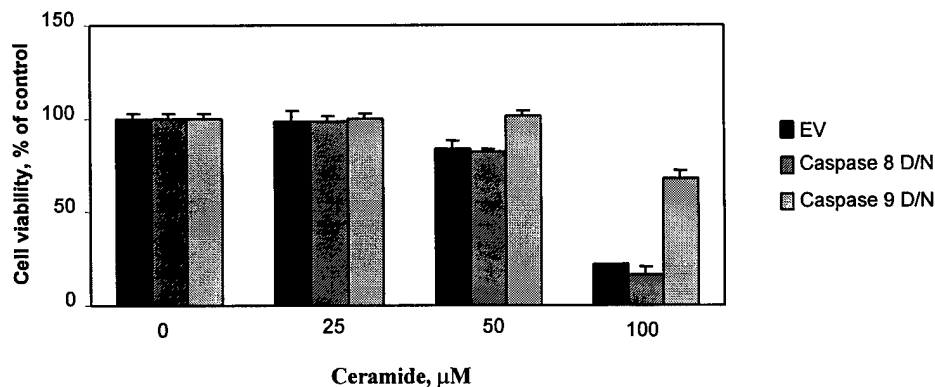


**Fig. 3** Effect of C<sub>2</sub>-ceramide on caspase-8 and -9 dominant-negative SHSY5Y (neuroblastoma) cells viability. Cell viability assessed by alamar blue after 36 h of incubation with indicated concentrations of C<sub>2</sub>-ceramide.

### PROJECT 3. ROLE OF AKT IN NEURONAL APOPTOSIS

Akt is a protein kinase that has been shown to modulate apoptosis in both neuronal and non-neuronal cells. We find that cell death following with either ceramide administration or activation of the tumor suppressor PTEN is associated downregulation of phosphorylated Akt that correlate with induction of apoptosis. Inhibition of Akt causes neuronal cell death (Fig. 4). These observations suggest that strategies to upregulate Akt after injury may be neuroprotective.

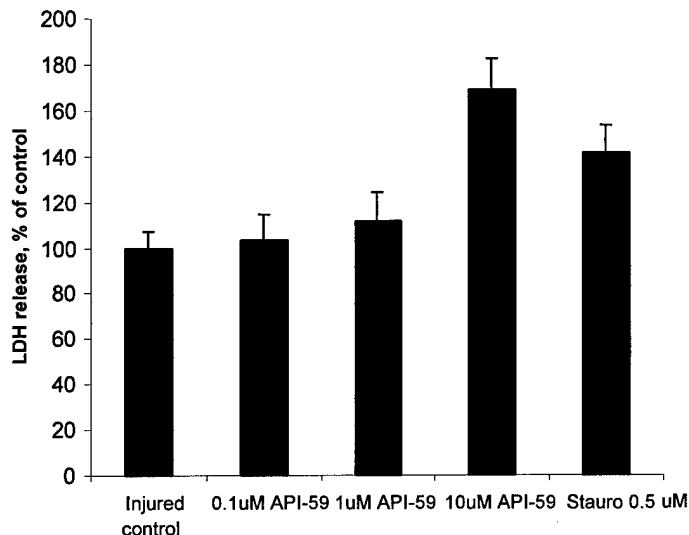


**Fig. 4** Cortical neuronal cell death induced by trophic support withdrawal is amplified by exposure to API-59 (Akt inhibitor). Cortical neurons were exposed to trophic support withdrawal alone (injured control), in the presence of increasing concentrations of API-59 (0.1mM, 1mM, 10mM) or in the presence of 0.5mM staurosporine for 24h. Cell death was estimated using the LDH release assay. There is a dose-dependent increase in cell death in the presence of API-59. At the highest concentration used (10mM) API-59 decreases cell survival to a larger extent than 0.5mM of the well-known pan-kinase inhibitor and apoptotic inducer staurosporine.

### PROJECT 4. ROLE OF MGLUR IN SECONDARY CELL DEATH

We have previously established, in prior years of this grant, that metabotropic glutamate receptors play an important role in modulating posttraumatic neuronal cell death. Specifically, we demonstrated that antagonists to group I mGluR were neuroprotective following traumatic neuronal injury *in vitro* or following lateral fluid percussion injury to rats *in vivo*. In contrast, activation of groups II and III mGluR were neuroprotective. Recent studies have suggested that under certain conditions, however, activation of group I mGluR may provide protection to neurons. We speculated that group I mGluR activation may have opposite effects on necrotic versus apoptotic stimuli. In our previous studies showing that activation of group I mGluR exacerbated injury and that antagonists were neuroprotective, the models shared largely necrotic profiles of cell death. Using mixed cortical glial cultures from rat cortex, we showed that in contrast to an exacerbating effect of group I mGluR on necrotic cell death, a Group I agonist had a clear neuroprotective effect to cells subjected to apoptotic stimuli using either staurosporine or etoposide. Group I mGluR consists of two subclasses, mGluR1 and mGluR5. We have previously demonstrated that mGluR1, but not mGluR5, activation exacerbates traumatic neuronal cell death in a model that is largely necrotic. Therefore, we speculate that in contrast to mGluR1, that mGluR5 may provide protection under conditions of apoptosis. Recent experiments using the specific agonist CHPG support this role. Other studies have compared the effects of mGluR1 and mGluR5 selective agonists and antagonists in traumatic brain injury in rats.

Both mGluR1 and mGluR5 antagonists were effective (see Dr. Vink's section). These studies support a role for mGluR modulation in the treatment of head injury.

## PROJECT 5. GENE PROFILING IN CNS TRAUMA

We have used both c-DNA based gene chips and those utilizing oligonucleotides (Affymetrix) to examine changes in gene expression after CNS trauma. A major objective was to examine the temporal clustering of genes of common function, with a goal of identifying both established and novel genes that play a role in secondary injury or recovery. Studies in traumatic brain injury established the feasibility of this approach using cluster analyses (Fig. 5). More recent ongoing studies in SCI using Affymetrix chips have extended these observations, showing distinct temporal clustering and coordinated gene regulation.

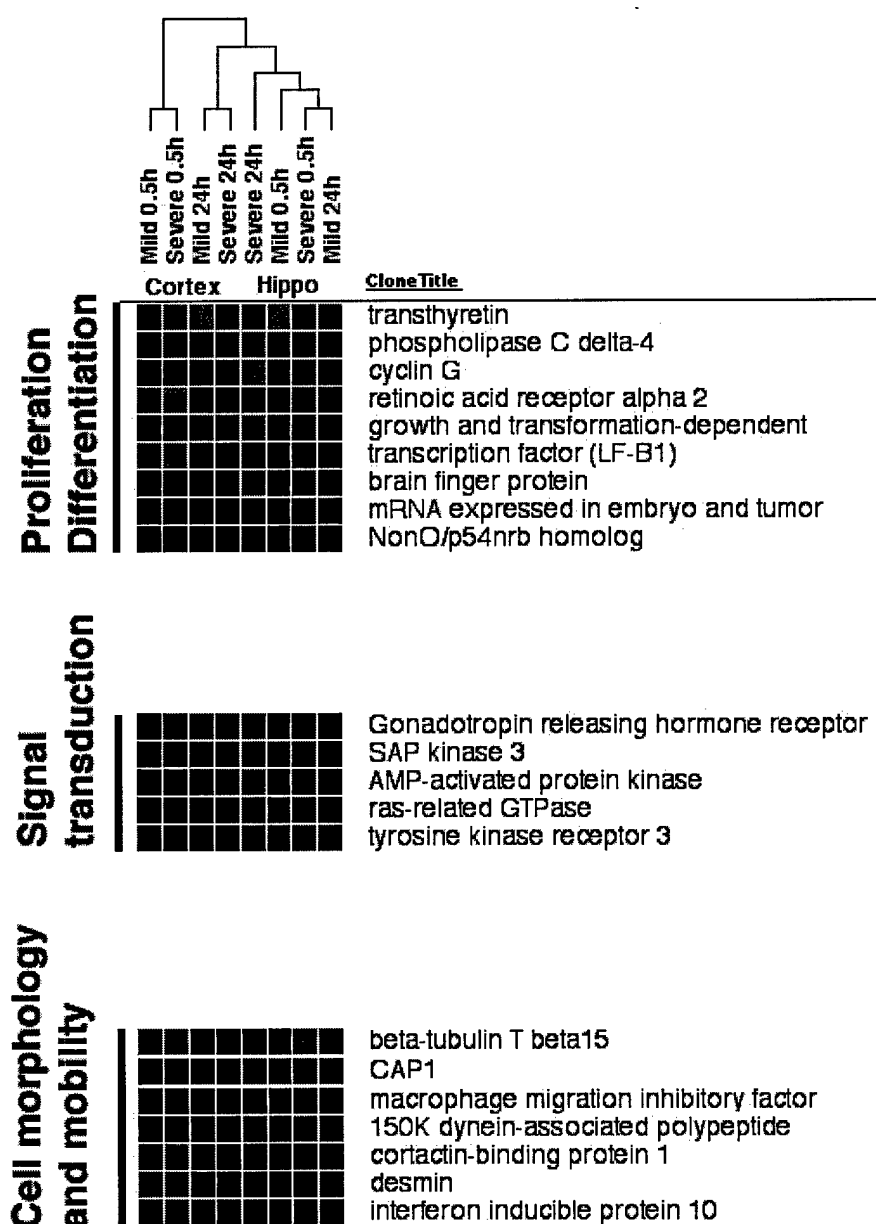


**Fig. 5** Partial gene expression patterns from two-dimensional cluster analysis of brain samples (horizontal axis) and genes (vertical axis, presented in segments). The partial data were from 2118 genes (out of 5147) with the average signal intensities higher than 600 and at least 2 fold changes in transcription levels. Genes implicated in cellular proliferation and differentiation, signal transduction and cell morphology and mobility are indicated. Brain tissue, treatment conditions, and dendrogram are indicated. The red squares represent genes with at least 2-fold increase in expression and the green ones indicate genes with at least 2-fold decrease in the expression, relative to sham rats.

## PROJECT 6. DRUG DISCOVERY

In collaboration with Dr. Alan Kozikowski at our Institute, we have continued to develop novel small peptides – tripeptides and diketopiperazines – which show both neuroprotection and cognitive enhancing properties. The compounds were originally developed from a structure related to naturally occurring hormone, thyrotropin releasing hormone (TRH). However, our compounds have been modified to exclude all the known major physiological effects of TRH – endocrine, autonomic, analeptic – while actually enhancing the neuroprotective and cognitive enhancing effects of this compound. For the past year we have extensively studied these compounds in both *in vivo* and *in vitro* model systems and also have designed second generation compounds with sidegroups that target additional specific proposed injury factors such as glutamate or free radicals. Recent studies have shown that these compounds can attenuate many types of cell death including apoptosis due to staurosporine, necrosis due to maitotoxin, free radicals, glutamate, and  $\beta$ -amyloid (see Dr. Knoblach's and Dr. Vink's sections).

**ROBERT VINK, Ph.D.**

## **NEUROBIOLOGICAL MAGNETIC RESONANCE LABORATORY**

The Laboratory is a core facility that provides both expertise and equipment associated with the application of magnetic resonance techniques to the study of nervous system injury. Magnetic resonance can be used to noninvasively acquire anatomical, physiological and biochemical data from the whole animal. As such, each animal serves as its own control and following the acquisition of data, the animal can be used for further studies such as behavioral analysis and histologic examination.

Over the past 12 months, there have been 4 major lines of investigation in the laboratory: 1) characterizing the development of brain lesions and their relationship to neurologic outcome following traumatic brain injury; 2) evaluating the role of metabotropic glutamate receptors on brain lesion development; 3) drug discovery related to neuroprotection; and 4) role of caspases in neuronal apoptosis and traumatic neuronal injury.

### **PROJECT 1. CHARACTERIZING THE DEVELOPMENT OF BRAIN LESIONS AND THEIR RELATIONSHIP TO NEUROLOGIC OUTCOME FOLLOWING TRAUMATIC BRAIN INJURY**

Previous studies have shown that location and direction of injury may affect outcome in experimental models of traumatic brain injury. Significant variability in outcome data has also been noted in studies using the lateral fluid percussion brain injury model (FPI) in rats. In recent studies from our laboratory, we observed considerable variability in localization and severity of tissue damage as a function of small changes in craniotomy position. To further address this issue, we examined the relationship between craniotomy position and brain lesion size/location in rats subjected to moderate FPI ( $2.28 \pm 0.18$  atmospheres). Induction of lateral FPI with the 5 mm craniotomy centered 2.6 mm from the sagittal suture resulted in both ipsilateral and contralateral lesion development on MR images (Fig. 1). The MRI lesions were generally restricted to the hippocampus and subcortical layers.

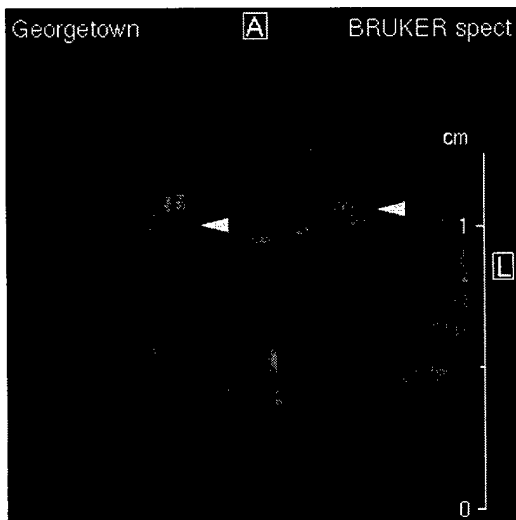


**Fig. 1** T2 weighted MR image of a rat brain 21 days after lateral fluid percussion injury. The craniotomy was centered 2.6 mm from the midline. Arrows indicate regions of hyperintensity that are indicative of tissue damage. Tissue damage was confirmed histologically.



Shifting of the craniotomy site laterally (away from the midline) was associated with increased ipsilateral tissue damage and a greater cortical component that correlated with distance from the sagittal suture (Fig. 2). In contrast, the contralateral MRI lesion did not change significantly in size or location unless the center of the craniotomy was placed more than 3.5 mm from the sagittal suture, under which condition contralateral damage could no longer be detected. Craniotomy position, and the associated ipsilateral tissue damage as determined from the MRI scans, was linearly correlated to motor outcome ( $r = 0.62$ ;  $p < 0.01$ ) but not with cognitive outcome as assessed by the Morris Water Maze.

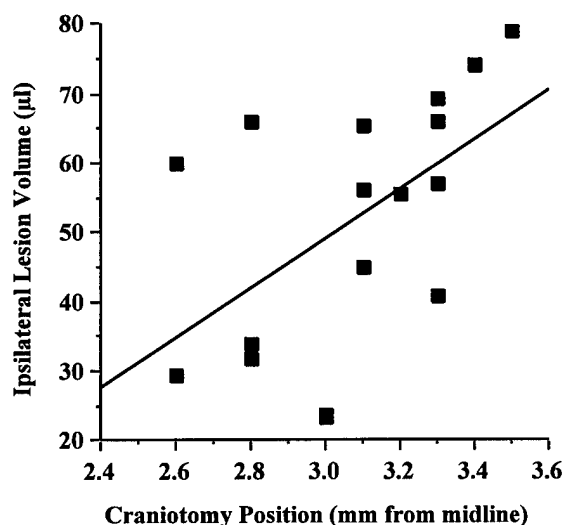


**Fig. 2** Relationship between craniotomy position and ipsilateral lesion size following lateral fluid percussion injury in rats ( $r = 0.54$ ;  $p < 0.05$ ). Over the range 2.6 to 3.5 mm from midline uniform contralateral injury was also consistently present

The present study has shown that small shifts in the location of injury induction using the lateral fluid percussion model of brain injury results in marked differences in tissue injury as indicated by lesion location, size and associated neurologic outcome. A more lateral craniotomy position resulted in unilateral injury with significant MRI lesions located in the ipsilateral cortex, hippocampus and other subcortical structures. A more medial craniotomy position (but still over the same, single hemisphere) resulted in bilateral MRI lesions to the hippocampus with reduced involvement of cortical tissue in the ipsilateral hemisphere, and no identifiable damage in the contralateral cortex. Craniotomy position was correlated to both ipsilateral MRI lesion size and motor outcome. These results indicate that even 1 mm shifts in craniotomy position can markedly alter the resultant injury profile following lateral FPI. This difference has important implications with respect to model reproducibility and it is critical that investigators using this model take this effect into account.

Following this model characterization and the recognition that injury site is critical in determining lesion size and outcome, we have now begun similarly characterizing lesion volume formation and its association with neurologic outcome following cortical contusion injury in the mouse.

## PROJECT 2. EVALUATING THE ROLE OF METABOTROPIC GLUTAMATE RECEPTORS ON BRAIN LESION DEVELOPMENT.

Metabolic glutamate receptors play an important role in modulating posttraumatic neuronal cell death. The work from Dr. Faden's laboratory has specifically demonstrated that antagonists to group I mGluR were neuroprotective following traumatic brain injury in rats. Our studies utilized magnetic resonance imaging to establish whether administration of group I mGluR antagonists influence development of a brain lesion following traumatic brain injury. Injury was induced by fluid percussion and magnetic resonance T2 weighted images were acquired at 21 days after injury for determination of lesion volumes. MCPG, [(+)- $\alpha$ -methyl-4 carboxyphenylglycine], an antagonist of both group I and group II glutamate receptors, was given IV 15 min after trauma. MCPG-treated animals showed markedly reduced post-traumatic lesion volume compared to controls. By comparing the highly selective mGluR1 antagonist AIDA to MCPG in the rat TBI model we demonstrated that both compounds significantly reduced post-traumatic lesion volume to a similar degree (Figure 3). This study confirmed that group 1 mGluR antagonists reduce lesion volume following traumatic brain injury.

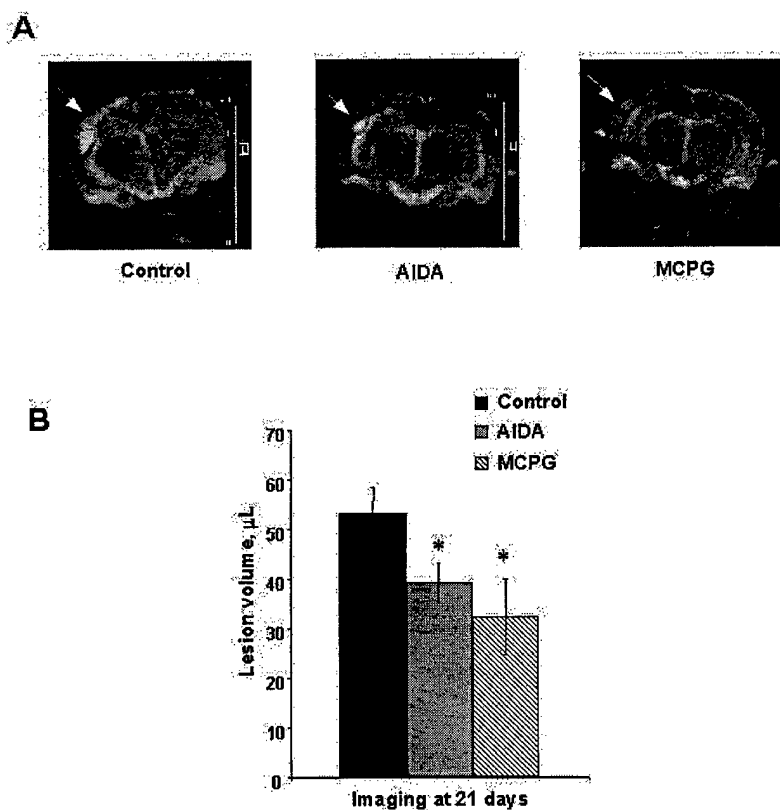


**Fig. 3** AIDA- and MCPG-treated animals developed significantly smaller lesions after TBI than vehicle-treated control animals. (A) Representative MRI T2-weighted images of control and mGluR1 antagonist treated rat brains at day 21 after TBI. (B) Summary of the effects of AIDA and MCPG treatments on lesion volume after TBI. The histograms represent average lesion volume ( $\mu\text{L}$ ) at day 21 after injury  $\pm$  SEM, as measured using T2-weighted magnetic resonance imaging;  $n = 9$  to 11 animals per treatment; \*,  $P < 0.05$  versus vehicle-treated controls.

### PROJECT 3. DRUG DISCOVERY RELATED TO NEUROPROTECTION

Novel small peptides – tripeptides and diketopiperazines – have been developed at this institution and shown to be both neuroprotective and able to enhance cognition. We have previously demonstrated using magnetic resonance spectroscopy that these compounds do not significantly affect bioenergetic state after traumatic brain injury and have since used magnetic resonance imaging to determine the effects of the compound on posttraumatic brain lesion size. Treatment with 35b significantly reduced lesion size in mice subjected to controlled cortical impact brain injury. This effect was particularly noticeable at 3 weeks after injury (Fig. 4), a timepoint at which the drug has demonstrable beneficial effects on neurologic outcome. This study confirmed that 35b significantly reduces posttraumatic brain lesion volume after traumatic brain injury in mice and that this reduction in lesion volume may contribute to the observed improvement in neurologic outcome with administration of these compounds.

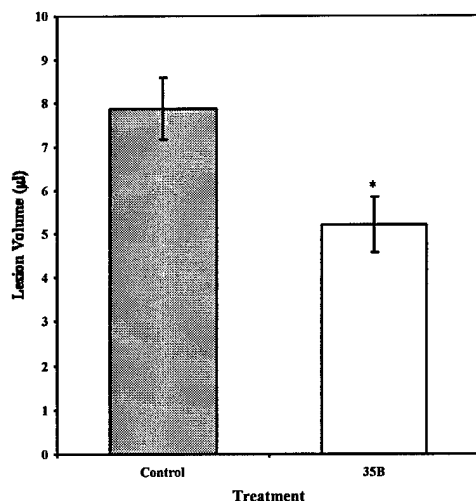


**Figure 4.** Average lesion volume ( $\pm$  standard error (ml)) was measured in mice subjected to the controlled cortical impact brain injury model using T2-weighted magnetic resonance imaging at 21 days after injury. Animals treated with 35B 1 hour after injury developed significantly smaller injury lesions ( $5.2 \pm 0.64$  ml) than control (vehicle treated) animals ( $7.9 \pm 0.7$  ml) ( $p < 0.05$ , 2 tailed T- test).

### PROJECT 4. ROLE OF CASPASES IN NEURONAL APOPTOSIS AND TRAUMATIC NEURONAL INJURY.

Studies in Dr. Alan Faden's laboratory have established an important role for the cysteine protease caspase-3 in posttraumatic cell death and neurological dysfunction. We are currently using magnetic resonance imaging to examine the effects of inhibitors of caspase-3 on brain lesion volume formation following traumatic brain injury. These studies are ongoing.

## SUSAN KNOBLACH, Ph.D.

Dr. Knoblach has worked on 2 major projects in collaboration with Dr. Faden. Project 1 focuses on the role of caspases and apoptotic cell death after traumatic brain injury. Clinical and experimental evidence supports the hypothesis that apoptosis contributes to secondary cell death after such injuries, and it may contribute to long-term functional deficits, as well. Caspases are protease enzymes that, when activated, serve as fundamental executors of coordinated, cellular programs that ultimately result in apoptotic cell death. To date, we have implicated caspases-1 and -3 and in apoptotic cell death after traumatic brain injury. Over the course of the past year, we evaluated whether other caspases may also be involved in the injury response. In addition, we assessed the effect of caspase inhibition on neurological outcome and tissue loss in rat and mouse models of traumatic brain injury.

Project 2 seeks to develop novel treatments for traumatic CNS injury, based on structure-activity relationships of thyrotropin-releasing hormone (TRH), its analogs, and metabolites. This year, we completed *in vitro* testing of novel compounds ty606lp and ty606mp, which confer protection against oxidative injury, and neuronal death induced in a model of mechanical trauma.

### PROJECT 1. APOPTOSIS AND CASPASE ACTIVATION AFTER TRAUMATIC BRAIN INJURY

#### Project 1a: Caspase activation and behavioral outcome in a rat model of experimental traumatic brain injury

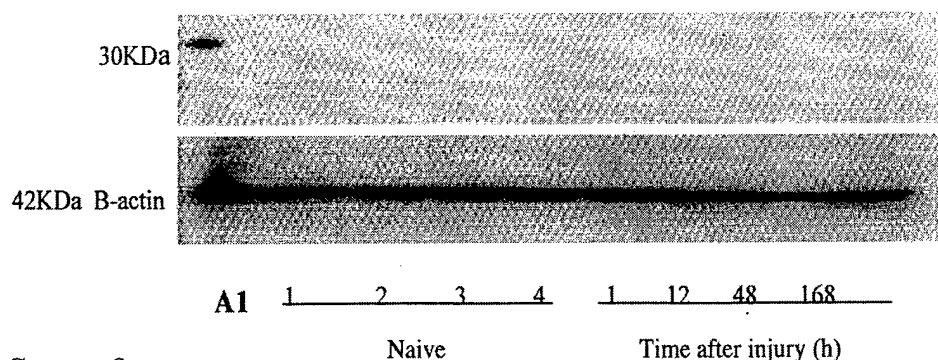
**Introduction:** Activation of caspase 3 appears to play a major role in apoptotic cell loss after TBI, however there is currently little information about the potential involvement of other caspases in this process. Upon activation, proforms of caspases are cleaved into large and small subunits which can be detected by specific antibodies. We utilized such antibodies to assess the temporal activation of caspases 2, 3, 8 and 9 in the injured cortex of rats subjected to moderate lateral fluid-percussion TBI. Separate studies examined the effect of treatment with z-VAD-fmk on motor and cognitive outcome measures after injury. Z-VAD-fmk is a broad spectrum inhibitor of multiple caspases.

**Methods:** The lateral fluid-percussion model of rat brain injury and related behavioral testing have been previously detailed in the original Department of Defense Proposal. Briefly, a craniotomy was performed over the left parietal cortex of anesthetized rats, ventilated on room air. Injury was induced by a brief, pressurized, saline pulse delivered through the craniotomy to the intact dura. At 1, 12 48 and 168 hr after injury, animals were sacrificed and the injured cortex removed, homogenized and analyzed via Western blot, for the presence of activated caspase(s). Brains from additional animals were subjected to fluorescent cell-type specific immunocytochemistry and TUNEL for precise localization of active caspase expression. For the drug treatment study, 25 mM z-VAD-fmk was dissolved in DMSO and injected intracerebroventricularly (5ul/2min.) at 15 min. after injury. Controls received equivolume injections of DMSO vehicle. Motor and cognitive function(s) were evaluated at 1, 7 and 14 days after trauma.

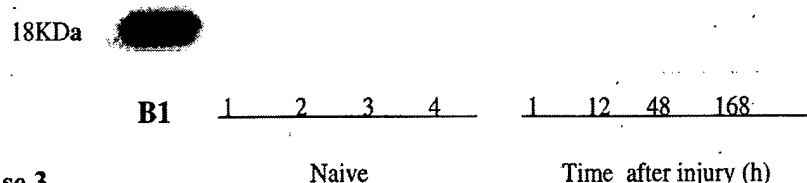
**Results:** Caspases 3 and 9 were activated from 1-48 hr after TBI. Cleavage fragments of these caspases were highly expressed from 1-12 hr after injury (Fig. 1). In contrast, there was no detectable activation of caspase 2 or 8 from 1 -168 hr after TBI. At 4 hr after TBI, activated caspases 3 and 9

were highly expressed by neurons localized within the injured cortex. Most astrocytes did not express these activated caspases at this time. TUNEL-positive cells with condensed or punctate nuclei characteristic of apoptotic morphology expressed activated caspase 9 and, particularly, caspase 3. However, the active forms of these caspases were not exclusively expressed by cells with this phenotype--neither did all cells with apoptotic morphology show immunohistochemical evidence of such caspase activation. Administration of the broad caspase inhibitor, z-VAD-fmk, just after TBI, significantly improved motor and cognitive function after injury (Fig. 2).

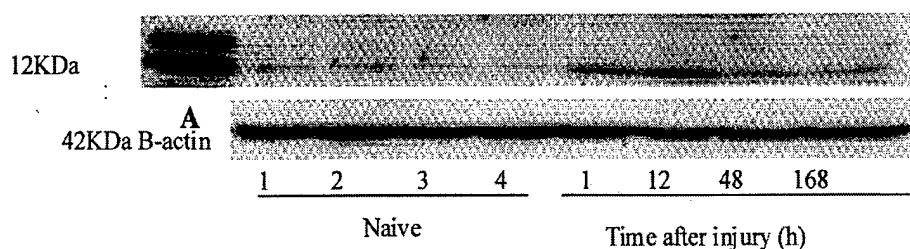
## Caspase 2



## Caspase 8



## Caspase 3



## Caspase 9

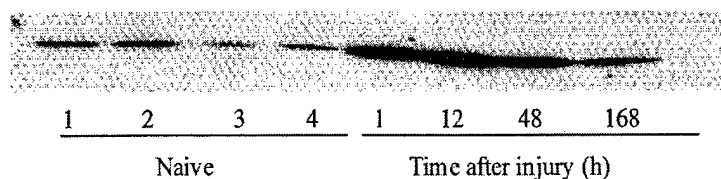
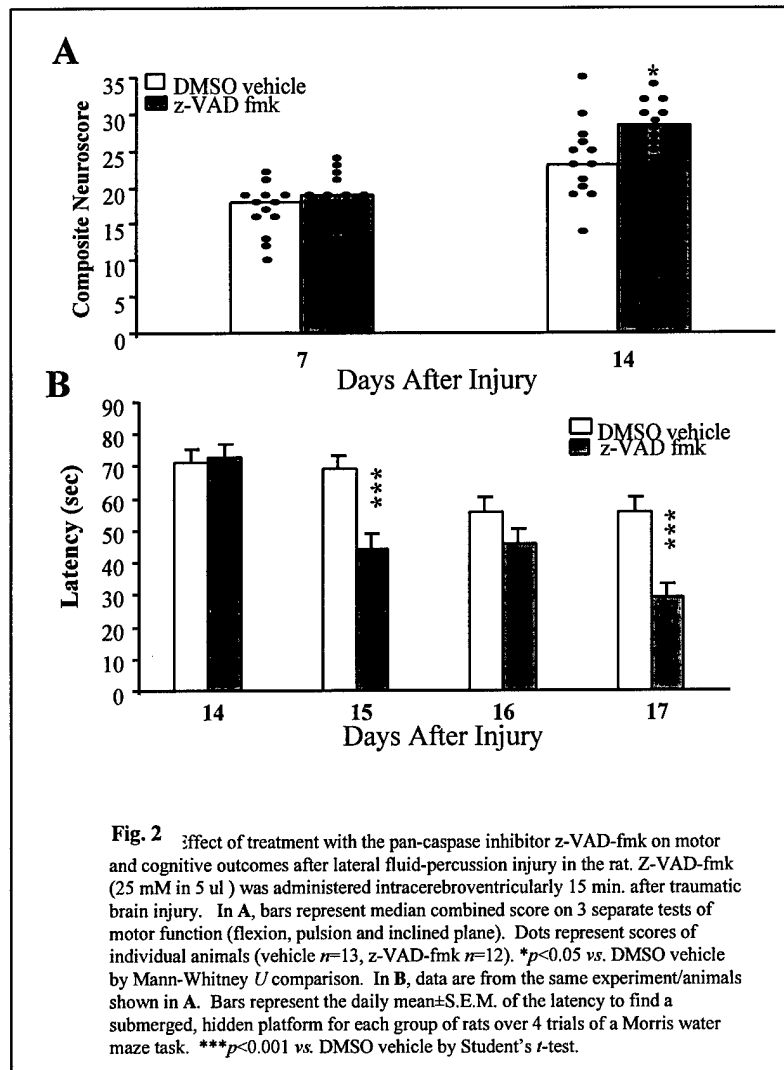


**Fig. 1.** Western blot analysis of caspase cleavage fragments over time after lateral fluid-percussion injury in the rat. For all, as denoted, Lanes 1-4 are from naive cortex. Hours after injury are marked as 1-168.  $\beta$ -actin served as an internal loading control for all Westerns, but is shown only for caspase 2 and 3. Results of individual caspases are shown from top to bottom. **Caspase 2:** antibody from Stressgen Biotechnologies (Victoria, B.C.) recognizes a 30 kDa fragment of cleaved caspase 2. Lane A1 contains extract from mouse spleen (+control). **Caspase 8:** SK440 from SmithKline Beecham, (King of Prussia, PA) detects an 18kDa fragment of cleaved caspase 8. Lane B1 contains active recombinant human caspase 8. **Caspase 3:** Antibody Bur 1797+ from the Burnham Institute (La Jolla, CA) recognizes a 12 kDa fragment of caspase 3. Lane A contains active rat recombinant caspase 3 (+control). **Caspase 9:** Bur81, also from the Burnham Institute, detects the 15kDa fragment of caspase 9.



**Conclusion:** Collectively, these data suggest that activation of caspases after TBI appears to be relatively selective, as well as cell-type specific. TBI may preferentially activate caspases through pathways that involve mitochondrial commitment (i.e. caspase-9). To our knowledge, this is the first report showing that a pan-caspase inhibitor improves neurological outcome following traumatic brain injury. Taken together, the data suggest that caspase inhibitors may be of potential therapeutic value, and moreover, that strategies which target multiple caspases may ultimately prove to be the most beneficial.

#### **Project1b: Caspase 3 activation and behavioral outcome in a mouse model of experimental traumatic brain injury.**

**Introduction:** Activation of caspase 3 appears to play a major role in apoptotic cell loss after TBI, however there is currently little information about the potential involvement of this caspase in the mouse model of traumatic cortical impact. Therefore, we assessed the activation of caspase 3 over time after injury, via Western blot and immunocytochemical methods. Separate studies evaluated the effect of treatment with a relatively specific caspase 3 inhibitor (z-DEVD) on motor and cognitive outcomes,

as well as lesion volume. In addition, we tested the hypothesis that z-DEVD may prevent necrotic cell death in an *in vitro* model of necrosis. Currently, we are evaluating the effect of z-DEVD on necrotic cell death *in vivo*.

**Methods:** The cortical impact model of mouse brain injury and related behavioral testing have been previously detailed in the original Department of Defense Proposal. Briefly, a craniotomy was performed over the left parietal cortex of an anesthetized mouse and an impact injury which resulted in 1 mm tissue deformation delivered to the intact dura. At 6, 12, 24 and 48 hr after injury, animals were sacrificed, and their brains removed and processed for fluorescent cell-type specific immunocytochemistry and TUNEL. A separate study evaluated the effect of treatment with z-DEVD-fmk (160 ng in DMSO) at 1, 4, 8 or 24 hr after injury on motor and cognitive recovery up to 21 days after trauma. z-DEVD-fmk is a relatively specific caspase 3 inhibitor. At 21 days after injury, lesion volume was assessed via T2-weighted MRI imaging. An additional set of animals received either z-DEVD-fmk treatment or DMSO 1 hr after injury, and their brains were removed for histological examination 2 hr later, to determine the number of necrotic and apoptotic cells in the area that later becomes a cavitation lesion. The last group of animals is still being processed, thus data from this group is not yet available. In separate experiments, rat cortical neuronal-glia co-cultures were prepared and, at 18 days *in vitro*, incubated with maitotoxin in the presence or absence of z-DEVD. Maitotoxin is a marine algal toxin that induces necrotic cell death. Eighteen hours later, LDH release was assessed as a measure of cell death.

**Results:** Although both apoptotic (TUNEL-positive cells with apoptotic morphology) and active caspase 3 positive neurons were detected throughout the injured cortex at from 6-24 hr after trauma (Fig. 3), this level of injury in the mouse model of cortical impact was primarily associated with necrosis. z-DEVD treatment improved both motor and cognitive function, and reduced lesion volume at 21 days after injury. z-DEVD (225-19 uM) was also neuroprotective against necrotic cell death induced by maitotoxin *in vitro*.

**Conclusion:** The marked improvement in motor and cognitive function, as well as lesion volume, seen after treatment with z-DEVD is notable in view of the amount of necrosis, rather than apoptosis or caspase-3 activation that was observed in our studies. Thus, we hypothesize that z-DEVD and/or caspase 3 inhibition, may prevent necrotic as well as apoptotic cell death. Data from the maitotoxin model of *in vitro* necrotic death support this. Our ongoing study will determine whether z-DEVD treatment reduces necrotic and/or apoptotic death *in vivo*, and thus provide important additional information about the effect of z-DEVD administration. The data could be interpreted as indicating possible multiple actions of z-DEVD, a compound which has been previously thought to be relatively specific, and/or cross-talk between apoptotic and necrotic pathways.

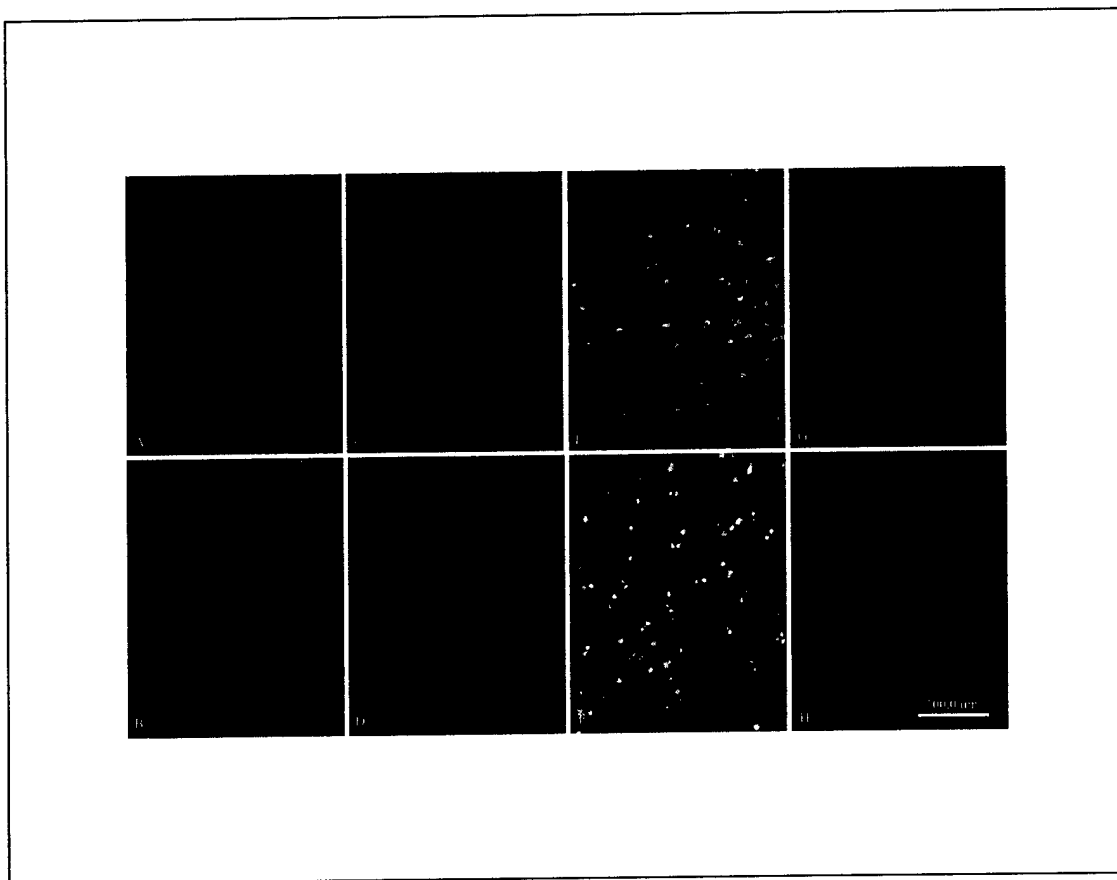


**Fig. 3** Co-localization of anti-NeuN staining (Texas Red/red) and TUNEL labeling (FITC/green) in mouse cortex 24 hr after controlled cortical impact brain injury. Images shown represent the inner (*A, C, E*) and outer cortex (*B, D, F*) of the injured (*A-F*) or contralateral (*G, H, J*) side. Many TUNEL- positive neurons displayed cytoplasmic TUNEL staining, whereas others showed condensed or fragmented staining consistent with apoptotic nuclear morphology (*E-F*). Fewer anti-NeuN-positive cells were observed in injured cortex than in the contralateral uninjured side (*C-D* vs. *G-H*).

## **PROJECT 2: NOVEL TREATMENTS FOR TRAUMATIC CNS INJURY, BASED ON STRUCTURE ACTIVITY RELATIONSHIPS OF THYROTROPIN-RELEASING HORMONE (TRH), RELATED ANALOGS AND METABOLITES.**

***In vitro* analysis of the potential neuroprotective activities of 2 new compounds, ty606lp and ty606mp.**

Cyclic dipeptide cyclo[His-Pro] (CHP) is synthesized *de novo* endogenously and as a breakdown product of thyrotropin-releasing hormone (TRH), a peptide with known neuroprotective activity. Our rationale was that the known structure of CHP, combined with the ability of certain phenols to act as scavengers for reactive oxygen species (ROS) might yield compounds with novel neuroprotective potential. In collaboration with the laboratory of Alan Kozikowski, we have synthesized several compounds based on the structure of CHP, with the exception that the histidine residue was replaced by 3,5-di-tert-butyltyrosine, a phenol group that traps reactive oxygen species.



**Methods:** The preparation of neuronal glial co-cultures and the traumatic injury method employed have been described in detail elsewhere (REF). All experiments were performed from 18-21 days *in vitro*. Agents that induce cell death via different mechanisms were used as injury models in a series of independent experiments. These included: 1) free radical /oxidative injury—FeSO<sub>4</sub> 2) excitotoxic injury—glutamate pulse 3) apoptotic injury—staurosporine 4) traumatic injury—mechanical disruption 5) necrotic injury--maitotoxin. The neuroprotective profile(s) of ty606lp and ty606mp were developed by treating injured cultures over a range of concentrations (100 uM-1 pM). LDH release and Hoescht staining and visualization via light and/or phase contrast microscopy were used as biochemical and morphological measures of cell death.

**Results:** Ty606lp and ty606mp prevented neuronal death in the *in vitro* model of traumatic injury. In addition, they dose-dependently prevented death caused by the direct induction of free radicals via FeSO<sub>4</sub>, and by calcium mobilization through maitotoxin, an agent that evokes rapid, necrotic death. The drugs showed activity against the latter at picomolar concentrations. The drugs did not show significant protection against injury induced by glutamate pulse or staurosporine.

**Conclusions:** These novel cyclic diketopiperazines show neuroprotective properties in a neuronal-glial model of trauma, which involves activation of multiple secondary injury factors. They are also able to block calcium-induced necrotic cell death initiated by maitotoxin as well as death induced by FeSO<sub>4</sub>, a free radical generator. This unique profile suggests that these agents act through several different mechanisms, and moreover, that they may have potential utility as treatments for acute CNS injuries such as stroke and trauma (Fig 4).

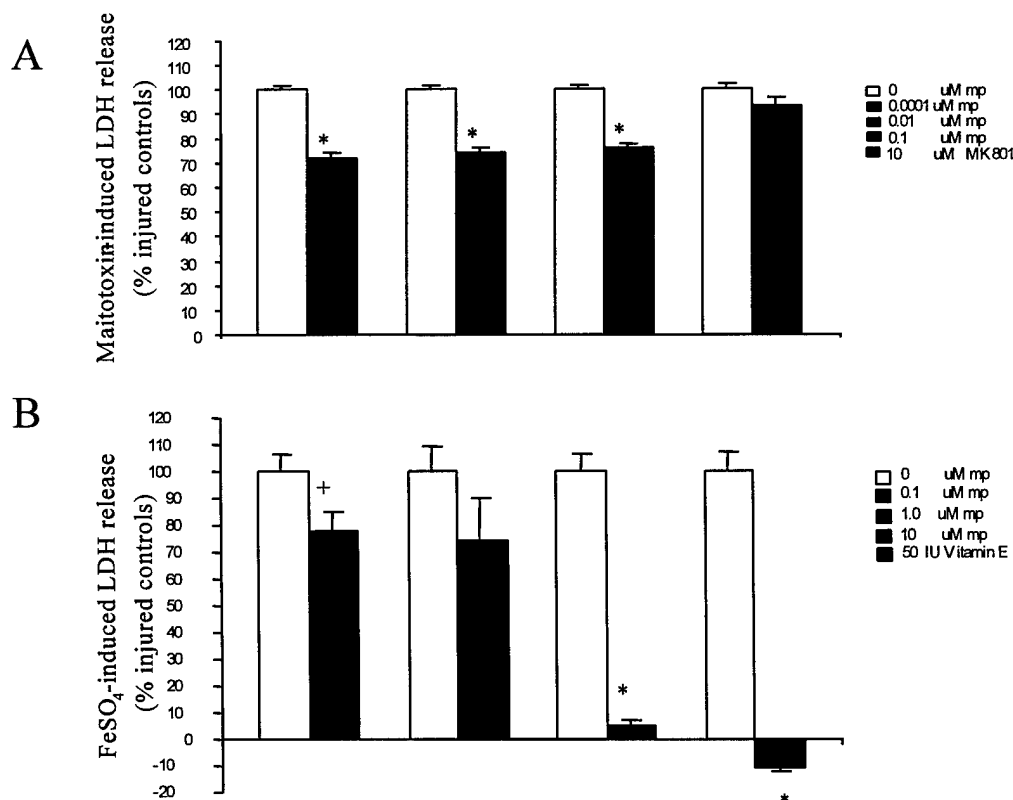


**Fig. 4** Ty606mp=mp significantly improved survival in *in vitro* models of A) necrotic injury induced by maitotoxin (0.0001-0.1 uM mp) or B) free radical induced death initiated by FeSO<sub>4</sub> (0.1 and 10 uM mp). Data are expressed as percentages of LDH release compared to injured, untreated wells (control). LDH release from uninjured, untreated controls was subtracted from all values. Treatment with MK-801 did not prevent cell death caused by maitotoxin, which causes necrosis via calcium mobilization. However, treatment with mp significantly increased survival in this model at concentrations as low as 1 picomole (data not shown). MP also increased survival in the FeSO<sub>4</sub> model, although at the doses tested it was not as effective as Vitamin E; LDH release in wells treated with FeSO<sub>4</sub> and Vitamin E was lower than in untreated, uninjured controls. Bars represent the mean  $\pm$  SEM for  $n=40-46$  wells per condition. \* $p<0.05$ , \* $p<0.0001$  for  $t$ -test with Bonferroni correction.

**CNS INJURY: MODELS, PLASTICITY AND REGENERATION:** Dr. MacArthur examines intrinsic factors that improve neuronal survival and regeneration after injury. Dr. Rosenberg has developed a new model of SCI in the mouse.

**LINDA MacARTHUR, Ph.D.**

The central underlying hypothesis being evaluated is that STAT (Signal Transducers and Activators of Transcription) proteins play a central role in neuronal homeostasis and that signal transduction through STAT proteins is required for survival and regeneration after axotomy.

The preliminary studies described below have been used to develop an RO1 submitted in February, 2001. The specific aims proposed seek to 1) define the role of STAT proteins in the survival of DRG neurons after injury and 2) define the role of STAT proteins in the regeneration of DRG neurons after injury.

**PROJECT 1. REGULATION OF STAT-LIKE PROTEINS BY NOXIOUS STIMULATION**

STAT activity is demonstrated by the binding of proteins to a STAT consensus sequence in a gelshift reaction and by increased tyrosine and/or serine phosphorylation. Alternatively, upon activation, changes in STAT localization occur and STAT proteins translocate from the cytoplasm and outer membrane to the nucleus. Preliminary results demonstrate that proteins that bind to a STAT consensus sequence are present in rat spinal cord and DRG and that they are regulated by noxious stimuli. Male Sprague Dawley rats received either a unilateral subcutaneous injection of formalin into the hindpaw, a model for acute inflammatory pain or ligation of the sciatic nerve at mid thigh (chronic constriction injury, CCI) a model for neuropathic pain that results from nerve injury. L4-L5 DRG (the site of sciatic nerve innervation) were removed. Whole cell extracts of L4-L5 DRG were prepared and gelshifts were performed as described using a STAT 1 consensus sequence (Fig. 1).

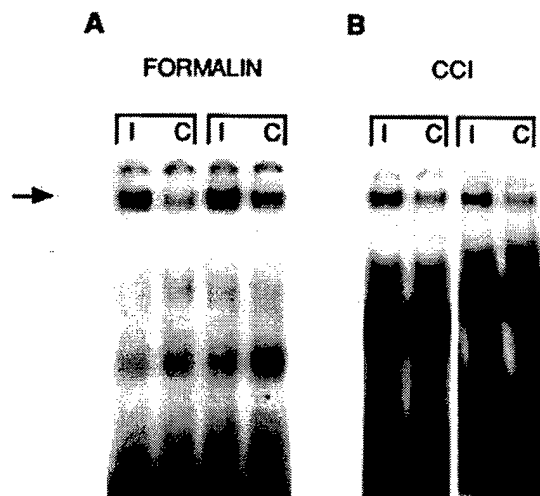


**Fig. 1** Gelshift analysis of STAT protein activity. Rats received a formalin injection into a single hindpaw (A) or ligation of the sciatic nerve (chronic constriction injury, CCI (B). L4-L5 DRG (the site of sciatic nerve innervation) were removed and examined for STAT protein activity. I=ipsilateral, C=contralateral.

There was an increase in binding of STAT-like proteins(s) to a STAT consensus sequence in extracts prepared from DRG from the ipsilateral side to the painful stimulus. This increase was detected at 60 minutes after formalin injection and 6 days after CCI, when rats exhibited thermal hyperalgesia for each

treatment, respectively. Although these data were obtained with a consensus sequence for the STAT 1 protein, other consensus sequences for STATs 2-6 gave similar results for detecting basal STAT binding activity.

## PROJECT 2. IDENTIFICATION AND LOCALIZATION OF STAT PROTEINS 1-6 IN RAT DORSAL ROOT GANGLIA.

Immunoblotting was done with antibodies against known STAT proteins (STATs 1-6) to determine if they were present in rat DRG extracts. STAT proteins 1-6 were detected in DRG whole cell extracts (Fig. 2). Antibodies against STAT 1 detected a faint band the same size of the STAT 1

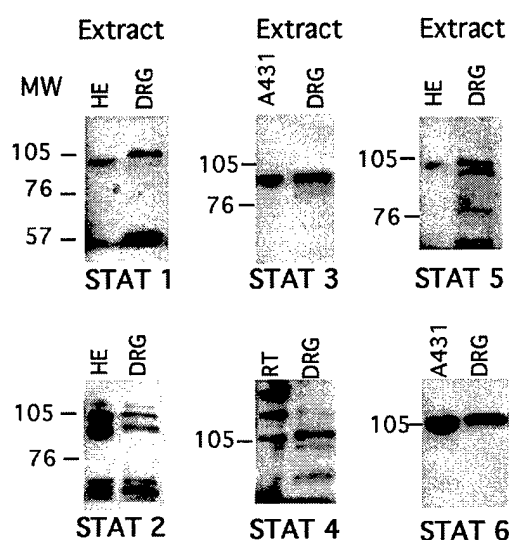


**Fig. 2** Immunoblotting was done with antibodies against STAT proteins 1-6. STATs 1-6 were detected in DRG whole cell extracts. STAT 1-5 antibodies detected more than one band suggesting modification or isoforms. Control extracts: HE=human endothelial cells, A431=carcinoma cells, RT=rat testes extract.

protein found in human endothelial cells (HE cells)(the expected forms are p91 and p84). However, the majority of the detectable protein was at a slightly higher molecular weight, approximately 105 kd. A prominent band also appeared at about 60kd. Antibodies against STAT 2 detected a triplet containing a band of 113 kd (the expected size of STAT 2) and two smaller bands. A lower molecular weight doublet of approximately 60 kd was also detected with both a mouse monoclonal and rabbit polyclonal antibody directed against STAT 2. STAT 3 antibodies detected a prominent band of approximately 92 kd (the predicted form) and two faint bands beneath it. Antibodies against STAT 4 detected a faint band at approximately p89 (the predicted form) as well as a higher molecular weight form. Antibodies to STAT 5 detected multiple bands. The predicted forms are 113 kd, 97 kd, 80 kd and 77 kd. The bands on the gel correspond well with these sizes. STAT 6 antibodies detected a single band at approximately 119 kd, the predicted size. These data suggest that DRG synthesize STAT proteins 1-6. The multiple bands, especially for the lower molecular weights, could be non-specific binding. However, at least for STATs 1 and 2, these bands were detected with additional antibodies, suggesting that these are STAT-like proteins.

Immunohistochemistry was used to determine if the STAT proteins were localized to neurons or satellite cells of the DRG. Two distinct types of staining were observed (Fig. 3).

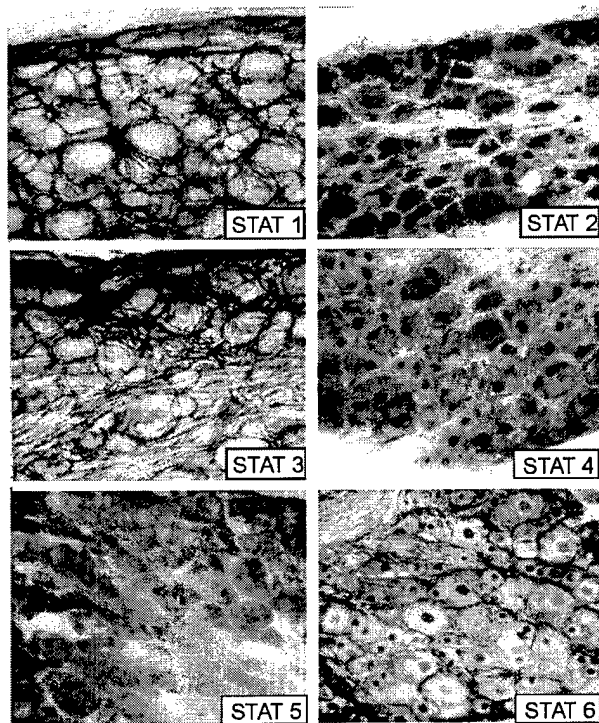


**Fig. 3** Localization of STAT proteins in adult DRG neurons by immunohistochemistry. Antibodies that gave specific staining by Western analysis were used. STATs 2,4, and 6 showed strong nuclear and cytoplasmic staining of small, medium, and large neurons. STAT5 was detected in the cytoplasm and more weakly in the nucleus. STATs 1 and 2 were not detected in either the cytoplasm or nucleus.

Antibodies to STATs 2,4, and 6 stained small, medium, and large neurons. The stain was most prominent in the nucleus with some cytoplasmic staining. Antibodies directed against STAT 5 detected proteins in the cytoplasm and more weakly in the nucleus. In contrast, antibodies against STATs 1 and 3 did not detect any nuclear staining in neurons, and little to none cytoplasmic staining. These antibodies produced staining that is either localized to the outer membrane of the neurons, or possibly to the satellite cells. Interestingly, STAT6 staining is present in P1 neonatal DRG (data not shown). However, the majority of the nuclear stain is in the small and medium sized neurons with large cell neurons exhibiting much weaker staining. This is potentially interesting since these cells have not made their connections in the CNS yet.

### PROJECT 3. REGULATION OF STAT6 ACTIVITY BY NERVE INJURY

We examined the effect of nerve injury on STAT6 protein localization. Sciatic nerve transection resulted in a dramatic loss of STAT6 nuclear staining ipsilateral to the treated side (Figure 4). This occurred in neurons with small, medium, and large cell bodies. Quantitative analysis of two animals that received sciatic nerve transection showed a 40-75% decrease in STAT 6 nuclear staining by seven days postoperative (Table 1). Chronic constriction injury also produced a decrease in STAT6 nuclear staining at ten days (data not shown). Formalin injection or complete Freund's adjuvant injection had no apparent effect on STAT 6 protein localization (data not shown). These data suggest that STAT 6 protein is responsive to nerve injury but not inflammatory mediators.

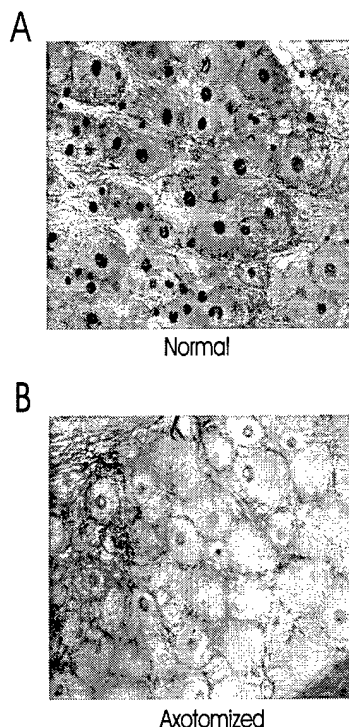


**Fig. 4** Localization of STAT6 protein by immunohistochemistry in adult rat DRG. A= uninjured tissue, B=axotomized tissue. Sections from normal and injured tissue were run simultaneously and mounted together.

**Table 1. STAT 6 Nuclear Staining in Dorsal Root Ganglia**

Dorsal Root Ganglia	Treatment	Percent Positive Cells	Percent Reduction
L5 Contra	Sciatic-X 7 days	63	
L5 Ipsi		38	40
L5 Contra	Sciatic-X 7 days	51	
L5 Ipsi		13	75
L5 Contra	Rhizotomy 3 days	59	
L5 Ipsi		28	53
L4 Contra	Rhizotomy 3 days	48	
L4 Ipsi		21	56

To determine if the loss of STAT 6 nuclear staining was the result of loss of trophic support from the periphery, versus a response to the injury per se, animals received a dorsal rhizotomy of the L4 or L5 dorsal root. Interestingly, rhizotomy produced similar changes in STAT 6 localization (note-this time point is 3 days after injury)(Table 1). The loss of STAT 6 nuclear staining after central rhizotomy suggests nuclear localization of STAT 6 protein is not maintained in neurons by peripheral trophic support.

**Conclusion-**we hypothesize that STAT proteins are a key component of neuronal survival and neurite elongation. Our preliminary data demonstrates that DRG neurons express STAT proteins naturally, and that the activity of these proteins is responsive to noxious stimulation and nerve injury. Future studies will examine STAT protein activation in during neuronal survival and regeneration after injury.

## **LISA ROSENBERG, Ph.D.**

Dr. Rosenberg's work focuses primarily on the mechanisms underlying white matter injury in the spinal cord following a traumatic insult. Spinal cord injury (SCI) produces in an acute dramatic loss of axons throughout the white matter (which is composed of axons that travel throughout the spinal cord) in and around the area of trauma. The loss of these axons results in a permanent disconnection between the brain and the spinal cord. It is this loss of communication that causes the paralysis that is associated with SCI.

Dr. Rosenberg, using a rat model of SCI, showed that much of the acute pathology and axonal loss associated with spinal cord injury (SCI) can be ameliorated by preventing/blocking the influx of extracellular sodium (Rosenberg et al., 1999a & b). Her findings suggest that the sodium influx significantly contributes to the degeneration and loss of axons seen after SCI. The evidence suggests that sodium influx is an upstream activator of biochemical and molecular pathways involved in the secondary injury mechanisms that continue to operate for hours to days after the initial insult. It is these secondary events that propagate the injury and ultimately bring about the widespread loss of axons.

### **DEVELOPMENT OF A MOUSE MODEL OF SCI**

**Introduction:** The development of transgenic mice has opened a new door for researchers. These animals provide scientists with a new tool by which they can study the role specific genes play in disease, aging and traumatic injury. Currently, there are a number of mouse strains that have been genetically manipulated so as to express or *not* express genes and/or proteins that are known to be activated by SCI and may be downstream events of sodium influx. Because of the importance of having a model of genetic manipulation with which to test the role a specific gene is playing in neuronal and axon loss, Dr. Rosenberg has developed a mouse model of SCI. The model will permit transgenic mice to be used to study genes that contribute to the recovery of neurological function following SCI.

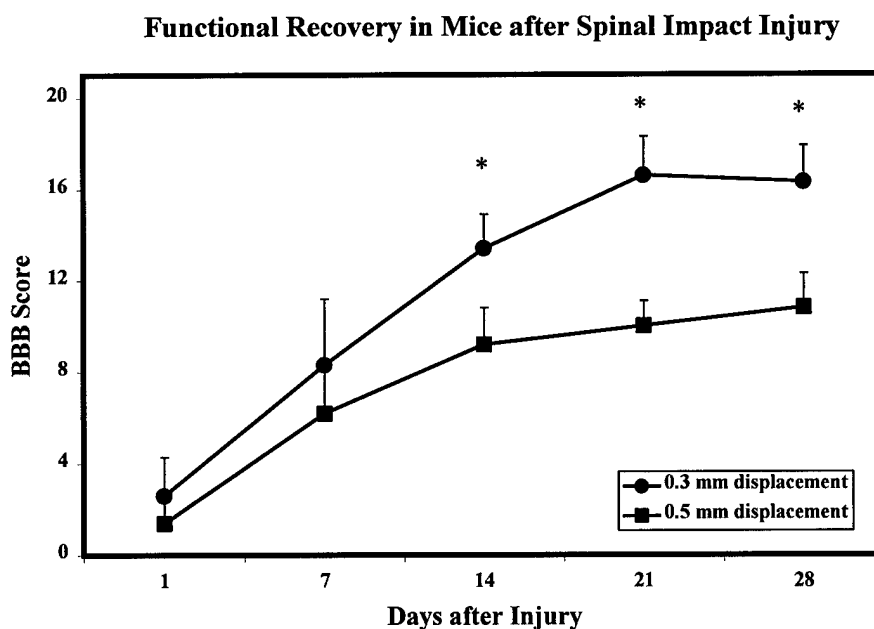
**Methods:** Spinal cord injury was produced using a microprocessor-controlled pneumatic impactor device. This device is a modified version of the well characterized controlled cortical impact device used to create traumatic brain injury (1). The device allows for spinal contusion injury to be performed in which the degree of tissue deformation, the duration and velocity of the impact can be precisely controlled.

The impact device is vertically mounted on a mill table and fitted with a 1.5mm beveled flat steel impounder tip. By changing the positive and negative (back) pressure settings, the researcher can vary the impact velocity. For the current study, impact velocity was held constant at 4.0 m/s. The dwell time (the length of time the impactor is in contact with the spinal cord) was also kept constant at 20 msec in the current study. Only the degree of tissue deformation was varied. We examined two degrees of tissue deformation, 0.3 mm and 0.5mm.

Briefly, adult C57 BL/6 male mice (30 g) were anesthetized with 2,2,2-tribromoethanol (125mg/Kg). A laminectomy was performed at 9th thoracic vertebra that included some removal of the 8th and 10th vertebra, opening an area approximately 2.0 mm in diameter. The laminectomized animal

was placed on the spinal impact device stage. The 7th and 11th vertebrae were clamped with small curved hemostats attached to ball and joint swivel arms. The swivel arms were adjusted so that the animal was suspended. The impactor tip was extended and dialed down so that the flat tip just rested against the exposed dura. The impactor was retracted and the degree of tissue displacement was set. The device was then triggered at which time the impactor was extended, displacing the dorsal surface of the spinal cord by 0.3 or 0.5 mm depending on the setting. The velocity of the hit and dwell time (length of time the impactor was in contact with the tissue) was recorded with a digital oscilloscope (Protec, Alexandria, VA).

**Results:** A tissue displacement of 0.3mm produced complete paralysis for approximately 48 h with a considerable amount of hind limb locomotion recovered over the next four weeks. The 0.5mm also produced complete hind limb paralysis for 48-72 h after injury. However, a more modest degree of hind limb function was recovered in these animals (see graph). Thus, we now have a model of SCI that can be used in mice, more importantly with genetically altered mice and by varying the tissue displacement, we can produce injuries of varying degree that have measurable behavioral outcomes.



Reference:

1. Fox GB, Fan L, LeVasseur RA and Faden AI. Sustained sensory/motor and cognitive deficits associated with neuronal apoptosis following controlled cortical impact brain injury in the mouse. *J Neurotrauma*, Vol. 15: 599-614, 1998.

## FULL-LENGTH PUBLICATIONS SUPPORTED DURING THE LAST YEAR

PAUL S. AISEN, M.D.

### Publications

Hull M, Pasinetti GM, Aisen PS. Elevated plasma neopterin levels in Alzheimer's disease. *Alzheimer Disease and Associated Disorders*, 14: 228-230, 2000.

Aisen PS. Anti-inflammatory therapy for Alzheimer's disease. *Neurobiology of Aging*, 21: 447-448, 2000.

Aisen PS. Anti-inflammatory therapy for Alzheimer's disease: implications of the prednisone trial. *Acta Neurologica Scandinavica*, S176: 85-89, 2000.

Aisen PS. Selective COX-2 inhibitors for the treatment of Alzheimer's disease. *American Journal of Medicine*, in press.

ALAN I. FADEN, M.D.

### Publications

Eldadah BA, Ren RF, and Faden AI. Ribozyme-mediated inhibition of Caspase-3 protects cerebellar granule cells from apoptosis induced by serum/potassium deprivation. *J Neurosci* 20(1):179-186, 2000.

Allen JW, Knoblach SM, and Faden AI. Activation of group I metabotropic glutamate receptors reduces neuronal apoptosis but increases necrotic cell death *in vitro*. *Cell Death Diff* 7(5):470-476, 2000.

Eldadah BA and Faden AI. Caspase pathways, neuronal apoptosis, and CNS injury. *J Neurotrauma* 17(10):811-29, 2000.

Toman RE, Spiegel S, and Faden AI. Role of ceramide in neuronal cell death and differentiation. *J Neurotrauma* 17(10):891-8, 2000.

O'Leary DM, Movsesyan V, Vicini S, and Faden AI. Selective mGluR5 antagonists MPEP and SIB-1893 decrease NMDA or glutamate-mediated neuronal toxicity through actions that reflect NMDA receptor antagonism. *Br J Pharmacol* 131(7):1429-37, 2000.

Movsesyan VA, O'Leary DM, Fan L, Bao W, Mullins PG, Knoblach SM, and Faden AI. mGluR5 antagonists 2-methyl-6-(phenylethynyl)-pyridine and (E)-2-methyl-6-(2-phenylethenyl)-pyridine reduce traumatic neuronal injury in vitro and in vivo by antagonizing N-methyl-D-aspartate receptors. *J Pharmacol Exp Ther* 296(1):41-7, 2001.



Movsesyan VA, Yakovlev AG, Fan L, and Faden AI. Effect of serine protease inhibitors on posttraumatic brain injury and neuronal apoptosis. *Exp Neurol* 167(2):366-75, 2001.

Faden AI, O'Leary DM, Fan L, Bao W, Mullins PG, and Movsesyan VA. Selective blockade of the mGluR1 receptor reduces traumatic neuronal injury *in vitro* and improves outcome after brain trauma. *Exp Neurol* 167(2):435-44, 2001.

Allen JW, Eldadah BA, Huang X, Knoblach SM, and Faden AI. Multiple caspases are involved in  $\beta$ -amyloid-induced neuronal apoptosis. *J Neurosci Res*, in press.

Allen JW, Vicini S, and Faden AI. Exacerbation of neuronal cell death by activation of group I metabotropic glutamate receptors: role of NMDA receptors and arachidonic acid release. *Exp Neurol*, in press.

Lea PM IV and Faden AI. Traumatic brain injury: developmental differences in glutamate receptor response and the impact on treatment. Special Issue: The glutamate signalling in developmental and in neonatal brain injury. *Mental Retardation & Developmental Disabilities Research Reviews*, in press.

#### **GEOFFREY GOODHILL, Ph.D.**

##### Publication

Goodhill, G.J. & Urbach, J.S. (2001). Axon guidance and gradient detection by growth cones. In Modeling Neural Development, ed. Arjen Van Ooyen, MIT Press, in press.

#### **SUSAN KNOBLACH, Ph.D.**

Knoblach SM and Faden AI. Cortical interleukin-1 beta elevation after traumatic brain injury in the rat: no effect of two selective antagonists on motor recovery. *Neurosci Lett* 289(1):5-8, 2000.

#### **ALAN KOZIKOWSKI, Ph.D.**

##### Publications

Nan F, Bzdega T, Pshenichkin S, Wroblewski JT, Wroblewska B, Neale JH, and Kozikowski AP. Dual function glutamate-related ligands: discovery of a novel, potent inhibitor of glutamate arboxypeptidase ii possessing mGluR3 agonist activity. *J. Med. Chem* 43(5), 772-774, 2000.

Qiao L, Zhao L-Y, Rong S-B, Wu X-W, Wang S, Fujii T, Kazanietz MG, Rauser L, Savage J, Roth BL, Flippen-Anderson J, and Kozikowski AP. Rational design, synthesis, and biological evaluation of rigid pyrrolidone analogs as inhibitors of prostate cancer cell growth. *Bioorg. Med. Chem. Lett.* 11, 955-959, 2001

Kozikowski AP, Nan F, Conti P, Zhang J, Ramadan E, Bzdega T, Wroblewska B, Neale JH, Pshenichkin S, and Wroblewski JT. Design of remarkably simple, yet potent urea-based inhibitors of glutamate carboxypeptidase ii (NAALADase) *J. Med. Chem* 44(3), 298-301, 2001.

## MICHAEL ULLMAN, Ph.D.

### Publications

Ullman MT. A Mental Model of Morphology: The Psychological and Neural Bases of the Computation of Complex Words. In K.K. Grohmann & C. Struijke (Eds.), *University of Maryland Working Papers in Linguistics, Volume 10. Special Issue: Proceedings of the Maryland Mayfest on Morphology 1999*. 127-156. 2000

Ullman MT and Izvorski R. What is special about Broca's area? *Behavioral and Brain Sciences*. 23(1) 52-54. 2000

Ullman MT. How the brain made language. *Science*. 289(5477) 251-252. 2000

Newman AJ, Izvorski-Pancheva R, Ozawa K, Neville H, and Ullman MT. An event-related study fMRI study of syntactic and semantic violations. *Journal of Psycholinguistic Research*. 30(2). 2001

Ullman MT. The neural basis of lexicon and grammar in first and second language: The declarative/procedural model. *Bilingualism*. 4(2). 2001

van der Lely HKJ and Ullman MT. past tense morphology in specifically language impaired and normally developing children. *Language and Cognitive Processes*. 16(2). 177-217. 2001

Steinhauer K, Pancheva R, Newman AJ, Gennari S, and Ullman MT. How the mass counts: An electrophysiological approach to the processing of lexical features. *Neuroreport*. 12(5). 999-1005. 2001

Ullman MT. The declarative/procedural model of lexicon and grammar. *Journal of Psycholinguistic Research*. 30(1). 37-69. 2001

Kensinger EA, Ullman MT, and Corkin S. Bilateral medial temporal lobe damage does not affect lexical or grammatical processing: Evidence from the amnesic patient H.M. *Hippocampus*. (in press)

Ullman MT. Evidence that lexical memory is part of the temporal lobe declarative memory, and that grammatical rules are processed by the frontal/basal-ganglia procedural system. *Brain and Language*. (in press)

Ullman MT, Izvorksi R, Love T, Yee E, Swinney D, and Hickok G. Neural correlates of lexicon and grammar: Evidence from the production, reading and judgment of inflection in aphasia. *Brain and Language*. (in press)

**ROBERT VINK, Ph.D.**

Publication

Vink R., Mullins PGM, Temple MD, Bao W, and Faden AI. Small shifts in craniotomy position in the lateral fluid percussion injury model are associated with differential lesion development. *J. Neurotrauma*, in press.

**SHAOMENG WANG, Ph.D.**

Publications

Wu X. and Wang S. Folding studies of a linear pentamer peptide adopting a reverse turn conformation in aqueous solution through molecular dynamics simulation, *J. Physical Chemistry* 104(33), 8023-8034, 2000.

Pak Y and Wang S. Application of a new molecular dynamics simulation method with a generalized effective potential to the flexible docking problems. *J. Physical Chemistry (B)* 104, 354-359, 2000.

Pak Y, Enyedy IJ, Varady, Kung JW, Lorenzo PS, Blumberg PM and Wang S. Structural basis of binding of high-affinity ligands to protein kinase c: prediction of the binding modes through a new molecular dynamics method and evaluation by site-directed mutagenesis, *Journal of Medicinal Chemistry* 44(11), 1690-1701, 2001.

**ALEXANDER YAKOVLEV, Ph.D.**

Publications

Yakovlev AG, Wang G, Stoica BA, Boulares H, Spoonde AY, Yoshihara K, Smulson ME A role of the  $\text{Ca}^{2+}/\text{Mg}^{2+}$ -dependent endonuclease in apoptosis and its inhibition by poly(ADP-ribose)polymerase. *J Biol Chem* 275(28):21302-21308, 2000.

Yakovlev AG, Di X, Movsesyan V, Mullins PG, Wang G, Boulares H, Zhang J, Xu M, and Faden AI. Presence of DNA Fragmentation and Lack of Neuroprotective Effect in DFF45 Knockout Mice Subjected to Traumatic Brain Injury. *Molecular Medicine* 7(3): 205-216, 2001.

Yakovlev AG and Faden AI. Apoptotic pathways and CNS injury. *Molecular Neurobiology* (in press).